

ALSF : Where Rivers Meet
Geophysical Survey at Catholme
Phase II Investigations.

Submitted By:
Meg Watters

University of Birmingham
Institute of Archaeology and Antiquity

Table of Contents

Table of Contents.....	1
Table of Figures	3
1.0 Report Contents	8
2.0 Project Summary.....	9
3.0 Review of Past Geophysical work at Catholme.....	13
3.1 Grey Literature.....	13
3.2 ALSF WRM Phase I Investigations.....	14
3.2.1 Phase I Geophysical Survey Goals and Methodology.....	14
3.2.2 Comparison to Grey Literature	16
3.3.3 Phase I Conclusions	17
4.0 Phase II Geophysical Survey at Catholme.....	21
4.1 Site Selection and Justification	21
4.1.1 Area A1	22
4.1.2 Area A2.....	23
4.1.3 Area B1	25
4.1.4 Area B2	26
4.1.5 Area F1.....	26
4.1.6 Area F2.....	27
4.2 Geophysical Survey Area Mapping and Data Collection.....	28
4.2.1 Magnetometry Data Collection.....	28
4.2.2 Magnetic Susceptibility	29
4.2.3 2m x 5m Sub-area Magnetic Susceptibility	29
4.2.4 Resistivity Data Collection	29
4.2.5 2m x 5m Sub-area Resistivity Data Collection.....	30
4.2.6 GPR Data Collection.....	31
4.2.7 2m x 5m Sub-area Dielectric Permittivity Data Collection.....	31
4.3 Geophysical Techniques and Methodology.....	33
4.3.1 Magnetometry	33
4.3.2 Magnetic Susceptibility	33
4.3.3 Resistivity	33
4.3.4 GPR.....	35
4.4 Geophysical Data Processing and GIS Integration.....	38
4.4.1 Magnetic Data Processing.....	38
4.4.2 Resistivity Data Processing.....	38
4.4.3 GPR Data Processing.....	38
4.4.4 GIS Data Integration.....	39
4.5 Geophysical Data Interpretation and Classification	40
4.5.1 General observations.....	41
5.0 Geophysical Survey Results	42
5.1 Area A1	43
5.1.1 Magnetometry Survey Results.....	43
5.1.2 Magnetic Susceptibility Results.....	45
5.1.3 Resistivity Survey Results	46
5.1.4 GPR Survey Results.....	54
5.1.5 A1 2m x 5m Sub-area	60
5.2 Area A2.....	63
5.2.1 Magnetometry Survey Results.....	63
5.2.2 Magnetic Susceptibility Results.....	66

5.2.3	Resistivity Survey Results	67
5.2.4	GPR Survey Results.....	73
5.2.5	A2 2m x 5m Sub-area	79
5.3	Area B2	82
5.3.1	Magnetometry Survey Results.....	82
5.3.2	Magnetic Susceptibility Results.....	86
5.3.3	Resistivity Survey Results	87
5.3.4	GPR Survey Results.....	90
5.3.5	B2 2m x 5m Sub-area	97
5.4	Area F1.....	100
5.4.1	Magnetometry Survey Results.....	100
5.4.2	Magnetic susceptibility Results	102
5.4.3	Resistivity Survey Results	103
5.4.4	GPR Survey Results.....	107
5.4.5	F1 2m x 5m Sub-area.....	111
6.0	Conclusions and Recommendations	114
6.1	Comments	114
6.1.1	Geophysical Survey	114
6.1.2	Resistivity Profiling	115
6.2	Recommendations.....	115
6.2.1	Continuation of the WRM geophysical survey project.....	115
6.2.2	GIS and ArcIms	116
6.2.3	Data Fusion, Modelling and Visualisation.....	117
7.0	Bibliography	122

Table of Figures

Figure 1. Oblique aerial photo with the 'Sunburst' and 'Woodhenge' monuments and pit-alignment cropmarks.	9
Figure 2. WRM Full Area.	10
Figure 3. Geophysical survey focus area of the WRM project.	11
Figure 4. WRM GIS: Magnetic survey results and interpretations are overlain on rectified aerial photograph showing the 'Woodhenge' cropmark.	12
Figure 5. Previous geophysical survey (purple areas) and excavation (blue lines) in the Catholme Ceremonial Complex area.	14
Figure 6. Phase I geophysical survey areas and interpreted anomalies.	15
Figure 7. Re-digitised cropmark features in blue.	16
Figure 8. Resistance survey results over the 'Sunburst' (a. and b.) and large ring ditch (c. and d.) monuments.	17
Figure 9. Comparison of magnetic survey results for the 'Sunburst' (a. and b.) and large ring ditch monuments (c. and d.).	18
Figure 10. Phase I geophysical survey interpretations for the 'Woodhenge' monument. GPR (green), resistance (pink) and magnetic (blue).	19
Figure 11. Re-assessment of the correct positioning of the cropmark data positions the 'Wood henge' feature over a probable geological resistance anomaly.	19
Figure 12. Phase II WRM geophysical survey areas as red blocks.	22
Figure 13. Phase II Field A area locations. A1 is in the north and A2 in the south.	23
Figure 14. Phase II survey area selected to investigate the 'Woodhenge' feature in Field A.	24
Figure 15. Rectified oblique aerial photo with 'Woodhenge' cropmark, Phase I geophysical interpretations and overlain operating cropmark GIS layer.	24
Figure 16. A2 positioned over the north-west section of the 'Woodhenge' cropmark.	25
Figure 17. Phase II survey areas in field B.	26
Figure 18. Field F area positions focused on anomalies defined through Phase I geophysical investigations.	27
Figure 19. G858 Cesium Vapor magnetometer (right) in vertical gradient mode and the FM256 Fluxgate Gradiometer (left).	28
Figure 20. Magnetic Susceptibility data were collected with the Bartington MS2 susceptibility meter.	29
Figure 21. RM15 resistivity meter configured to collect readings at multiple depths across the site. The second image illustrates the basic premise behind this multiplexing technique.	30
Figure 22. Data were collected using the RM15 resistivity meter on a custom-designed square array. Three data samples were collected at each station: α , β and γ	30
Figure 23. The SIR3000 GPR unit was used with a shielded 400 MHz antenna.	31
Figure 24. The Adek Pyrometer v.6 was used to collect dielectric permittivity data in the 2m x 5m sub-areas.	32
Figure 25. Resistivity data samples a volume of earth dependent upon probe separation distance.	34
Figure 26. Orthogonal grid display.	36
Figure 27. Vertical profiles can be stacked together to create a 3D cube of information for use in data imaging and analysis.	36

Figure 28. GPR data can be displayed as 2D vertical profiles (greyscale at the bottom of the figure), or sliced along the x, y, and z axes.	37
Figure 29. Greyscale division for magnetic interpretation labeling.	40
Figure 30. A1 magnetic surface survey data (top left) with interpretations (top right) and overlain excavation plan.	43
Figure 31. A1 magnetic gravel survey data (top left) with interpretations (top right) and overlain excavation plan.	44
Figure 32. A1 surface magnetic susceptibility results (left) with overlain excavation plan.	45
Figure 33. A1 gravel magnetic susceptibility results (left) with interpretations (right) and overlain excavation plan (bottom).	46
Figure 34. Resistivity survey data from 0.25m depth (left) with overlain interpretations (right).	47
Figure 35. Resistivity survey data from 0.50m depth (left) with overlain excavation plan (right).	47
Figure 36. A1 gravel resistivity survey results at 0.25m (left) with overlain excavation plan (right).	48
Figure 37. A1 gravel survey at 0.25m with data interpretations that map the same details as the excavation plans.	49
Figure 38. A1 resistivity at 0.50m depth (left) with interpretations (right).	50
Figure 39. A1 resistivity gravel survey at 0.5m (right) with overlain excavation plans (left). The red arrows identify anomalies that do not correspond directly to the plan.	50
Figure 40. Two examples of pits from area A1's pit-alignment. The sketch defines F212, the pit one the eastern edge of the area.	51
Figure 41. A1 resistivity from the gravel survey at 0.75m depth (right) highlighting possible pit structural responses to resistivity survey (right).	51
Figure 42. Image a. represents demonstrates the vertical component of the multiplexed resistivity data. The three plots of measured resistivity in b. present a single pseudosection inversion. The data represented here are a profile across the pit-alignment (red line in a.).	52
Figure 43. Comparison of apparent resistivity plan to graph of raw resistivity pseudosection.	53
Figure 44. Resistivity inversion graph after three iterations with apparent resistivity plan.	53
Figure 45. A1 GPR profile over the pit-alignment showing the changes in velocity of the radar wave due to saturated pit fill.	54
Figure 46. GPR plan views and vertical profiles detailing the pits of the pit-alignment and potential interpretation pitfalls. A. are the pit anomalies in the GPR plan views and B. shows the depth of the plan view at the position of the yellow line.	55
Figure 47. The ground coupling zone at the top of the GPR record measures approximately one wavelet.	56
Figure 48. Time zero position for GPR trace.	57
Figure 49. Adjusted time 0 setting to include the direct wave amplitude.	57
Figure 50. A1 GPR slice at time zero. The red line in the top image designates the position of the vertical profile on the bottom.	57
Figure 51. GPR plan map showing pit-alignment anomalies (blue) in A1.	58
Figure 52. GPR profile across pit-alignment in A1. A is a processed profile and B is the same profile with preliminary interpretations.	59

Figure 53. A1 2m x 5m magnetic susceptibility survey results.....	60
Figure 54. A1 2m x 5m sub-area resistivity survey results.....	61
Figure 55. A1 2m x 5m sub-area dielectric permittivity survey results.....	62
Figure 56. A2 surface magnetometry map (top left) with interpretations (top right) and overlain excavation plan (bottom).	63
Figure 57. A2 gravel magnetometry map (top left) with interpretations (top right) and overlain excavation plan (bottom).	64
Figure 58. A2 gravel FM256 magnetometry map (top left) with interpretations (top right) and overlain excavation plan (bottom).....	65
Figure 59. A2 surface magnetic susceptibility results (left) with interpretations (right) and overlain excavation plan (bottom).	66
Figure 60. Area A2 resistivity survey map at 0.25m depth (left) with overlain highlighted anomalies (right) and excavation plan (bottom).	67
Figure 61. Area A2 resistivity (left) with identifications (right) and overlain excavation plan (bottom). Notice the high percentage of post-pits that have been mapped (circled in red).	69
Figure 62. A2 resistivity gravel survey data at 0.50m (left) with interpretations (right). Note the lack of distinct post-pit anomalies.	70
Figure 63. A2 resistivity gravel survey at 0.75m (left) with interpretations (right). ..	70
Figure 64. A2 resistivity gravel survey at 0.75m with interpretations and excavation plan.....	71
Figure 65. A2 resistivity gravel survey at 1m depth (left) with interpreted anomalies (right) and overlain excavation plan (bottom).	72
Figure 66. A2 GPR plan map at 0.75m (left) with interpretations (right).	73
Figure 67. A2 GPR anomaly interpretation with overlain blue arcs at possible post-pit alignment (left). The image on the left shows the excavation plan mapping the position of post-pits.....	74
Figure 68. A2 GPR natural subsoil plan map at the ground coupling position.	75
Figure 69. A2 GPR natural subsoil at 0.55m depth (left) with interpretations (right) overlain excavation plan (bottom).	76
Figure 70. A2 GPR profile across post-pit features.....	77
Figure 71. A2 GPR profile across post-pit features with yellow crosshair identifying position of post-pit in the plan map.	77
Figure 72. A2 GPR plan map at approximately 0.65m depth.....	78
Figure 73. A2 2m x 5m sub-area magnetic susceptibility survey results.	79
Figure 74. A2 2m x 5m sub-area resistivity survey results.....	80
Figure 75. A2 2m x 5m sub-area dielectric permittivity survey results.....	81
Figure 76. B2 surface magnetometry map (top left) with interpretations (top right) and overlain excavation plan (bottom left).	83
Figure 77. B2 gravel magnetometry map (top left) with interpretations (top right) and overlain excavation plan (bottom).	84
Figure 78. B2 gravel FM256 magnetometry map (top left) with interpretations (top right) and overlain excavation plan (bottom).....	85
Figure 79. B2 surface magnetic susceptibility results (left) with overlain excavation plan (right).	86
Figure 80. B2 gravel magnetic susceptibility results (left) with interpretations (right) and overlain excavation plan (bottom).	87
Figure 81. B2 resistivity surface survey (left) with interpretations (right) and overlain excavation plan (bottom).	88
Figure 82. B2 resistivity gravel survey at 0.25m (left) with interpretations (right)....	89

Figure 83. B2 resistivity gravel survey at 0.25m with interpretations and overlain excavation plan.	89
Figure 84. B2 surface GPR plan views showing the appearance of the ring ditch.	90
Figure 85. GPR surface survey plan map at 0.57m (left) with interpretations (right) and excavation plan (bottom).	91
Figure 86. B2 'Sunburst' Monument. GPR record from the ground coupling signal (left) with interpreted archaeological and geological features (right).	92
Figure 87. B2 'Sunburst' Monument ring ditch in GPR data.	92
Figure 88. B2 'Sunburst' monument GPR data at 0.4m depth showing distinct ring ditch property contrasts with background material (red arrows) and the lack of contrast and ditch definition (yellow arrows).	93
Figure 89. B2 GPR image of profile through ring ditch. A and C are the ring ditch (blue) and B is one of the plough furrows (green) passing through the ring ditch.	94
Figure 90. B2 GPR profile through archaeological features: A - pit, B- plough furrow, C- burial, D- pit with <i>in situ</i> burning, E- ring ditch.	95
Figure 91. B2 2m x 5m magnetic susceptibility survey results.	97
Figure 92. A1 2m x 5m resistivity survey results.	98
Figure 93. B2 2m x 5m dielectric permittivity survey results.	99
Figure 94. F1 surface magnetometry map (top left) with interpretations (top right) and overlain excavation plan (bottom).	100
Figure 95. F1 gravel magnetometry map (top left) with interpretations (top right) and overlain excavation plan (bottom).	101
Figure 96. F1 surface magnetic susceptibility results (left) with overlain excavation plan (right).	102
Figure 97. F1 gravel magnetic susceptibility results (left) with overlain interpretations and excavation plan (right).	102
Figure 98. F1 resistivity map at 0.25m depth (left) with interpretations (right).	103
Figure 99. F1 resistivity map at 0.50m depth (left) with interpretations (right).	104
Figure 100. F1 resistivity survey at 0.50m depth with overlain interpretations and excavation plan.	104
Figure 101. F1 resistivity gravel survey at 0.50m (left) with interpretations (right).	105
Figure 102. F1 resistivity gravel survey at 0.75m depth (left) with interpretations (right).	106
Figure 103. F1 resistivity gravel survey at 0.75m depth with interpretations and excavation plan.	106
Figure 104. Ground coupling GPR map of gravel survey surface F1 over the Large Ring Ditch with extensions. The map on the right has the excavation features mapped that correspond with the GPR information.	108
Figure 105. GPR interpretations from the surface of the GPR gravel survey area F1.	108
Figure 106. F1 gravel GPR data at 0.6m depth (left) with overlain interpretations (right).	109
Figure 107. F1 ring ditch feature defined by high amplitude reflection at approximately 0.90m depth (left). The image to the right highlights in yellow the response of the GPR to archaeological features at 0.90m depth, this anomaly is overlain on previous GPR interpretations.	110
Figure 108. F1 2m x 5m magnetic susceptibility survey results.	111
Figure 109. F1 2m x 5m resistivity survey results.	112

Figure 110. F1 2m x 5m dielectric permittivity survey results..... 113
Figure 111. Traditional GPR profiles (a.), fence diagram (b.) and 3D cube with time slices (c.) 118
Figure 112. Resistivity plan maps (a.) and inverted pseudosections (b.) 119
Figure 113. 3D visualised GPR and resistivity data from A1..... 120

1.0 Report Contents

This report presents the results of Phase II of geophysical survey undertaken by Birmingham Archeology at Catholme in Staffordshire. The survey was conducted as part of the Where Rivers Meet: Landscape, Ritual, Settlement and the Archaeology of River Gravels project (hereafter WRM) and was funded through the Aggregates Levy Sustainability Fund by English Heritage.

2.0 Project Summary

Within the boundaries of the project, a 'Focus Area' encompassing an important concentration of monuments known as the 'Catholme Ceremonial Complex' was targeted for geophysical investigation. The Neolithic/Early Bronze Age monuments include a 'Woodhenge' feature comprising concentric rings of post-pits, a 'Sunburst' monument comprising a central ring ditch with radiating pit-alignments and a large ring ditch with associated linear features.



Figure 1. Oblique aerial photo with the 'Sunburst' and 'Woodhenge' monuments and pit-alignment cropmarks.

The location of these monuments is of particular archaeological significance not only because of the variety of archaeological features but also the geological nature of the area with complex river channel activity at the confluence of the Tame, Trent, and Mease Rivers.

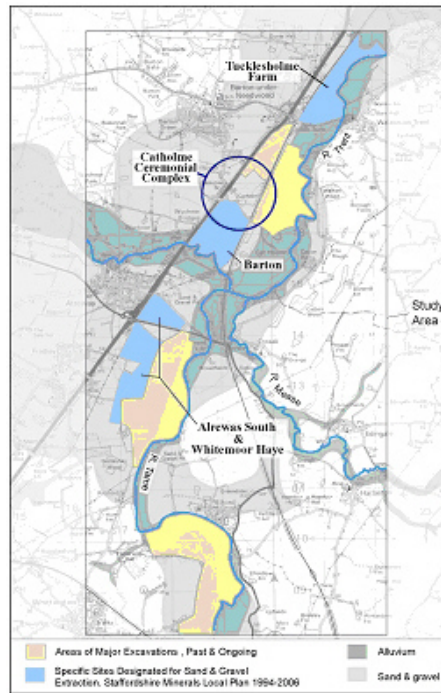


Figure 2. WRM Full Area.

Originally the ‘Catholme Ceremonial Complex’ was discovered as cropmarks and subsequently partially protected as a series of Scheduled Ancient Monument (SAMs). The archaeological features were described generally as a type “not readily susceptible to detection by conventional archaeological prospection techniques” (Buteux *et al.* 2002, p. 11). This description was based on the results of previous geophysical survey conducted in the Focus Area. The WRM survey objectives were to better classify the geophysical survey methods that may or may not positively identify this particular type of archaeological feature. Additionally, the project attempted to gain a more informed sub-surface view of the properties of the archaeology and how various geophysical survey methods responded to them, the aim being to better inform future archaeological investigation.

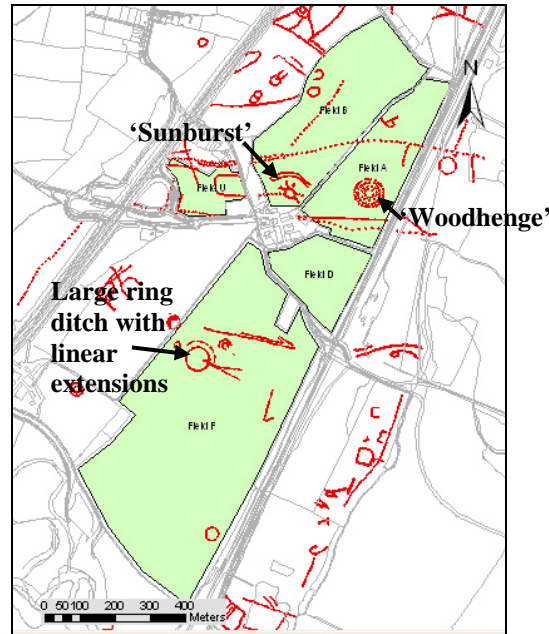


Figure 3. Geophysical survey focus area of the WRM project.

The Phase I geophysical surveys were undertaken with the aim of quickly and effectively covering large areas with conventional geophysical techniques. The surveys were successful and identified a number of anomalies, some of which were clearly archaeological. The main emphasis of the work was to classify the effectiveness of geophysical survey methods in identifying archaeological features in the Catholme area.

Phase II investigations were focused on ‘ground truthing’ the results from the Phase I work. This process employed a programme of further geophysical survey, soil analysis and excavation aimed at gaining a more in depth understanding of the site. The focus was to better understand the relationship between the geophysical survey data, below-ground archaeology and soil properties as a means to enhance the interpretation of survey results, and as a guide to future geophysical practice. A study of the relationship between the processes and materials by which the deposits obtained their geophysical properties was attempted in order to better comprehend the results of the geophysical survey and plan for more informed and effective work in the future.

Six areas of significant interest were selected for intensive investigation, three 20m x 10m areas and three 10m x 10m areas. An additional four sub-areas measuring 2m x 5m were selected for further geophysical sampling, soil analysis and excavation. Intensive geophysical surveys were conducted on the ground surface in each area and repeated on the subsoil surface following the removal of the plough zone. Geophysical sampling was continued within the 2m x 5m sub-areas at 0.2m deep intervals, then excavated and planned at each exposure until the base of the archaeology was reached.

Techniques used for each survey area included magnetometry, magnetic susceptibility, resistivity and ground penetrating radar (hereafter GPR).

The results of the geophysical surveys were processed and rectified into a larger WRM geophysical GIS. The multi-layered spatial nature of a GIS was necessary for the integration not only of multiple geophysical data types and interpretations, but also of excavation information and data from soil sampling and analysis. The management of project data in a GIS was an essential step toward potential full data integration between different geophysical surveys, soil analysis results and excavation information.

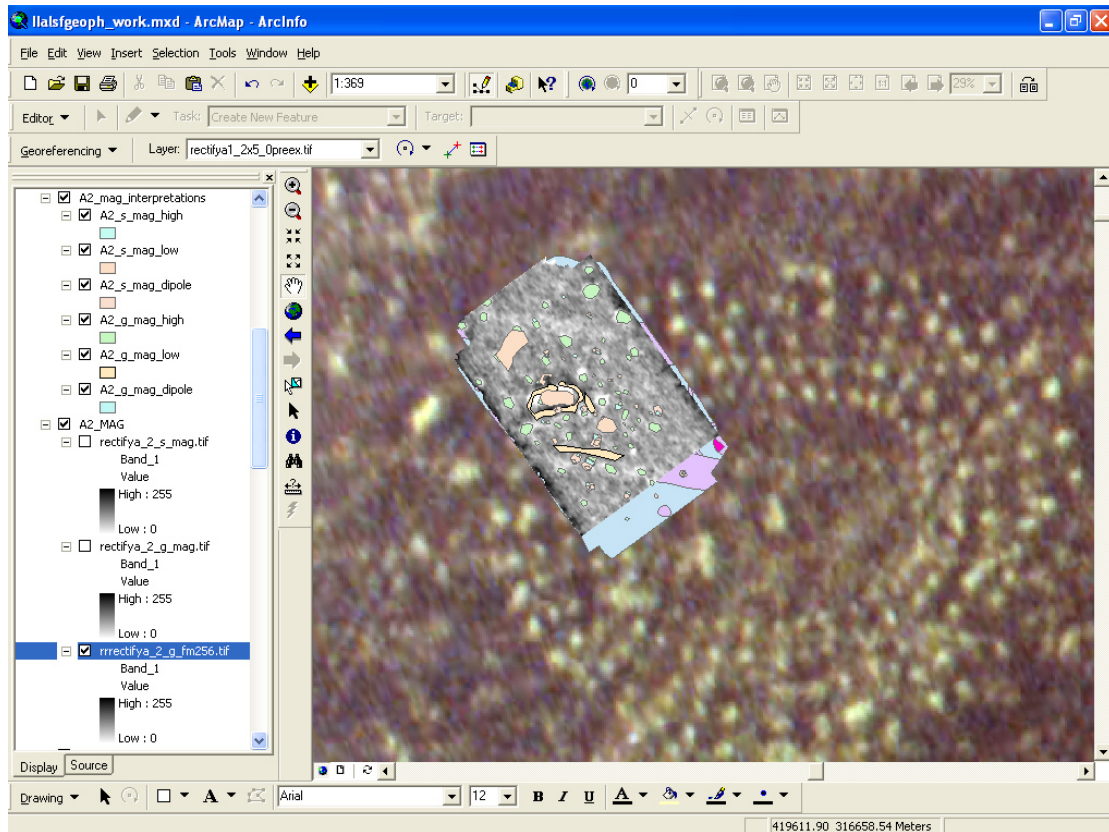


Figure 4. WRM GIS: Magnetic survey results and interpretations are overlain on rectified aerial photograph showing the 'Woodhenge' cropmark.

Data have been interpreted with an emphasis not only on the identification of archaeological features, but equally importantly, on the nature of the sub-surface response to each geophysical technique. Further investigations and analyses of the project data will provide a unique insight into the nature of the archaeology and environment and the impact of contemporary land use on it.

3.0 Review of Past Geophysical work at Catholme

Geophysical surveys have been conducted in the WRM Full Area previously as part of archaeological investigations in the early 1990s. The Focus Area, which includes the 'Catholme Ceremonial Complex', was first targeted in 1999 as part of a commercial project. This did not, however, include the areas of the three scheduled monuments (Bartlett 1999). Approximately 16ha was surveyed as part of Phase I of the WRM project during 2002-2003 (Watters, forthcoming). This survey covered broad swathes of the landscape around and over the scheduled monuments in an attempt to gather more information on the cropmark features and their surrounding environment.

3.1 Grey Literature

A general review of geophysical survey results in the Full Area indicated that potential archaeological features were successfully located, such as at Whitmore Haye (Bartlett 1998, 1995). But in general, geophysical evaluation in this region has not successfully located known cropmarks or other possible archaeological features.

Specific geophysical survey work in the Focus Area was conducted as part of an archaeological evaluation of the site extending to the north and east of Catholme Farm in August of 1999. The survey was commissioned by Phoenix Consulting Archaeology Ltd and undertaken by the Bartlett-Clark Consultancy Company on behalf of Hanson Aggregates (Bartlett 1999). The purpose was to assess whether archaeological features in addition to the known cropmarks might be identified.

Geophysical areas were located to provide an overall sample of the site and to include archaeological features which had previously been recorded as cropmarks, all but those in the scheduled areas (Bartlett 1999). This project was undertaken mostly using magnetometry. Small areas were also covered using resistivity over selected features which had been identified previously by magnetometry. This survey did not provide conclusive results (Bartlett, 1999, p.3-4).

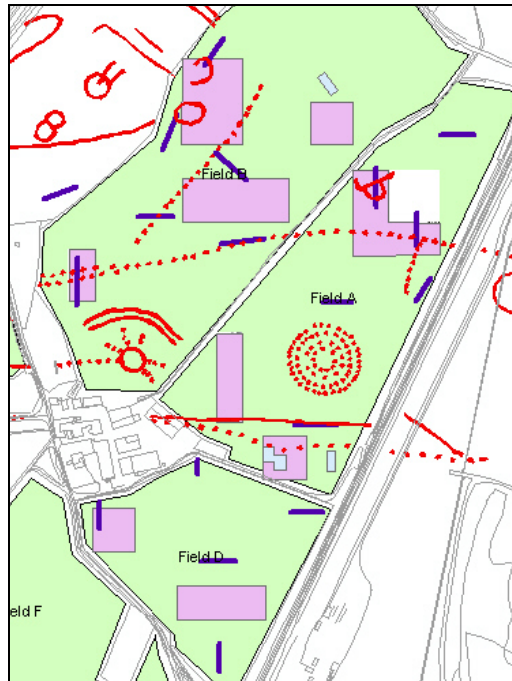


Figure 5. Previous geophysical survey (purple areas) and excavation (blue lines) in the Catholme Ceremonial Complex area.

Following the geophysical survey a series of trial trenches was excavated. These were located over possible anomalies which had been highlighted in the geophysical data, over known cropmarks and in unrelated areas to provide a measure of control. Some geophysical anomalies were identified positively as archaeological features but, in general, the geophysical survey did not contribute significantly to the archaeological project (Hughes and Coates 1999).

3.2 ALSF WRM Phase I Investigations

Phase I investigations were implemented in order to study a number of aspects of the archaeological landscape. These included specific archaeological monuments and the impact of modern land-use and hydro-geological patterns on the state of archaeological preservation.

3.2.1 Phase I Geophysical Survey Goals and Methodology

Geophysical surveys were conducted with the aim of:

- Non-invasive mapping and identification of archaeological features.
- The establishment of methodologies for effective geophysical mapping.
- Assessing the impact of contemporary land-use.
- Contributing to a larger dynamic landscape model for a better understanding of the site and the human use and occupation of the area over time (Watters, *forthcoming*).

Resistivity, magnetometry and GPR techniques were each employed in the geophysical mapping of the project area. Magnetometry and resistivity were selected on the basis that they are the most commonly used techniques employed in most archaeological investigations, and were also readily accessible. GPR was used

because it was an appropriate method to employ in this environment and has often been overlooked in British archaeological investigations. Data collection began with a resistivity survey in April 2003, since this method typically takes up to twice as long as the other methods to conduct. A magnetometry survey followed in June 2003 and GPR survey in October 2003.

A review of the grey literature which related to the Full Area showed that most archaeological investigations were conducted in the field on the basis of the location of known cropmarks. The geophysical survey of the Focus Area was also based on the location of the cropmarks. As with previous projects, one of our primary objectives was to establish whether we would be able to map the cropmarks and other features, whilst the process of mapping these features was itself assessed.

The area covered during Phase I of this project was more extensive than is usual in order that more of the landscape could be mapped than the isolated ‘postage stamp’ areas more conventionally targeted. The project coverage totaled *c.*26.5ha, resistivity survey measuring *c.*13ha, magnetometry survey *c.*10ha and GPR *c.*3.5ha.

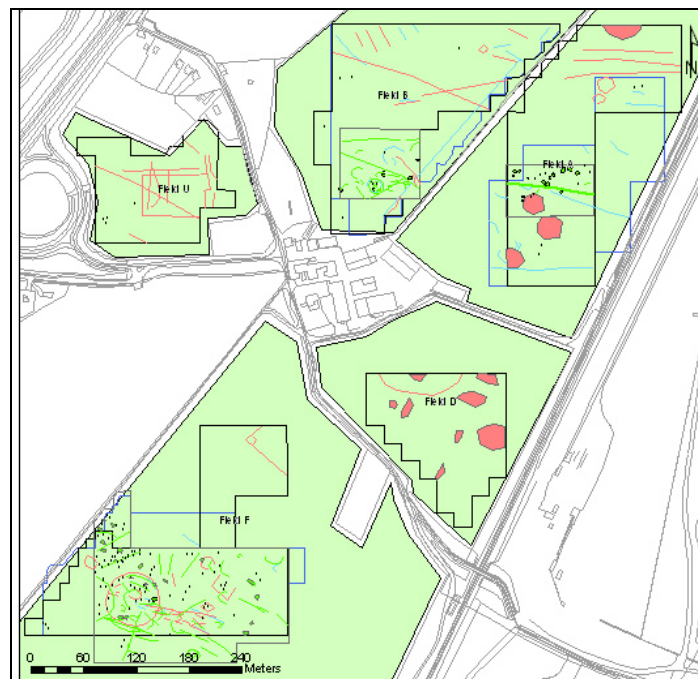


Figure 6. Phase I geophysical survey areas and interpreted anomalies.

The geophysical survey conducted over the five fields of the Focus Area revealed many geophysical anomalies. One objective of the survey was to determine whether the known cropmarks could be detected by non-invasive means. The ring ditch of the ‘Sunburst’ monument in Field B was mapped definitively as was almost the entire group of cropmark features in Field F. Field A produced some good results over the pit-alignment in the north, but failed to produce positive results for the cropmarks which correspond with the ‘Woodhenge’.

The survey in the Focus Area successfully mapped many known cropmarks as well as a number of new potential archaeological anomalies. This research provided a thorough assessment of basic geophysical methodologies in general use in the field.

The results of the survey contained some surprises and posed interesting questions which perhaps challenge present archaeological practices.

In addition to mapping the cropmarks, the GPR survey provided a geophysical profile of the Focus Area. This three dimensional perspective provided the opportunity for analysis of the effects of modern and past land-use on the archaeological resource. It provided information which suggested the 'Sunburst' monument in Field B had been directly affected by more recent land-use, probably from the medieval period onwards, as evidenced by remnants of possible ridge and furrow.

Analysis of the GPR results in Field F provided information that present and past land-use appeared not to have directly impacted upon the buried archaeological resource. Field F may well therefore contain the best preserved archaeology.



Figure 7. Re-digitised cropmark features in blue.

3.2.2 Comparison to Grey Literature

The results of the extensive survey undertaken as part of the WRM project was compared with the results of earlier geophysical surveys, both in the Focus Area and the Full Area. The earlier surveys were undertaken mostly as part of commercial projects. A review of the relevant grey literature revealed that while some of this work was effective in identifying archaeological targets only a small proportion of the overall work done might be described as successful and most employed only a single technique, on a limited scale.

A number of factors might explain the variable results revealed in the review of the grey literature:

- Technique used (resistivity, magnetometry, *etc.*).
- Geology and soils.
- Feature properties.
- Ground conditions (for example saturation).
- Extent of coverage.
- Data sampling intervals/rates.
- Processing, analytical and display techniques.

3.3.3 Phase I Conclusions

Two key points emerge from the results of Phase I geophysical investigations:

- The ring ditches in Fields B and F responded differently to resistivity and magnetic survey, but similarly to GPR. The ring ditch in Field B was clearly located with GPR and magnetic survey methods whilst the ring ditch in Field F was located by GPR and resistivity survey. The questions that arise from these results are:

- I. Why was the ring ditch in Field F located with the resistivity method whilst that in Field B was not?

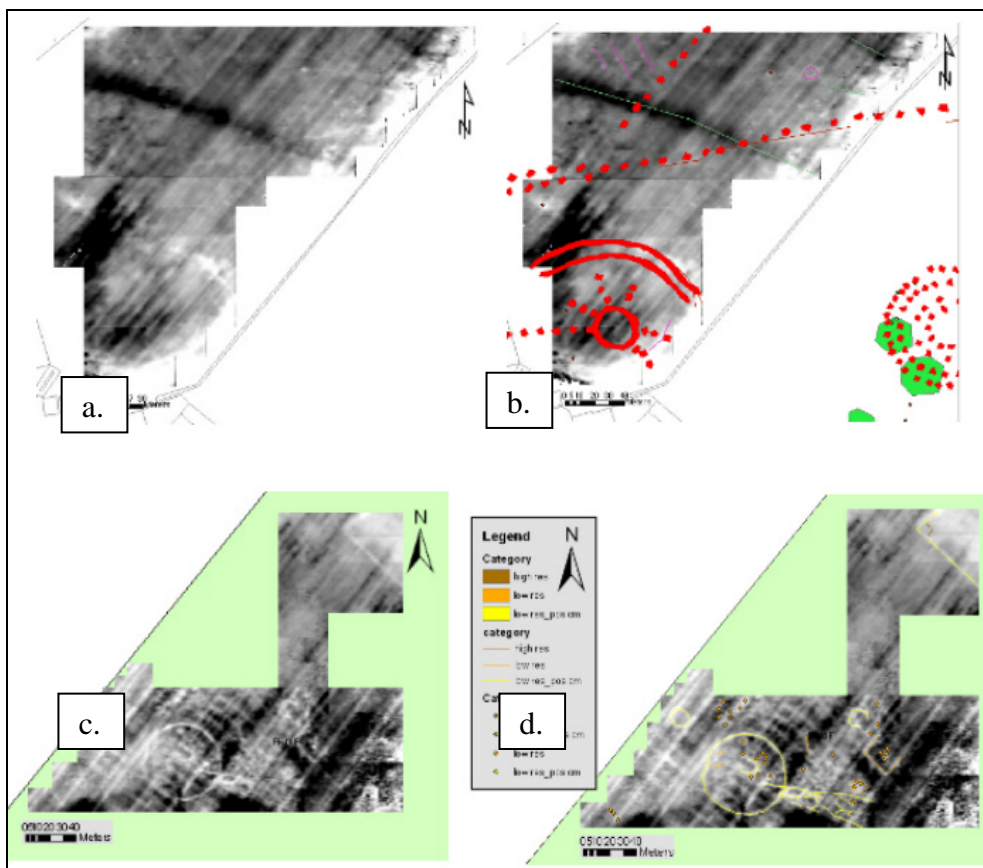


Figure 8. Resistance survey results over the 'Sunburst' (a. and b.) and large ring ditch (c. and d.) monuments.

The contrast in resistivity survey results in this instance could be explained by the possible difference in ground saturation during data collection. The resistivity data for Field F was collected during rain while Field B was very dry during data collection. If this is the explanation, why did GPR work effectively in both cases? It is often dependent upon the same site properties as resistivity, for example saturation which enhances the contrasts in dielectric properties. GPR and resistivity clearly differ enough in their sensitivity to different physical properties such that they do not always respond in the same manner to ground conditions.

II. Why did the ring ditch in Field B appear as a strong anomaly in the magnetic data - although there were some very weak signatures in places - whilst the ring ditch in Field F did not appear so clearly?

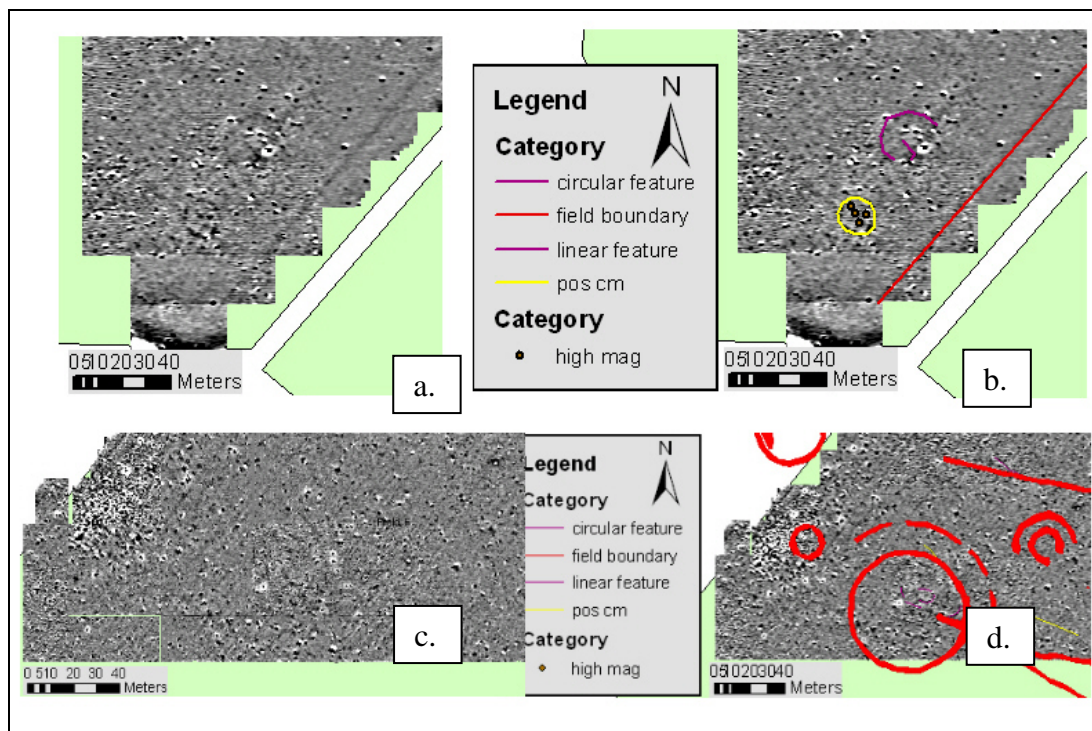


Figure 9. Comparison of magnetic survey results for the 'Sunburst' (a. and b.) and large ring ditch monuments (c. and d.).

This could be explained with reference to the remanent magnetism of the ploughed soil which is characteristic of recent ploughing events. If a field is surveyed by magnetometry soon after ploughing the remanent magnetism may still be relatively strong in the topsoil and may overshadow underlying magnetic features. Alternatively the variable results may have been a product of different fill compositions in the ring ditches in each of the fields.

- All three survey methods failed conclusively to map any features of the 'Woodhenge' monument.

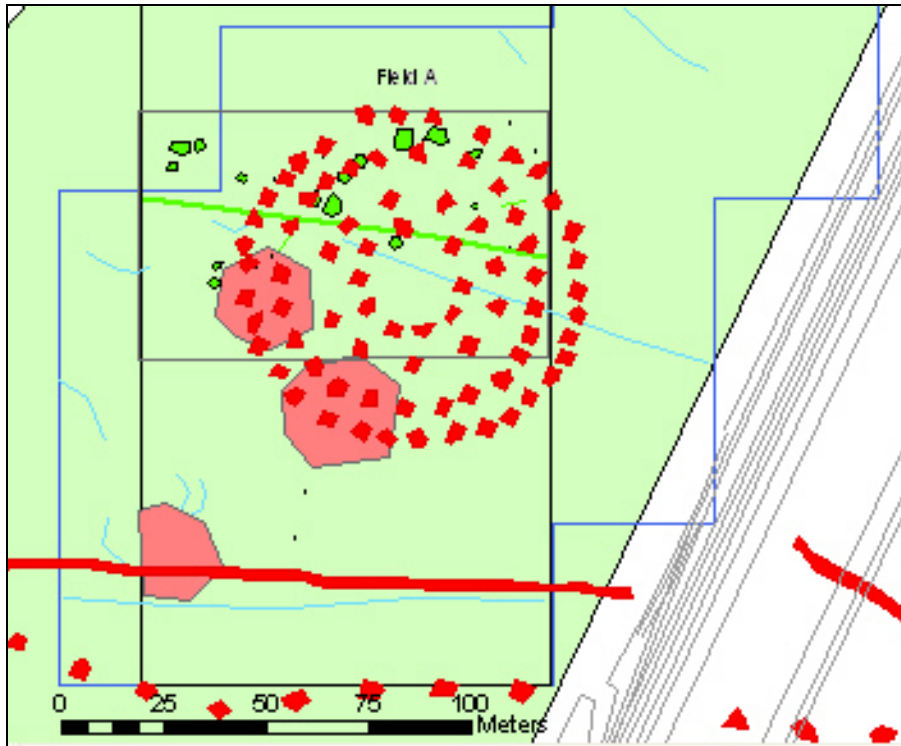


Figure 10. Phase I geophysical survey interpretations for the 'Woodhenge' monument. GPR (green), resistance (pink) and magnetic (blue).

Examination and rectification of oblique aerial photographs relocated the 'Woodhenge' feature. Magnetic and GPR surveys do not record any obvious archaeological anomalies in the newly positioned location of the 'Woodhenge' monument. The area of high resistivity that is in this area is most likely geological in nature.

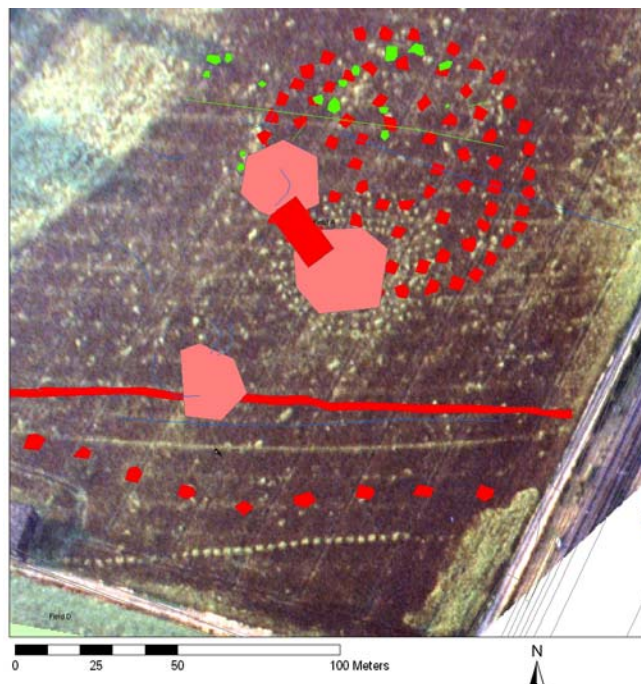


Figure 11. Re-assessment of the correct positioning of the cropmark data positions the 'Woodhenge' feature over a probable geological resistance anomaly.

Location of the 'Woodhenge' monument could have failed for a number of reasons:

- Physical properties: The features of the 'Woodhenge' may have been too small to be located with the sampling methods utilised in this survey.
- The properties of the 'Woodhenge' monument were perhaps not detectable with the techniques employed.
- The sampling methods utilised for data collection may not have been robust enough for these types of features.
- The archaeological features may have been severely damaged by past and/or contemporary land-use.

Answers to these questions could only be achieved through further geophysical survey data analysis, additional geophysical survey, soil analysis and excavation.

4.0 Phase II Geophysical Survey at Catholme

Phase II investigations provided the opportunity to continue the geophysical research in the 'Catholme Ceremonial Complex'. This work sought further to investigate areas of interest brought to light in Phase I, in order to better understand the relationship between the survey data, archaeology and soil properties, as a means to enhance the interpretation of survey results and as a guide to future best practice.

The bulk of survey work which was undertaken at Catholme produced varied results. Some clearly showed well-defined anomalies closely corresponding to the cropmarks. Other results, however, showed weak or indistinct anomalies corresponding in part to known features, although with some not represented at all.

4.1 Site Selection and Justification

Six areas were selected for ground truthing which focused on the three principal monuments of the 'Catholme Ceremonial Complex'. Three of these areas measured 20m x 10m and three measured 10m x 10m. In order to limit disturbance to the monuments these were the minimum believed necessary to achieve the project aims.

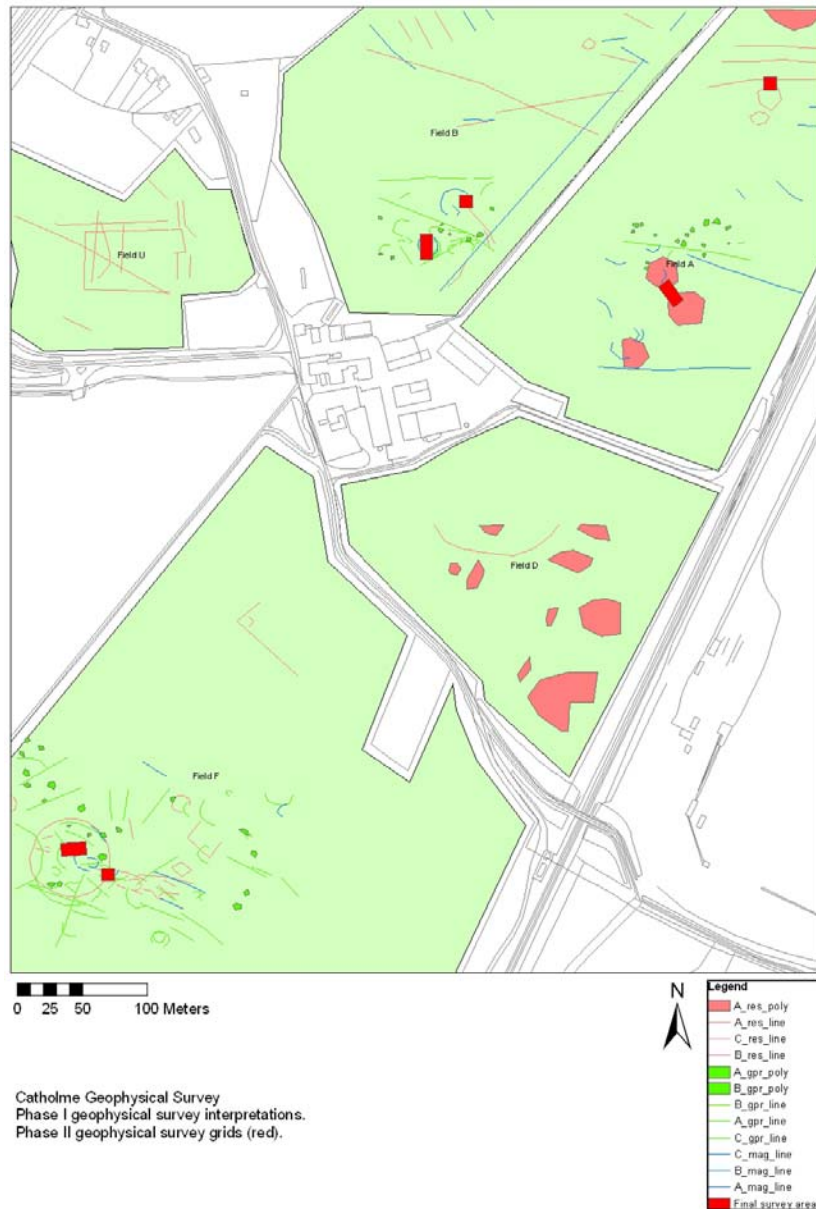


Figure 12. Phase II WRM geophysical survey areas as red blocks.

Detailed geophysical surface surveys were undertaken in each target area using multiple techniques, as described below. Following the surface survey the topsoil was removed, and detailed geophysical survey repeated. Four 2m x 5m sub-areas were then selected over archaeological and geophysical features of interest. Further geophysical measurements, along with measurement of soil properties and sampling for laboratory analysis was conducted in these smaller sub-areas.

4.1.1 Area A1

The survey area in A1 was positioned over one of the pit-alignments that cross the WRM landscape. The pit-alignment was mapped in Phase I of survey at Catholme along with two other linear features to the north of the pit alignment. With consideration of the inaccuracy of the cropmark map, Area A1 was positioned over the linear feature that continues into Field B to the west.

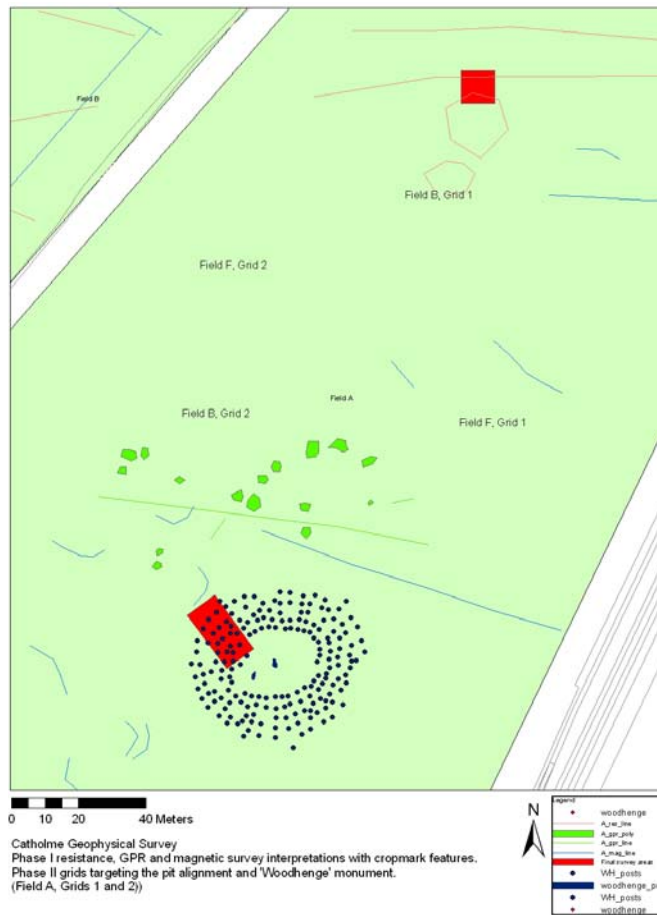


Figure 13. Phase II Field A area locations. A1 is in the north and A2 in the south.

The objective of this investigation was to establish the location of the pit-alignment and to investigate the properties of the pit fills, along with other potential archaeological features and the surrounding gravels.

4.1.2 Area A2

The area of the 'Woodhenge' had a number of GPR and resistance anomalies which were thought to correspond with the cropmark.

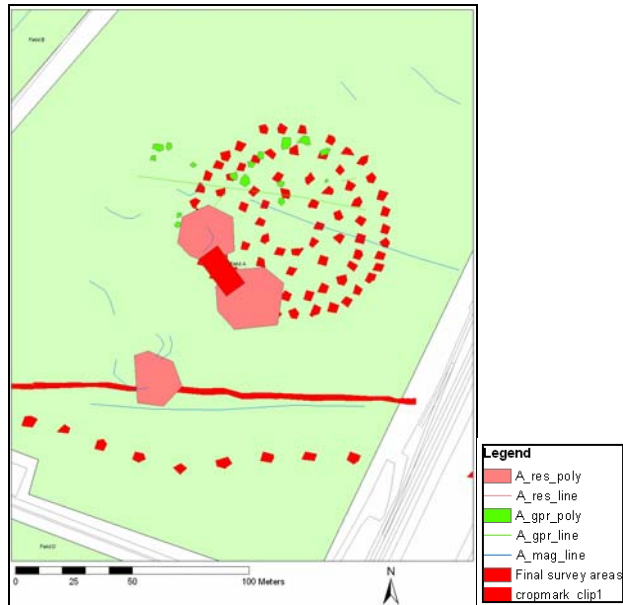


Figure 14. Phase II survey area selected to investigate the 'Woodhenge' feature in Field A.

For the best placement over this feature, the oblique aerial photograph was rectified to the project GIS. The results of this rectification altered the supposition that hitherto mapped geophysical anomalies may have corresponded to the 'Woodhenge' monument. The correct location of the cropmark meant a shift of between 17m - 53m, with the 'Woodhenge' altered in size to 47m in diameter.

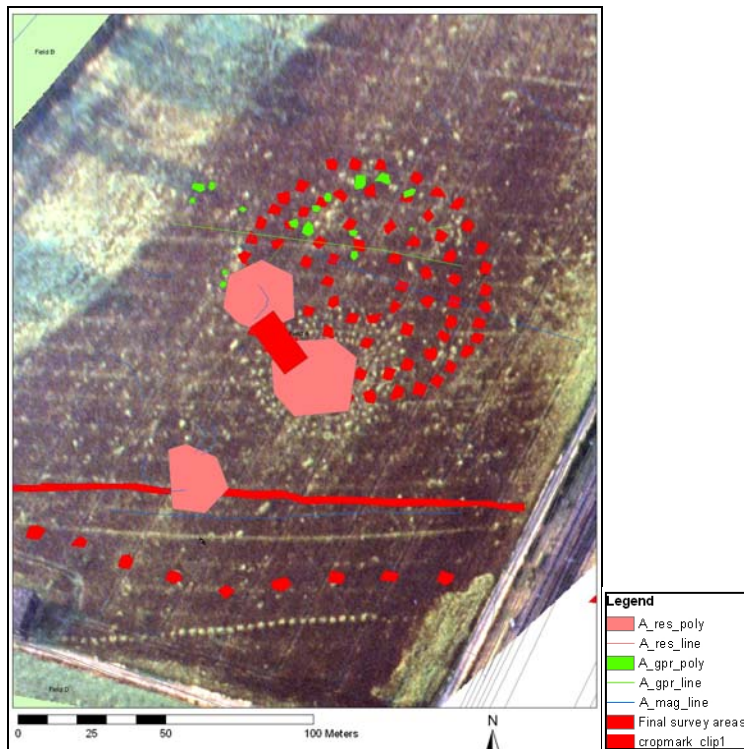


Figure 15. Rectified oblique aerial photo with 'Woodhenge' cropmark, Phase I geophysical interpretations and overlain operating cropmark GIS layer.

The location of the 10m x 20m area was established over the northwestern edge of the 'Woodhenge' monument. The aim was to attempt an assessment of the monument, in

terms of its archaeological structure, and to gather information about its geophysical and geological properties.

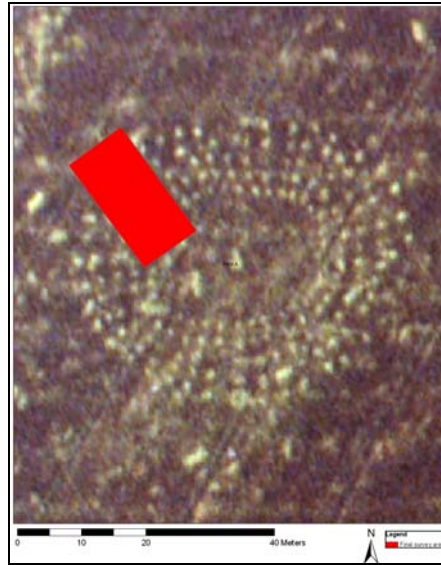


Figure 16. A2 positioned over the north-west section of the 'Woodhenge' cropmark.

4.1.3 Area B1

The 10m x10m area in Field B was selected in order to investigate the potential location of a possible outer ring of a double ring ditch which was identified as a cropmark across the northern section of the 'Sunburst' monument. B1 was established over an area which corresponded to known cropmarks and an area of low resistivity. A semi-circular magnetic anomaly occurred at the same location. The area was established in order to sample anomalies from the resistivity and magnetic surveys to attempt to understand the causes of anomalies and the archaeological potential of the cropmark at this location.

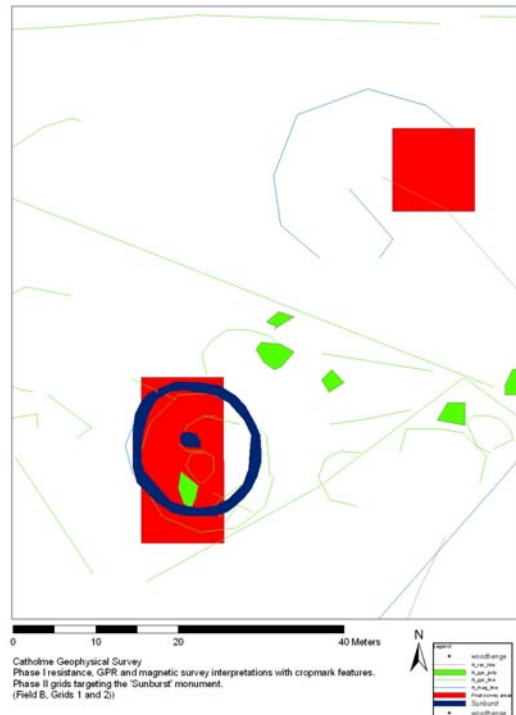


Figure 17. Phase II survey areas in field B.

4.1.4 Area B2

The second area measured 20m x 10m and was established at a location where magnetic and GPR anomalies corresponded with the ‘Sunburst’ monument (Fig. 17). Both magnetic and GPR data revealed a ring ditch and various anomalies within and surrounding the ditch. The area was positioned with the intention of mapping the ring ditch from both the interior and the exterior. The strong magnetic and GPR anomalies at the centre of the ring ditch and immediately east of the centre were also important targets for assessment.

The aim was to understand the nature of the magnetic and GPR anomalies. Equally important was the intention to assess known cropmark features which were not identified in the geophysical results, such as the radiating pit-alignments of the ‘Sunburst’ monument, and to determine why the resistivity survey failed to locate the ring ditch here in Field B when it clearly did so in Field F.

4.1.5 Area F1

The cropmark in Field F was mapped successfully with GPR and resistivity techniques. The magnetic survey revealed only the vague outlines of the ring ditch and radiating linear features. Due to the size of this monument, measured at approximately 60m in diameter, with associated linear features extending a further 80m to the southeast, the placement of both ground truthing areas was very important.

Area F1 measured 10m x 10m and was located directly over the ring ditch at a point where the two extending linear features appeared to cross the ring ditch. The previous survey results produced extensive anomalies within and surrounding the ring ditch and the linear features. The area was located with the intention of investigating the

ring ditch and its properties, as well as those of the linear features. In addition, an assessment of additional archaeological and geological features was undertaken.

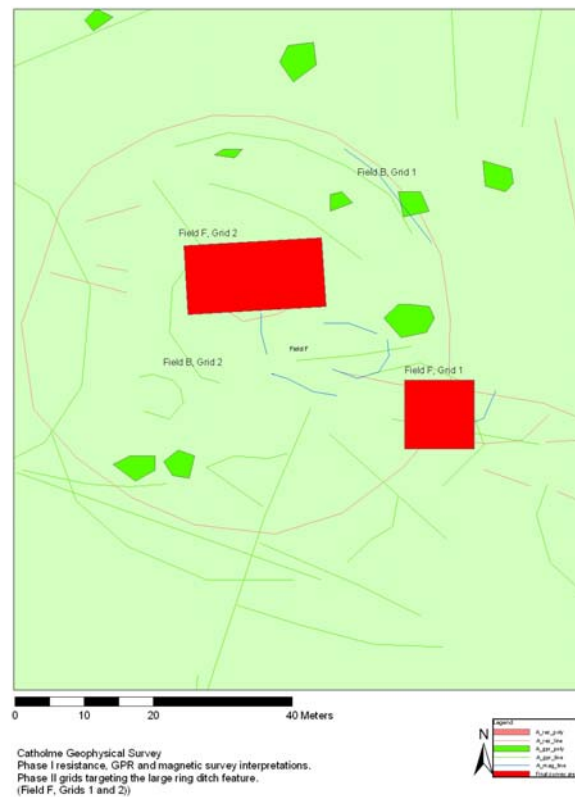


Figure 18. Field F area positions focused on anomalies defined through Phase I geophysical investigations.

4.1.6 Area F2

Area F2 measured 20m x 10m and was located in the interior of the ring ditch at a point of distinct overlapping resistivity and GPR anomalies. The cause of these anomalies was unknown, but was suspected to represent some form of activity, structure, or other anthropogenic feature located within the confines of the large ring ditch. The investigation sought to assess the possible significance of the archaeological and geophysical anomalies within this area.

4.2 Geophysical Survey Area Mapping and Data Collection

All the survey areas were selected after careful consideration of Phase I geophysical survey results, past geophysical and archaeological investigations in the Full Area, aerial photography and cropmark information. Once the Phase II survey areas were established and justified, they were plotted in the project GIS. Files were generated in order for accurate (± 2 cm) GPS location in the field. A Leica 500 series differential GPS unit was used to establish the areas. Geophysical survey grids were set directly on the established corners of each area.

All geophysical data were collected on the basis of guidelines set out in the project design. Data collection was conducted in three main stages: at the modern surface, at the surface of the natural subsoil and in each of the 0.2m spits of the four 2m x 5m sub-areas.

4.2.1 Magnetometry Data Collection

The vertical gradient of the vertical magnetic field was collected with the G858 cesium vapor magnetometer with a sensor spacing of 1m, positioned at 0.3m from the ground surface. Samples were collected every 0.2m across the survey area. Data were collected through manually triggered readings following a uni-directional survey grid. This enabled accurate sensor position and orientation (vertical) for the best quality data.



Figure 19. G858 Cesium Vapor magnetometer (right) in vertical gradient mode and the FM256 Fluxgate Gradiometer (left).

A remote magnetometer station collected a single total field of magnetic field strength at regular intervals of 1 per second at a fixed position significantly distant from the area and all project activities. Areas A2, B2, F1 and F2 were also surveyed with the FM256 fluxgate gradiometer on the surface of the natural subsoil (and in F1 and F2,

also on the modern surface). Data were collected with a sampling interval of 0.125 m along transects spaced at 0.25m apart.

4.2.2 Magnetic Susceptibility

Magnetic susceptibility data were collected with the Bartington MS2 susceptibility meter. Data were collected manually, values recorded by hand and later entered into digital spreadsheets. Magnetic susceptibility data were collected at 0.5m sample intervals across the survey area.



Figure 20. Magnetic Susceptibility data were collected with the Bartington MS2 susceptibility meter.

4.2.3 2m x 5m Sub-area Magnetic Susceptibility

Magnetic susceptibility data were collected with the Bartington MS2 susceptibility meter. Data were collected manually, values recorded by hand and later entered into digital spreadsheets. Magnetic susceptibility data were collected at 0.2m sample intervals across the 2m x 5m sub-area along strips at 0.2m depth from the ground surface to the terminus of archaeological features.

4.2.4 Resistivity Data Collection

Resistance data were collected with the RM15 resistivity meter and converted to resistivity data for analysis. Data collection employed the RM15 multi-plexer which enabled multiple depths to be recorded at each position. The resistivity array comprised 6 probes at a spacing of 0.25m. Six readings were collected at each array position at 0.25m, 0.5m, 0.75m, 1m, 1.25m and 1.5m. Data were collected along a uni-directional survey grid with a 0.25m sample spacing.

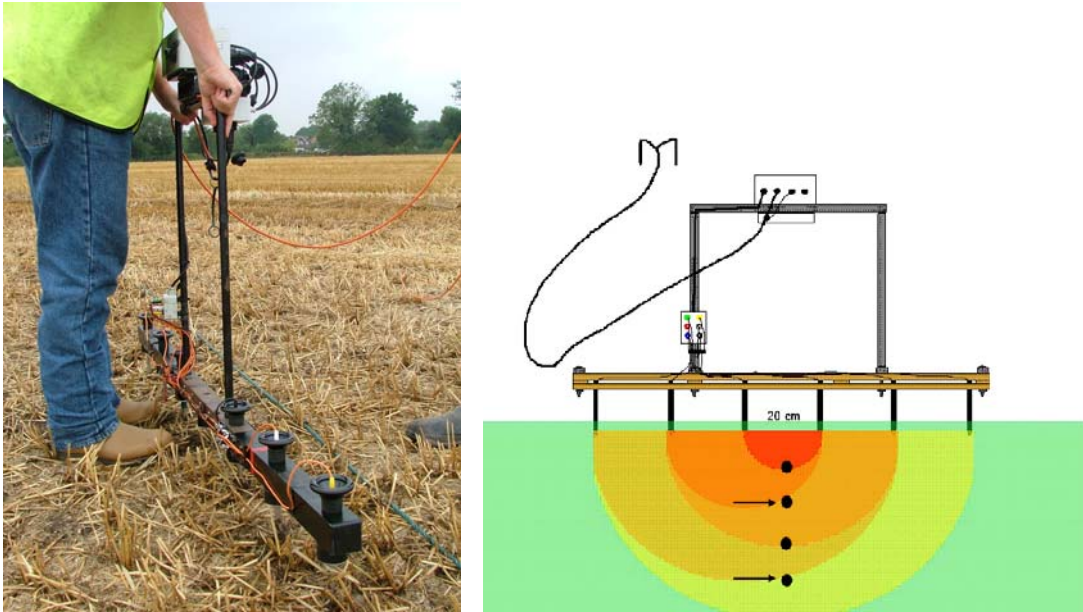


Figure 21. RM15 resistivity meter configured to collect readings at multiple depths across the site. The second image illustrates the basic premise behind this multi-plexing technique.

4.2.5 2m x 5m Sub-area Resistivity Data Collection

A specially built square array was used to collect resistivity data in the 2m x 5m sub-areas. The square array had 6 probes at 0.25m spacing that enabled the collection of 2 positions of data per array position. Data were recorded with the RM15 multi-plexer unit collecting the α , β and γ readings at each position. The α value is used in this report. Data were collected at 0.25m spacing across the grid.

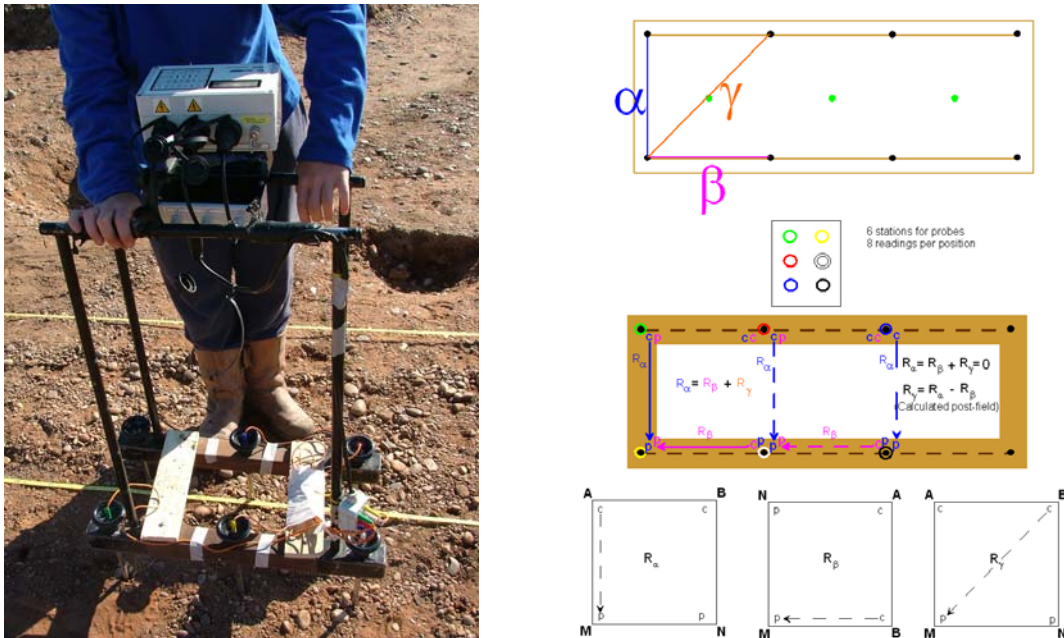


Figure 22. Data were collected using the RM15 resistivity meter on a custom-designed square array. Three data samples were collected at each station: α , β and γ .

4.2.6 GPR Data Collection

GPR data were collected with the SIR3000 GPR system using a shielded 400 MHz antenna. Data collection was regulated with a survey wheel ensuring a regular and measured record. Basic high pass and low pass vertical filters were set according to each survey area. Because of potential gain issues encountered in the Phase 1 survey (see Watters, *forthcoming*) a 2 point linear gain was set to ensure consistent data across the site.



Figure 23. The SIR3000 GPR unit was used with a shielded 400 MHz antenna.

GPR data were collected along a uni-directional survey grid to an approximate depth of 2m (targeted between 1.5m and 2m in order to complement the vertical aspect of the resistivity survey). The data sampling rate was 512 samples per scan and 100 scans per metre with 0.25m transect spacing. GPR data were collected in orthogonal grids with the first oriented east-west and the second oriented north-south. There was, however, some variation west-east and south-north from area to area. Depth conversion was conducted for each survey area based on velocity data collected in each area.

4.2.7 2m x 5m Sub-area Dielectric Permittivity Data Collection

The Adek Pyrometer v.6 with a surface probe was used to collect dielectric permittivity, conductivity and temperature. Data were recorded at 0.2m sample intervals across the 2m x 5m sub-areas. Data were manually collected with a data logger.



Figure 24. The Adek Pyrometer v.6 was used to collect dielectric permittivity data in the 2m x 5m sub-areas.

4.3 Geophysical Techniques and Methodology

4.3.1 Magnetometry

Magnetic survey measures the variation of the magnetic fields of the Earth and buried features across a site. Different soils and features can be mapped through their contrasting magnetic values. Examples of features that can be detected through this process include ferrous materials, soil affected by human occupation (rubbish pits and middens with organic materials), fired materials such as kilns and hearths, tiles, bricks, and concentrations of ceramics. Differences in soil type or soil perturbation are also detected through magnetic survey enabling identification of ditches, pits, foundations, graves and other excavated features (Clark 1996).

When interpreting data for archaeological purposes we look at the gradient of the magnetic field that best reveals archaeological features. Magnetometry collects two total fields from two separate magnetometer sensors. These sensors measure the total magnetic field at their respective distance above the earth. The gradient is calculated from the two total fields and effectively removes broader scale background noise. This background noise includes larger geological trends and diurnal effects and acts as an edge filter (Breiner, 1973).

The Geometrics G858 cesium vapor gradiometer collects the magnetic total field (uncorrected for diurnal influence) at a height above the ground from which the magnetic gradient can be derived. The G858 was used in the vertical gradient mode with the two sensors mounted on a vertical staff. The sensors were arranged so that the center of the lower sensor was 0.3m from the survey surface and the top sensor was 1m from the lower sensor. An additional remote station was set to collect continuous readings on a single sensor in order to record a steady record of diurnal variations. Data were collected by a two person team, one person moving the sensor array and the second person with the computer/batter pack collecting data as discrete stations. The sensors and computer and battery pack were kept as far apart as possible to regulate and reduce any effect of the iron in the computer/battery pack array.

4.3.2 Magnetic Susceptibility

Magnetic Susceptibility measures the effect of sediment magnetisation when subjected to a magnetic field. The more magnetised the material becomes the higher its susceptibility but it is a temporary response and only possible when a magnetizing field is present. Archaeological sites may have enhanced susceptibility due to the disturbance of underlying archaeological features through ploughing or other activities (Gaffney *et al* 2003).

4.3.3 Resistivity

Resistivity survey measures the change in the resistance of the earth. The twin probe array was used in the WRM project where current and potential probes are paired on a mobile frame that measures the variation in resistance across a grid. A second pair of current and potential probes is fixed at a great distance from the area being surveyed (approximately 100m in the case of this project). With a fixed separation distance of

0.5 m, the roving probes map an effective volume of resistivity to a depth of approximately 0.75 m, measured in Ohms/m. In the case of this research data were collected at a variety of depths with different probe separation readings controlled through the multi-plexer.

Resistance effectively looks at the saturation level of the materials in the survey area, thus is sensitive to soil compaction, soil type, geological features and objects that may be buried with in the soil. Resistance survey can map features that include pits, trenches, foundations, compacted or disturbed surfaces, and changes in soil type (Clark 1996).

Resistivity data were collected with the multi-plexer in order collect information across the site at different depths. Resistivity survey samples at each position across the site and at each depth are influenced by the surrounding soils. This method sends an electrical current into the earth and records the resistivity value for a volume of earth controlled by the probe separation distance. For example, if the twin probe spacing is 0.50 m, a resistivity value for a volume of earth measuring approximately 0.50m from the central point of the frame is recorded.

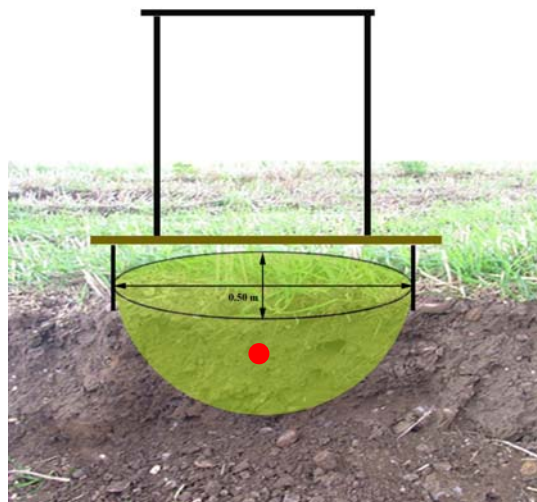


Figure 25. Resistivity data samples a volume of earth dependent upon probe separation distance.

The wider the probe spacing the deeper the penetration with a larger volume of earth sampled. The deeper the sampling, the more interference is potentially introduced to the resistivity record because the sampling is recording the resistivity representative of the entire volume of earth. Features closer to the surface have an effect on the deeper readings. This is important to keep in mind while interpreting deeper resistivity anomalies.

A good example of this effect can be seen in the resistivity data interpretation section of this report for area A1. Data collected at different depths with the multi-plexer can be assembled into vertical profiles called pseudosections that are graphic plots of measured resistivity. In order to assess the true resistivity at each depth, pseudosections must be inverted to remove artefacts introduced by the data collection method.

Due to time constraints all resistivity data are presented in this report as plan views. Preliminary pseudosection inversions have been tested over area A1 in order to prove the necessity for more effective data assessment.

4.3.4 GPR

GPR maps the form of contrasting electrical properties (dielectric permittivity and conductivity) of a soil or other materials below the ground surface. The stronger the difference between the electrical properties of two materials, the stronger the reflected signal in the GPR profile. The conductivity of soils and buried features causes the attenuation, or loss, of the GPR signal that impacts the effectiveness of GPR survey. Though a highly conductive material will attenuate the GPR signal, it can also be an effective mapping tool contributing information to the nature of the subsurface and features within it. (Daniels 1996, Conyers and Goodman 1997)

GPR records information on the amplitude, phase and time related to the capture and induction properties of the antenna in addition to the energy propagation, scattering and reflection off of subsurface features. Unlike resistivity or other archaeological-based geophysical methods, GPR data are collected as 2D vertical profiles into the earth. The 2D profiles are made up of a number of traces (or scans) at a particular location (x, y) that record the response of sub-surface properties to the radar's electromagnetic wave at discrete points at a particular time (or depth) in the earth. The horizontal axis represents surface distance along a transect with the vertical axis recording time (often referred to as two-way travel time.) The time is recorded in nanoseconds (ns). Time can be easily converted to depth in two ways: the first is by having a known dielectric permittivity value for the material in the survey area, the second through having a known depth to a feature that appears in the radar profile. The more accurate of these two methods is the latter but this requires digging or coring. It must be kept in mind that earth properties are not constant and can change drastically over an area. Depth conversion should be checked at intervals across a site if possible.

When considering feature resolution, differences are best viewed based on a relative scale. The outline of features may be identified at the lowest resolution and individual features such as bones and artefacts within for example, a grave, may be imaged at the highest resolution (to date, no conclusive research has been conducted that has positively imaged bones within a grave, although Watters and Hunter *in press* propose a method through which this may be possible). GPR is easily adaptable to these different scales because of its range of antenna frequencies. These frequencies range between 10 MHz and 1.5 GHz with the lowest frequencies used to map geological and environmental targets with a typical penetration of approximately 30m. The highest frequency, 1.5 GHz, will effectively penetrate to about 1.5 – 2m in basic, dry loamy soils but often much less, particularly in wet, clay-rich material. The deeper penetration achieved with lower frequency antennas provides a coarser resolution while the finest feature resolution is achieved with higher frequency antennas (but with a limited depth penetration). The most suitable antennas for archaeological feature location and detailed imaging are the 200, 400, 900, and 1500 MHz antennas. This group provides a range of depth and resolution flexibility.

GPR Data Viewing and Imaging:

GPR data are collected along a grid as vertical slices into the ground. Grid lines (transects) are collected in parallel lines typically spaced 0.5 to 1m apart. Due to the form of the beam of radar wave propagation into the earth, survey transects are most effective if oriented perpendicular to known archaeology. To record the most information on buried features, data can be collected orthogonally, or on a grid with perpendicular transects.

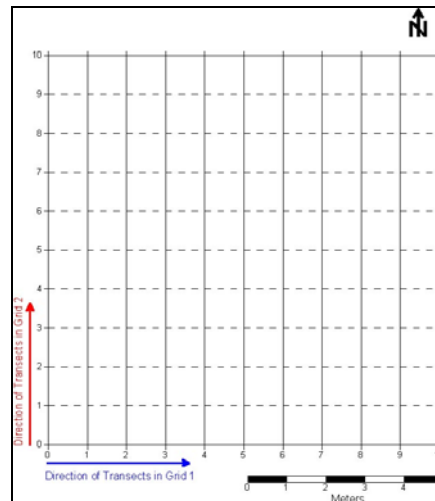


Figure 26. Orthogonal grid display.

Initial data review is conducted on these vertical profiles. Anomalies can be identified in individual profiles. Time slicing enables anomalies from individual profiles to be merged in order to view plan maps of the GPR data in a similar format to magnetic and resistivity data.

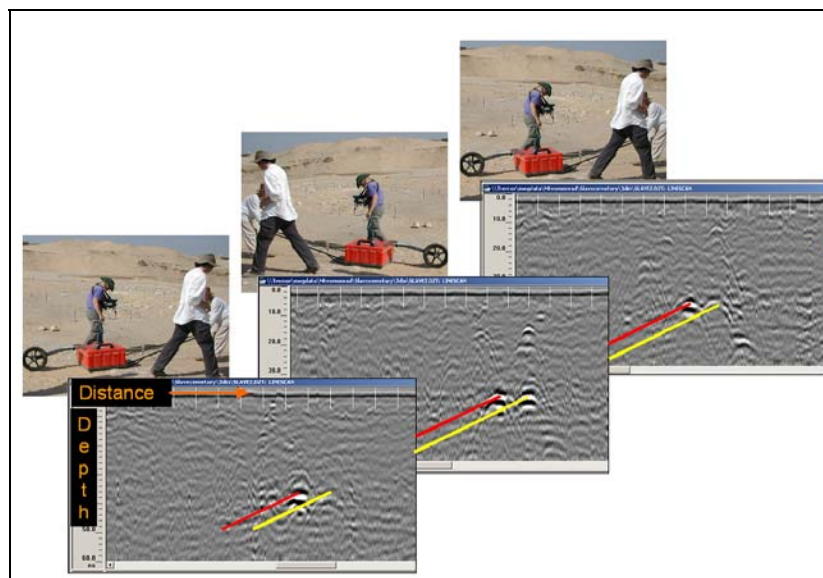


Figure 27. Vertical profiles can be stacked together to create a 3D cube of information for use in data imaging and analysis.

Time slicing is when the vertical slices are stacked next to each other and the data interpolated to form a cube. This cube is then sliced on the horizontal plane to create plan views of the area. As GPR data records the nature of the subsurface to a certain

depth, a number of time slices can be created that depict the nature of the subsurface at given depths. Further assistance in feature mapping can be achieved through displaying all three axes of the GPR cube x, y, and z. This helps define feature shape and volume.

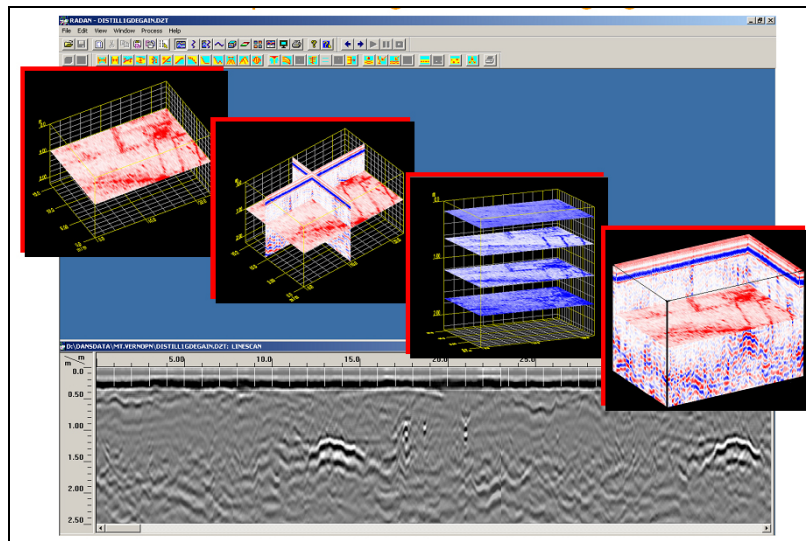


Figure 28. GPR data can be displayed as 2D vertical profiles (greyscale at the bottom of the figure), or sliced along the x, y, and z axes.

Each area surveyed with GPR during the WRM project was reviewed in both vertical profile and plan views. Each area is represented by a selection of plan views in the GIS which best represent the nature of the sub-surface. Images included in this report are time slices for each area that best represent the archaeology, whilst not depicting all features. The images with interpretations include interpretations from every time slice in the GIS for an overall depiction of identified features.

4.4 Geophysical Data Processing and GIS Integration

All geophysical data were processed in proprietary software. After data were processed they were converted to .tif formats for rectification into the GIS. The steps listed below for each geophysical survey method are basic techniques employed in the process of data analysis. A thorough assessment and study of the geophysical data went beyond the listed techniques to present end results of high confidence.

4.4.1 Magnetic Data Processing

1. The G858 data are adjusted for grid orientation and during data export corrected for diurnal influence with data from the base station.
2. Data are then sorted in Surfer according the field strength and the outliers clipped from the file.
3. Data are gridded and imaged as contours or images in Surfer.
4. Data are exported as .tif files for input to the GIS.

FM256 magnetic data processing:

1. FM256 data are filtered to remove any background noise, de-spiked and clipped of data outliers in Geoplot.
2. Data are then interpolated along the y axis to generate an equally spaced data sample.
3. Data are exported and imaged as contour files or images in Surfer.
4. Data are exported as .tif files for input to the GIS.

Magnetic susceptibility data processing:

1. Data are converted to digital format and gridded in Surfer.
2. Data are exported as .tif files for input to the GIS.

Post processing software for data analysis and interpretation included Magmap2000, Geoplot 3.0, Surfer 8, and ArcGIS 8.3.

4.4.2 Resistivity Data Processing

1. The RM15 data are filtered to remove any background noise, de-spiked and clipped of data outliers in Geoplot for each layer of data.
2. Data are then converted to resistivity and exported and imaged as contour files or images in Surfer.
3. Data are exported as .tif files for input to the GIS.

Post processing software for data analysis and interpretation included: Geoplot 3.0, Excel, Surfer 8, and ArcGIS 8.3.

4.4.3 GPR Data Processing

1. GPR survey transects are compiled into 3D cube format in RADAN.
2. Data are processed to adjust for the correct time zero, gain adjustment and migrated. If it was necessary, additional vertical and horizontal background removal filters were applied.

Note: the Catholme GPR data was mostly very clean and needed little data processing other than time zero adjustment and migration. A Hilbert transform

function was also applied to all the GPR data and data fully investigated for the best end results.

3. Data are then viewed and exported as plan views (or time slices) from the 3D cube as .csv files.
4. The .csv files are converted to .dat files and gridded in Imagine to create .img files that are exported as .tif files for input to the GIS.

Post processing software for data analysis and interpretation included RADAN 6.0.0.1, Erdas Imagine 6.0, and ArcGIS 8.3.

4.4.4 GIS Data Integration

During Phase I of the WRM project a GIS was created to manage, analyse and present the breadth of information utilised in the study. This encompassed airborne data including aerial photography and LiDAR, ground based Ordnance Survey and geological maps and geophysical survey maps and data interpretations.

A separate geophysical data GIS has been maintained and expanded to include all of the geophysical survey results from the Phase II investigations. This GIS is the core organisational tool for the huge amount of data which was collected throughout the WRM project. The layers in this GIS include: OS base maps, the Full Area LiDAR and aerial photographic surveys, the oblique ortho-rectified photograph over the 'Woodhenge monument, all the geophysical survey maps and interpretations from Phase I and all the geophysical survey maps and interpretations from Phase II. Not only does the GIS enable data management, it is a powerful tool for data assessment and analysis especially following the integration of the archaeological database and results from the soil sampling studies.

4.5 Geophysical Data Interpretation and Classification

All data have been processed and imported into the project GIS. Data interpretations are based on the author's knowledge of geophysical survey methods, predicted results, and site specific archaeology and geology. Due to the visual nature of geophysical data as well as the more complex 3D component of GPR data, all interpretations presented are the culmination of intensive and exhaustive examination in a number of forms.

Data interpretations and classifications are based not only on the identification of possible archaeological features in the geophysical data, but look deeper into the data in an attempt to gain greater insight into the geophysical properties of the archaeological features and their surrounding environment. This detailed interpretation is meant for integration with the results of the archaeological excavations and soil analysis.

In an attempt to keep geophysical data classifications consistent throughout, a relatively simple scheme is presented which identifies geophysical properties by levels of intensity or strength. These are high, medium high (med-high), medium-lowb (med-lowb), medium-low, low and, for magnetometry, dipole.

Not all categories are used on every site. The reasoning behind this is:

- High and low are the strongest values that appear as distinct black and white anomalies.
- med-high is a dark-grey but not black.
- Med-highb is mid -grey at the centre of the black and white scale.
- med-lowb is more to the white end of the grey spectrum (but not as light as med-low)
- Med-low is light-grey but not white.
- In the case of magnetometry, dipole groups the high and low parts of dipole features - not all black/white contrasting areas are identified as dipoles, as is evident in the case of B2, the southern part of the ring ditch is not identified as a dipole.

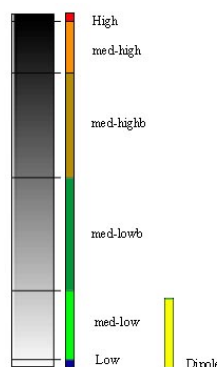


Figure 29. Greyscale division for magnetic interpretation labeling.

The variation between med-high, med-highb, med-lowb, and med-low in the magnetic data is to have distinct values that define features. As can be seen as an example in

the B2_g_FM256 interpretations, the ring ditch is identified mostly as a medium-low feature, containing areas of low, and bordered by areas of med-high and high magnetic field strengths.

These differentiations are done with the thought that the actual soil properties are responsible for the signature in the geophysical data. The intent is not to simply identify the 'ring ditch', but to identify differences in the strength of the geophysical anomalies recorded irregardless of their match to a larger archaeological feature.

In addition to data strengths, data are classified in the GIS according to which data sets contain the interpretations - surface or gravel - and also the depth layers for each of the interpreted anomalies. This type of classification is done in order to create a fully analytical database, one that can be queried not only on geophysical method type, but field strength, surface or gravel survey and, where appropriate, the approximate depth of the sample. This is deemed necessary because techniques such as GPR and resistivity will map archaeological features according to the method array and survey methodology. As will be seen in the cases of pits, ditches and post-holes, resulting geophysical anomalies do not always appear in the data as may be assumed.

4.5.1 General observations

Though visible in data results, plough furrows were not identified as geophysical anomalies in the interpretations. Geophysical interpretations of the data were done to specifically highlight the archaeological features and their geophysical characteristics. Occasionally, geological background features are identified in order to place archaeological features within their geological background.

Occasionally plough furrows are highlighted but mostly because sections stand out as particular contrasts to surrounding values. Because the survey areas are quite small, it is possible that isolated areas of contrasting geophysical values, whether related to plough furrows or not, may also have some relationship to archaeological features, or contribute to the value of archaeological geophysical values. For example, if one area is particularly low resistivity that may coincide with a plough furrow, it identifies an area of slower drainage or otherwise higher water retention. This, though natural, may contribute to the resistivity of underlying archaeological features.

5.0 Geophysical Survey Results

The second phase of geophysical survey at the Catholme Ceremonial Complex produced a massive amount of data. Multiple geophysical survey methods mapped the ground surface and the natural subsoil (after removal of the topsoil) in 6 designated areas. Further geophysical surveys were conducted in four 2m x 5m excavation trenches at regular 0.2m intervals.

The dense sampling rate and careful data collection were done with the intent to collect the most detailed and scientifically rigorous data examples possible. The use of multiple geophysical methods was undertaken in order to study the results of each method individually and to study the comparison of the results. Additional sampling and testing were undertaken through the efforts of Mark Hounslow and David Jordan. Results from these three main survey efforts should be integrated to the large-scale geophysical survey in order to gain the most informed understanding not only of the response of geophysical methods to archaeological features but also the relationship between the properties of archaeological features and the relationship to their surrounding environment.

The results presented below are the culmination of intensive data assessment that has been conducted throughout the project from data collection in the field, post-processing, analysis up to the present interpretations and results in this report. The process of data evaluation employs multiple software packages, processing, assessment, and interpretation and presentation methods. Final images that are put forth below are the culmination of work conducted over the past seven months. Images in the report are data images and interpreted maps exported from the GIS. Though the graphic presentation of some of the data in this format is not the best possible, the format of a GIS enables the most accessible and comprehensive organisation of data.

5.1 Area A1

5.1.1 Magnetometry Survey Results

The magnetometry survey conducted over the area of the pit-alignment in A1 was dominated by a strong dipolar feature in the northeastern section of the area. This magnetic anomaly did not have any specific shape that reflected expected archaeological features and after excavation was proved to be geological in nature. The pits of the pit-alignment were not mapped from the surface of the survey area. A few medium-low magnetic anomalies were identified in the areas of the pits, but they could not be identified as archaeological in nature. The plough furrow or ditch crossing the area from the east to west was not identified through the surface survey.

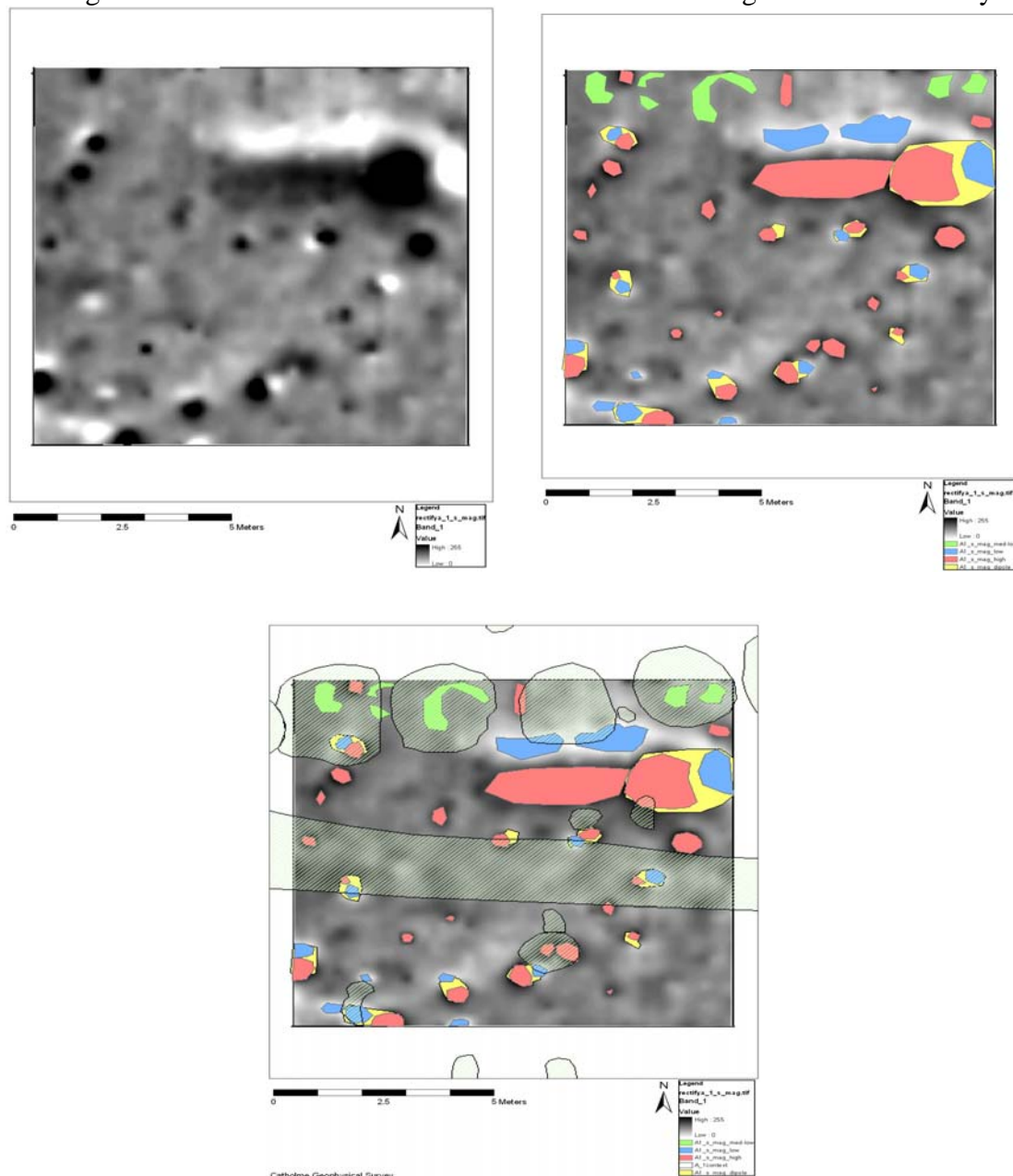


Figure 30. A1 magnetic surface survey data (top left) with interpretations (top right) and overlay excavation plan.

The magnetic survey on the natural subsoil was dominated even more than the surface survey by the strong magnetic dipole feature in the northeastern section of the area. Despite this fact, the pits of the pit-alignment were visible as weak, or low magnetic anomalies. The ditch that passes through the area could not be differentiated from the general magnetic background and patterns of the geological signature. The pit in the center of the southern edge of the area stood out as strong high magnetic anomaly.

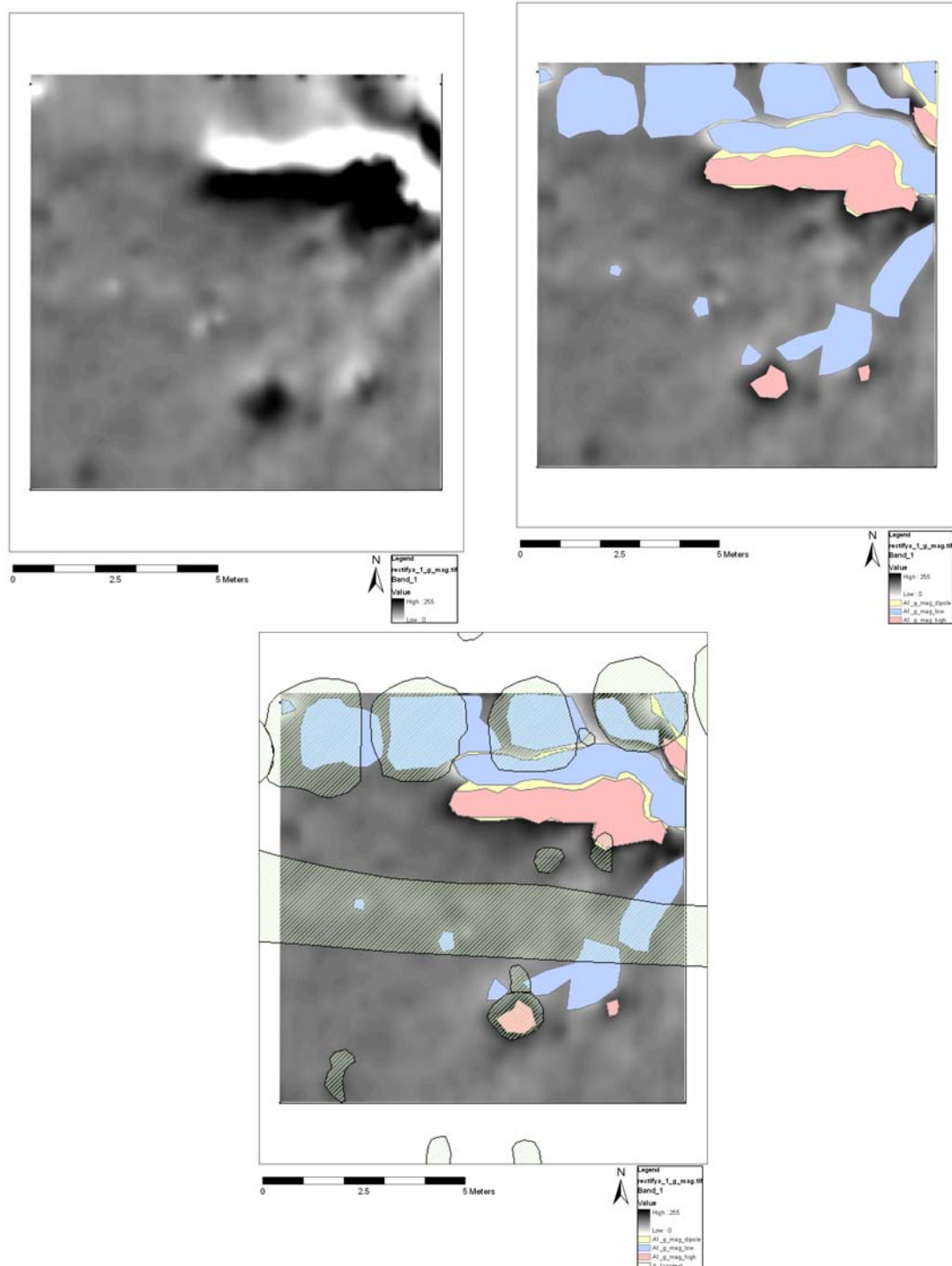


Figure 31. A1 magnetic gravel survey data (top left) with interpretations (top right) and overlain excavation plan.

5.1.2 Magnetic Susceptibility Results

Preliminary assessment of the results of the A1 magnetic susceptibility results did not show any obvious archaeological anomalies. A few linear features trending northeast-southwest were probably effects from plough furrows.

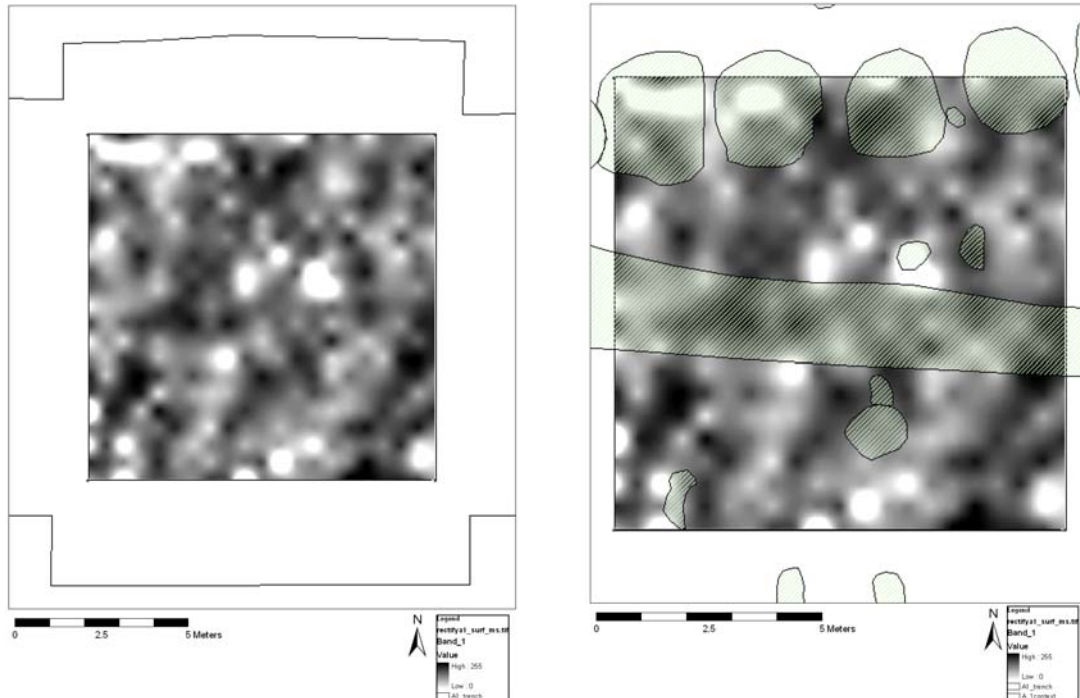


Figure 32. A1 surface magnetic susceptibility results (left) with overlain excavation plan.

The results from the gravel magnetic susceptibility survey revealed information on the archaeological features that were uncovered. Three of the pits in the pit-alignment were marked with low to medium low values and the pit features on the southern edge were also mapped as low susceptibility features. The ditch crossing through the middle of the area was mapped as a medium low feature.

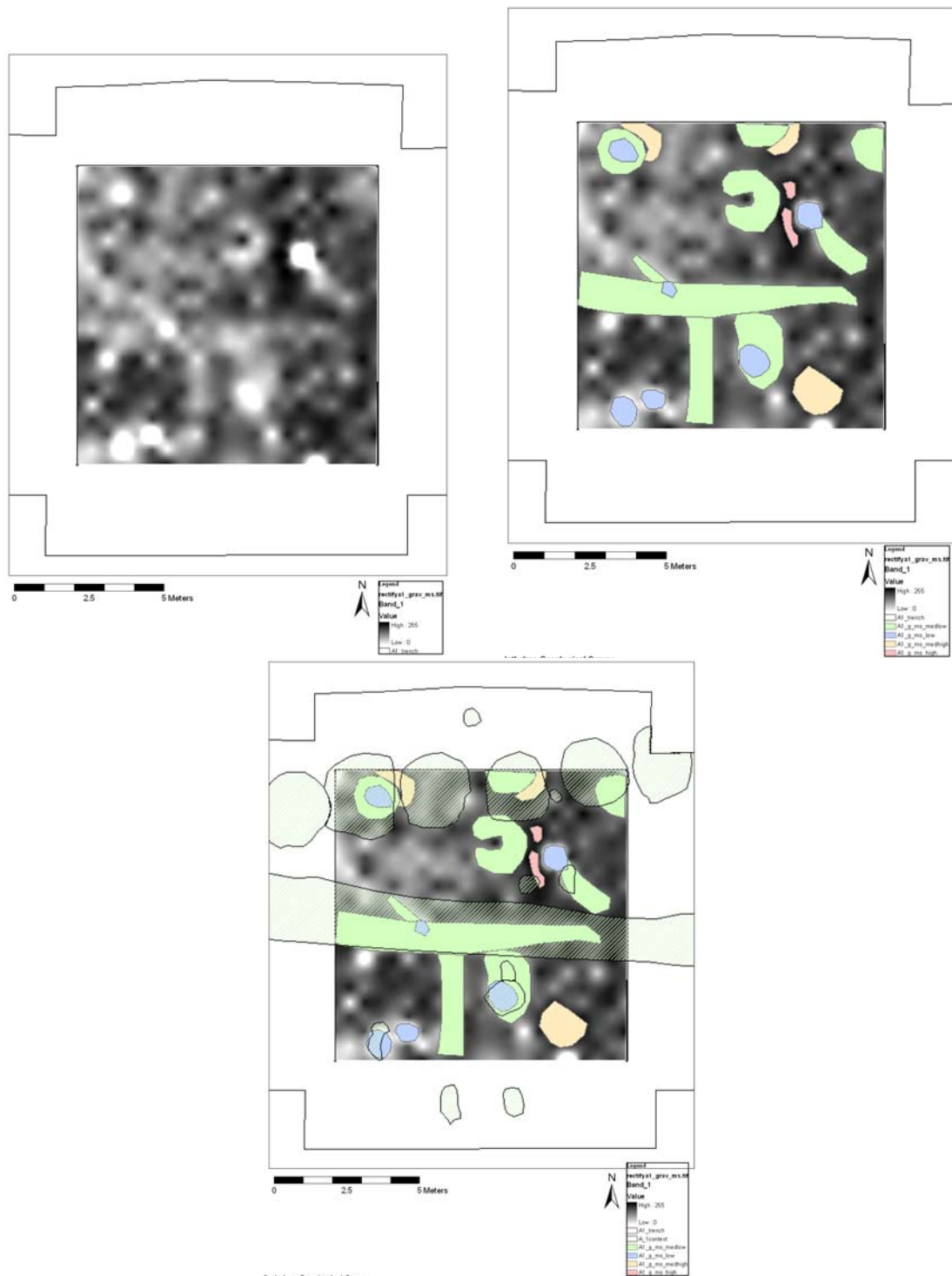


Figure 33. A1 gravel magnetic susceptibility results (left) with interpretations (right) and overlain excavation plan (bottom).

5.1.3 Resistivity Survey Results

Resistivity surface survey did not clearly reveal the underlying archaeological pit-alignment and ditch features. Plough furrows and general areas of high and low resistivity were most prominent in the surface survey data.

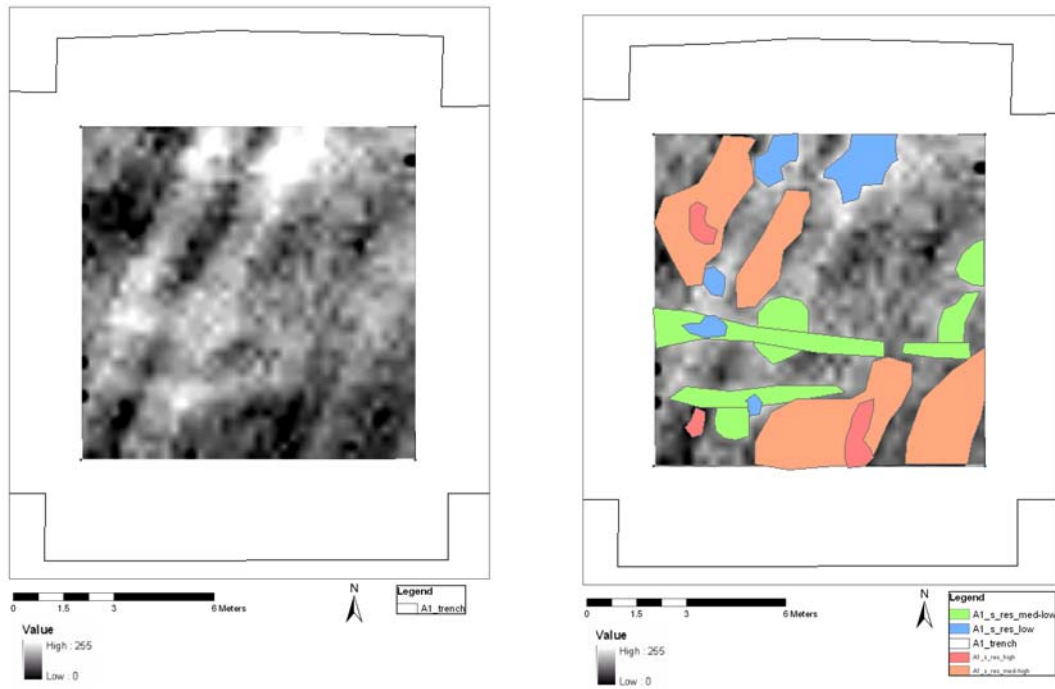


Figure 34. Resistivity survey data from 0.25m depth (left) with overlain interpretations (right).

One or two anomalies in the surface resistivity data may reflect the underlying pits of the pit-alignments. In the image below the very bright white, or low resistance anomaly in A1 resistivity level 0.50m corresponds with a pit (A) and the light grey linear feature corresponds with the shallow ditch (B) crossing the area. If background knowledge and ground truthed results were not known these anomalies would not stand out as probable archaeological features.

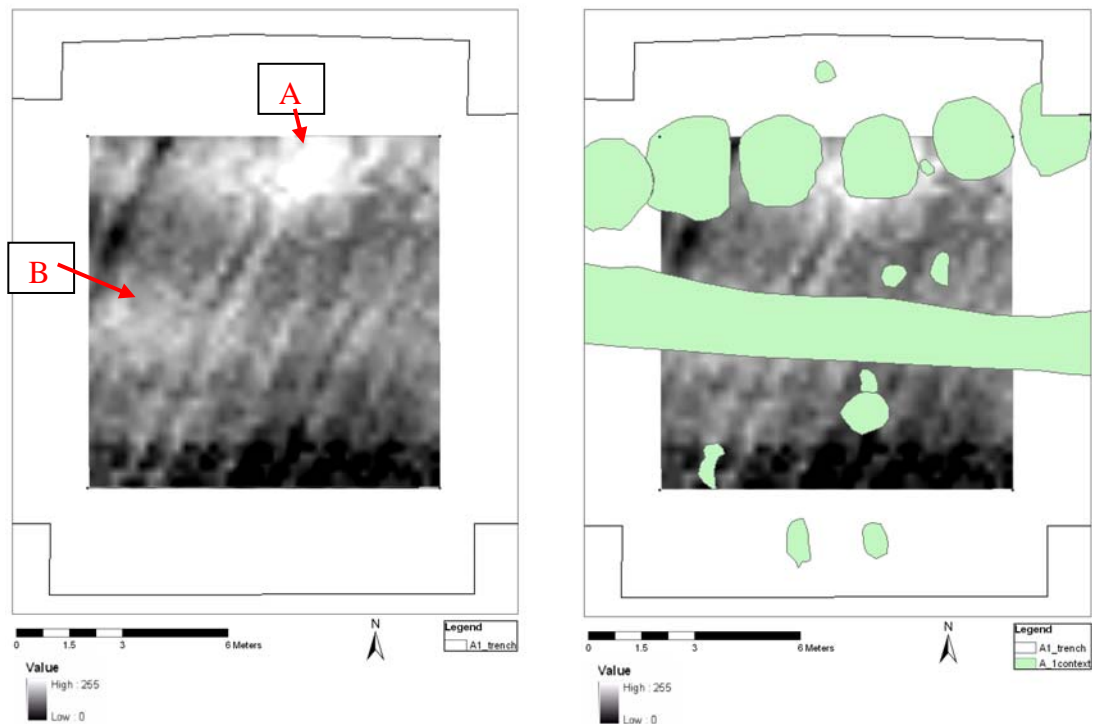


Figure 35. Resistivity survey data from 0.50m depth (left) with overlain excavation plan (right).

Despite surveying to multiple depths, the interference of the topsoil properties was significant and the archaeology was not easily mapped. If we were to rely upon just this survey, even with the high density sampling rate (0.25m x 0.25m) and multiple layers that we believe should provide more detailed information to underlying features, we would not have been able to accurately map the pit-alignment and the ditch. The criteria for identifying a feature such as a pit-alignment were to find anomalies (like the low resistivity anomaly in the above image) that may represent the pits. A pit-alignment would have multiple pits in a line, so the positive interpretation of this feature would be a repeating pattern of low resistivity anomalies. With only one high resistivity anomaly, it was not possible to identify it as a pit or as part of the pit-alignment.

After the topsoil was removed and the area re-surveyed with resistivity, not only were the archaeological features mapped, but additional information was collected regarding specific background material and archaeological feature resistivity properties. Due to the sandy gravel material in the majority of the survey areas, resistivity probe contact was difficult at times, this accounts for the missing data that are seen as black dots in some of the data layers.

The first resistivity map to a depth of 0.25m showed all of the archaeological features. The pits of the pit-alignment were low resistivity anomalies and the ditch running across the trench appeared as a medium-low resistivity anomaly. The difference between these signatures may have been that the ditch feature was much shallower than the pits, thus retained a smaller percentage of moisture. Other reasons for higher or lower resistivity values of different archaeological features were the composition of the fills that define each feature. The pits may have had a different purpose, and thus fill material, while something like the ditch across the trench may have been filled mostly with the surface plough material.

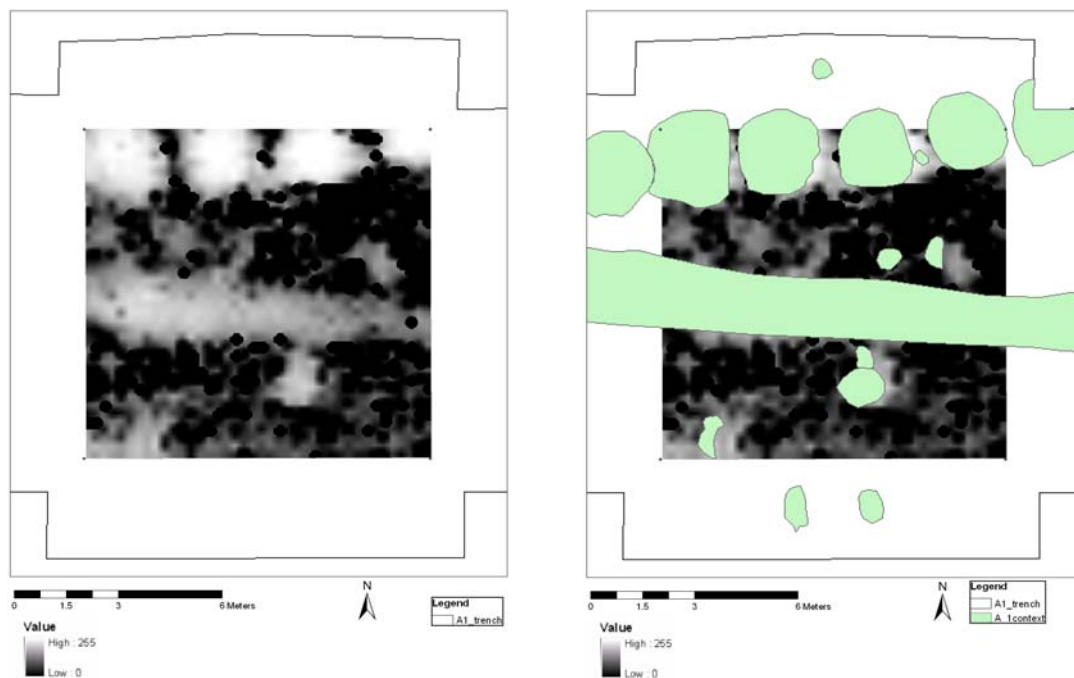


Figure 36. A1 gravel resistivity survey results at 0.25m (left) with overlain excavation plan (right).

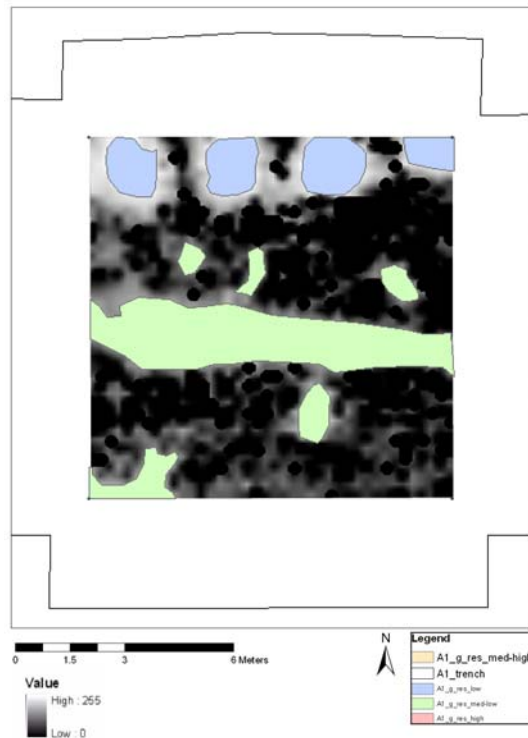


Figure 37. A1 gravel survey at 0.25m with data interpretations that map the same details as the excavation plans.

The results above were expected from the resistivity survey, as from other geophysical methods. If we can see the archaeological features, we should be able to map them by geophysical means, and if not, as in the case of the magnetic survey in this area, be able to provide an explanation.

As the resistivity maps increased in depth, it is important to keep in mind the potential introduction of artefacts from near surface features into the data. Close scrutiny of the data attempted to contribute to a better understanding of the archaeological features and their relationship with the surrounding soils but only after inversion of pseudosections could a more intrinsic comprehension of the resistivity data be gained.

Without the consideration of inverted pseudosections there is great danger of over interpreting the apparent resistivity maps. As an example, area A1 has been interpreted taking each depth of the resistivity mapping as a valid representation of the earth at that approximate depth. At the end of this section, an example of pseudosection inversion is presented which highlights that further work should be undertaken in order to gain a detailed understanding of what lies beneath the surface of our survey areas.

Example considering only apparent resistivity maps at each depth sampled:

At 0.50m depth, the pit-alignment continued to be a strong anomaly with the pits' resistance to the current passing through them slowly increases.

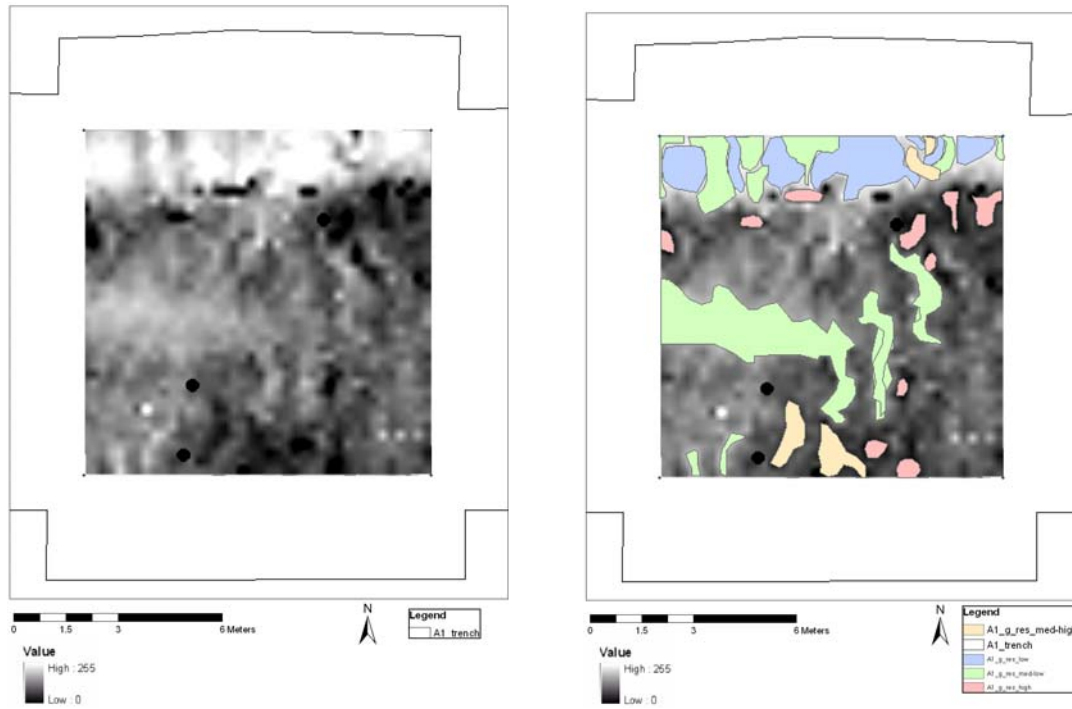


Figure 38. A1 resistivity at 0.50m depth (left) with interpretations (right).

One explanation was that the pits change in shape, becoming narrower with depth. The pits changed in the resistivity data at 0.5m and other low resistivity anomalies appeared at the same depth that did not correspond to the pit anomalies.

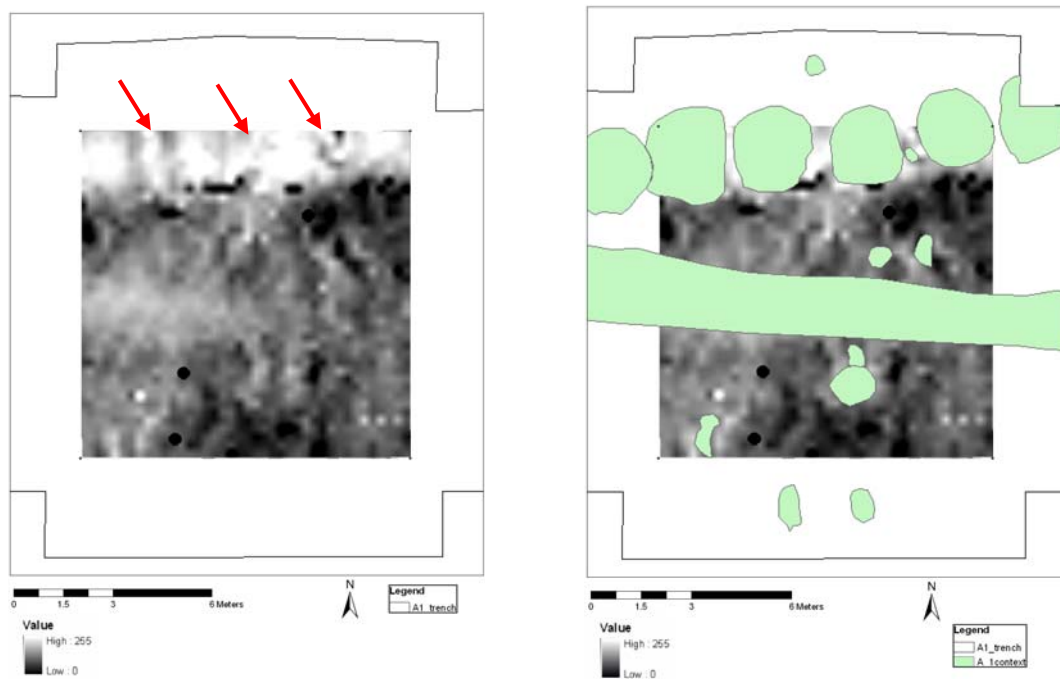


Figure 39. A1 resistivity gravel survey at 0.5m (right) with overlain excavation plans (left). The red arrows identify anomalies that do not correspond directly to the plan.

These smaller low resistivity anomalies may be mapping the actual edge of the pit where there could be a higher contrast between the saturation of the edge of the pit and the surrounding sandy gravel material of the background.

Further investigation of the data down to 0.75m depth showed the pit anomalies as higher resistivity anomalies. Some specific areas remained low resistivity. This may reflect the shape and fill of the pits in that the area toward the edges has a gradual dip (A) down toward the pit then approaches a steeper (in some cases almost vertical) dip (B) toward to bottom of the pit.

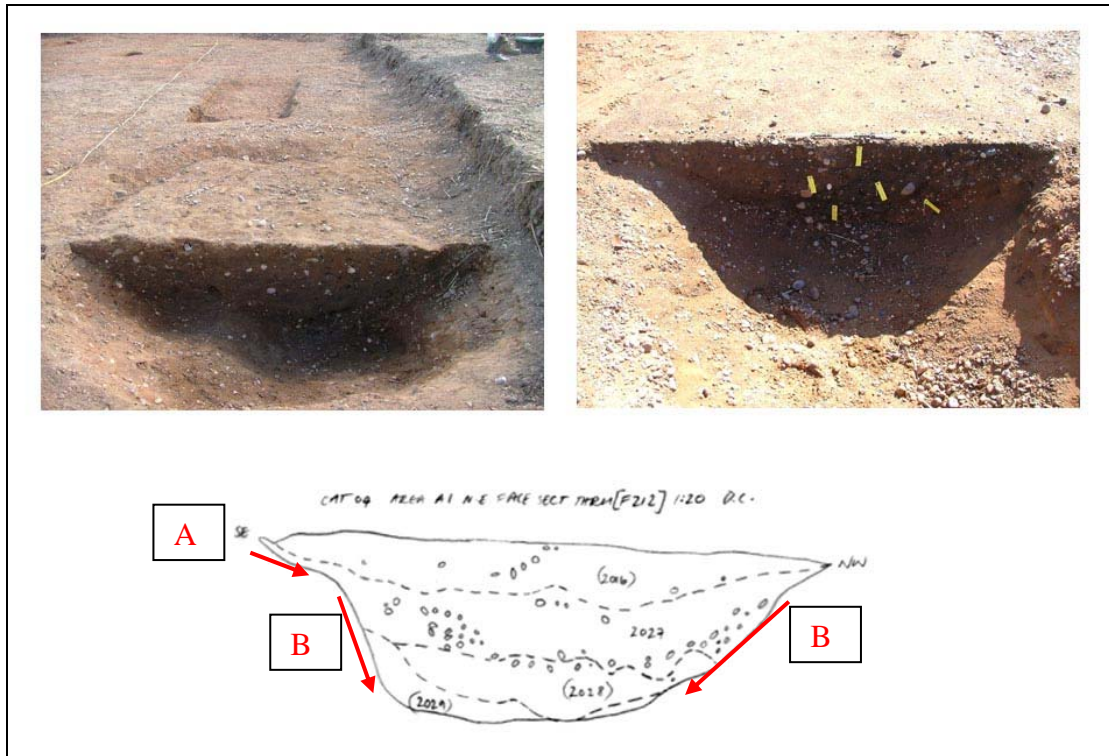


Figure 40. Two examples of pits from area A1's pit-alignment. The sketch defines F212, the pit on the eastern edge of the area.

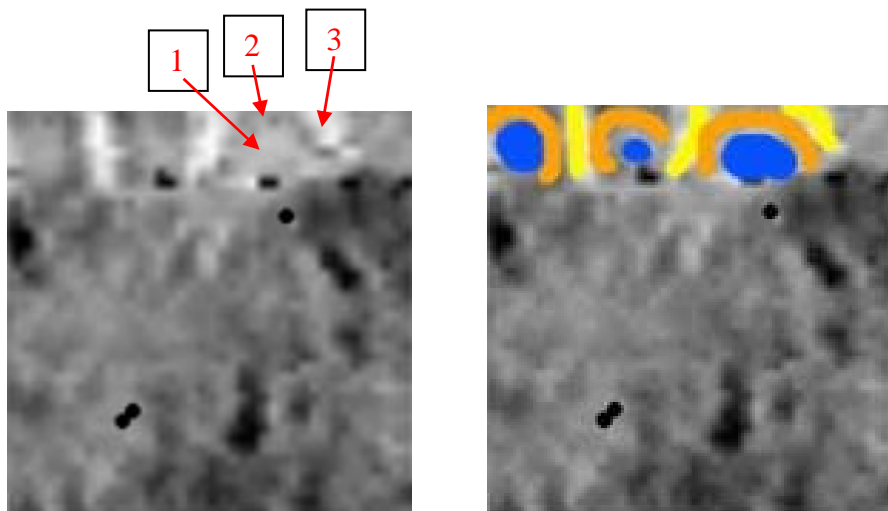


Figure 41. A1 resistivity from the gravel survey at 0.75m depth (right) highlighting possible pit structural responses to resistivity survey (right).

At 0.75m the difference between the centre of the pit as a low or mid-low resistivity anomaly (1 - blue), to the mid-high resistivity (2 - orange) again to the very low

resistivity (3 - yellow) anomalies that appear may reflect the structure of the pit and pit fill detected at each point. This might explain the low resistivity (3) at the edges where it is a stronger feature on the surface that is showing in the 0.75 level; then the higher resistivity (2) reflecting the steep dip of the pit, thus the sand-gravels having some influence on the readings at the edges of the pits, and (1) the lower resistivity at the centre of the pit actually being the reading from the mass of pit fill that again would retain more moisture.

Up to this point, all the possible explanations to explain details in the resistivity maps are feasible. However, examination of inverted pseudosections over the pit-alignment feature clearly illustrates the danger of over interpretation.

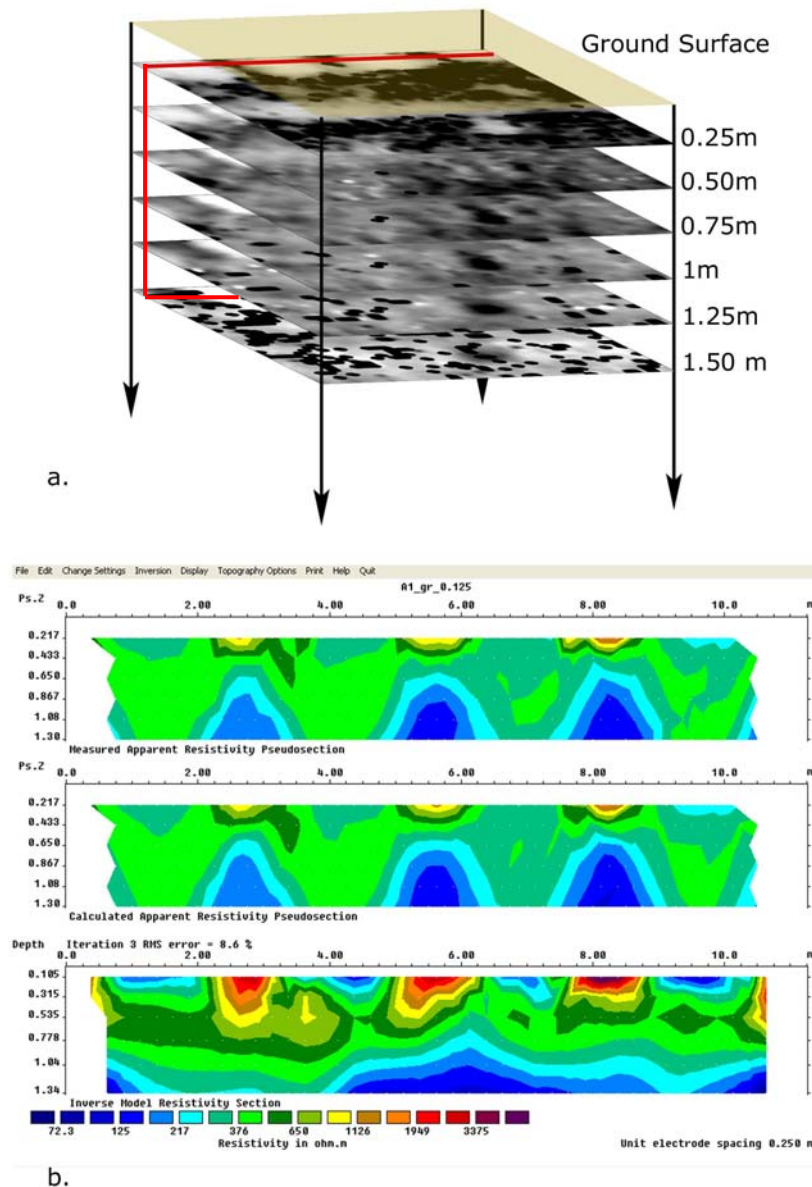


Figure 42. Image a. represents the vertical component of the multi-plexed resistivity data. The three plots of measured resistivity in b. present a single pseudosection inversion. The data represented here are a profile across the pit-alignment (red line in a.).

The resistivity plots above clearly illustrate the importance of pseudosection inversion (Figure 42b). The interpretations conducted in the section above can be directly compared with the top pseudosection of plotting raw resistivity data. The anomalies that have been identified in fact are artefacts in the data that are removed after inversion.

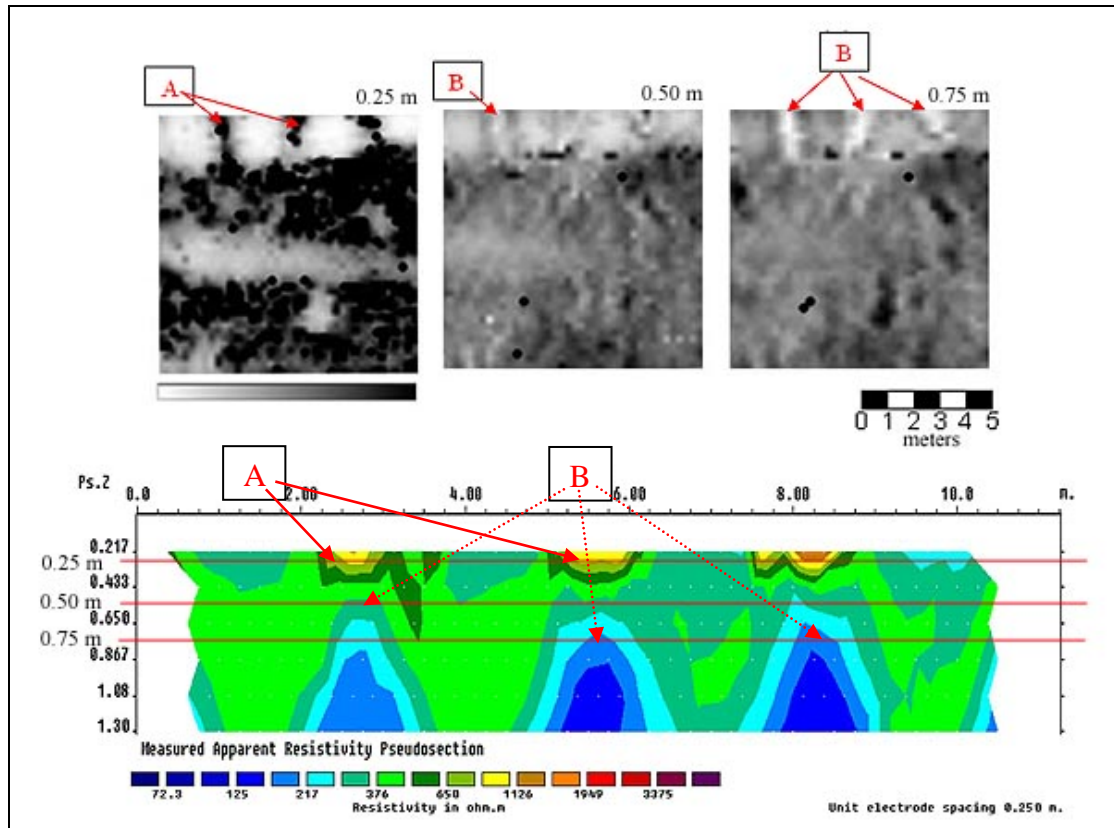


Figure 43. Comparison of apparent resistivity plan to graph of raw resistivity pseudosection.

Once the pseudosection is inverted the results sharpens the high resistivity anomalies and the low resistivity anomalies disappear (Figure 44). This confirms that the low resistivity anomalies are artefacts of the data collection method.

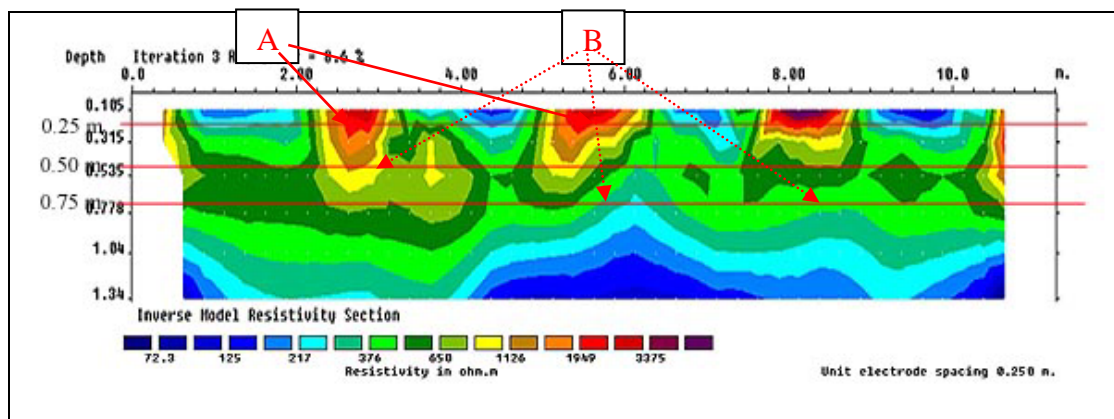


Figure 44. Resistivity inversion graph after three iterations with apparent resistivity plan.

The final inverted image gives the most realistic representation of the actual structure of the archaeological features and background materials through resistivity property mapping.

Further assessment of these resistivity anomalies and their correlation to the archaeological features in area A1 should be pursued through full data pseudosection inversion and careful consideration of excavation data and thorough resistivity profiling. In order to best integrate with the archaeology, it is necessary for the geophysics specialist to work closely with the archaeologists who excavated and recorded the site.

5.1.4 GPR Survey Results

Data interpretation was based on a full assessment of all geophysical data. In the case of the surface data for area A1, plough furrows and a rough survey surface have generated significant noise in the data. This noise made it more difficult to identify archaeological anomalies. After thorough investigation of the GPR surface survey data the pits were visible in three different areas of the data.

GPR data act in a similar manner to resistivity data in that possible distortions are introduced to the data with increasing depth. In GPR, features called hyperbolas are created due to the geometry of the propagation pattern of the radar waves. These hyperbolas are removed through migration, a method that effectively reduces the ‘tails’ of the hyperbolas based on a velocity curve formed by selecting representative hyperbolas across the data set. Migration has been performed on all the GPR data sets in this report.

Area A1 is a unique example of another form of data distortion caused by varying velocities of materials. GPR data are recorded as the time delay between the release of the radar signal, its penetration into the earth, reflection off of an interface of contrasting materials, and reception back at the ground surface. In the case of the pit-alignment, the pit fill contained a significant amount of water in contrast to the surrounding sandy gravel material. The velocity of a radar wave is fastest in air that has a dielectric permittivity of 1 and slowest in fresh water that has a dielectric permittivity of 81. All other materials (excepting metals) have dielectric properties in between 1 and 81. GPR profiles over the pit-alignment depict the position of the pits, not by obvious contrasts between the pit fill and gravel materials as would be expected, but by the change in the velocity of the GPR signal in the data. The changing velocity affected the position of a flat layer of stratigraphy at approximately 1m depth that can be seen across most of the survey area.

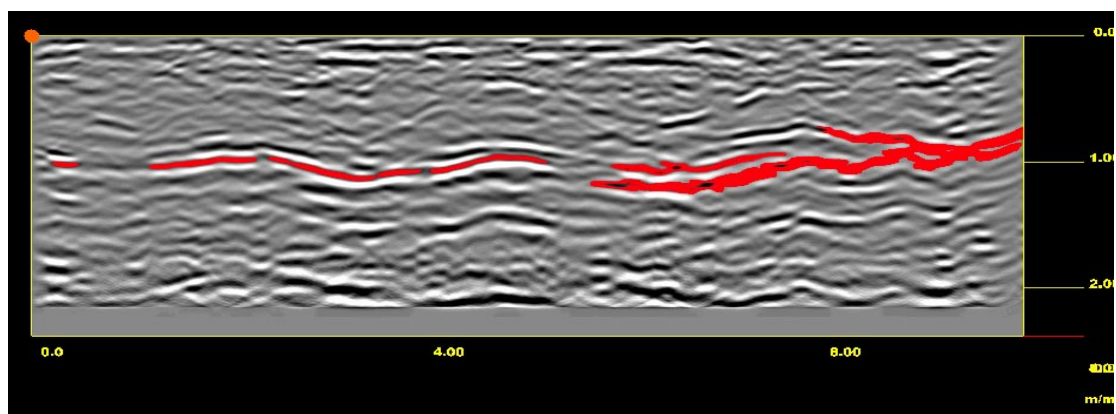


Figure 45. A1 GPR profile over the pit-alignment showing the changes in velocity of the radar wave due to saturated pit fills.

The position of the pits in this instance is centered on the lowest point in each dip in the layer highlighted in red in Figure 45. Once this change in velocities was observed, closer investigation of the data provides an intersection through the pits. This profile, however, is not obvious and if the change in signal velocity was not identified through a single layer of stratigraphy that happened to be in that particular location, these pits would be difficult to recognise.

Additionally, though the saturation of the pit fill was significant enough to affect the velocity of the radar signal in this instance, it is not guaranteed. If the area was surveyed after a long period of hot and dry weather, the results may be different.

To further investigate this type of feature GPR assessment was conducted adjacent to area A1 just after the topsoil was removed. With the pits of the alignment visible on the natural subsoil, the GPR was run over the position where the alignment would continue across the field. As many times as the GPR was run in the field over the position of the alignment, the pit features were not visible in the data in the field. The identification of this particular feature was made in the post-field data analysis.

Another note for data assessment of the pit-alignment pit features is that data must be investigated carefully, with a comprehension of the depth of the plan view (or slice) being assessed and the nature of GPR data. The pits are visible in their real positions, and if one is not paying attention, below their real positions. This is the case in any survey that has similar characteristics to this one.

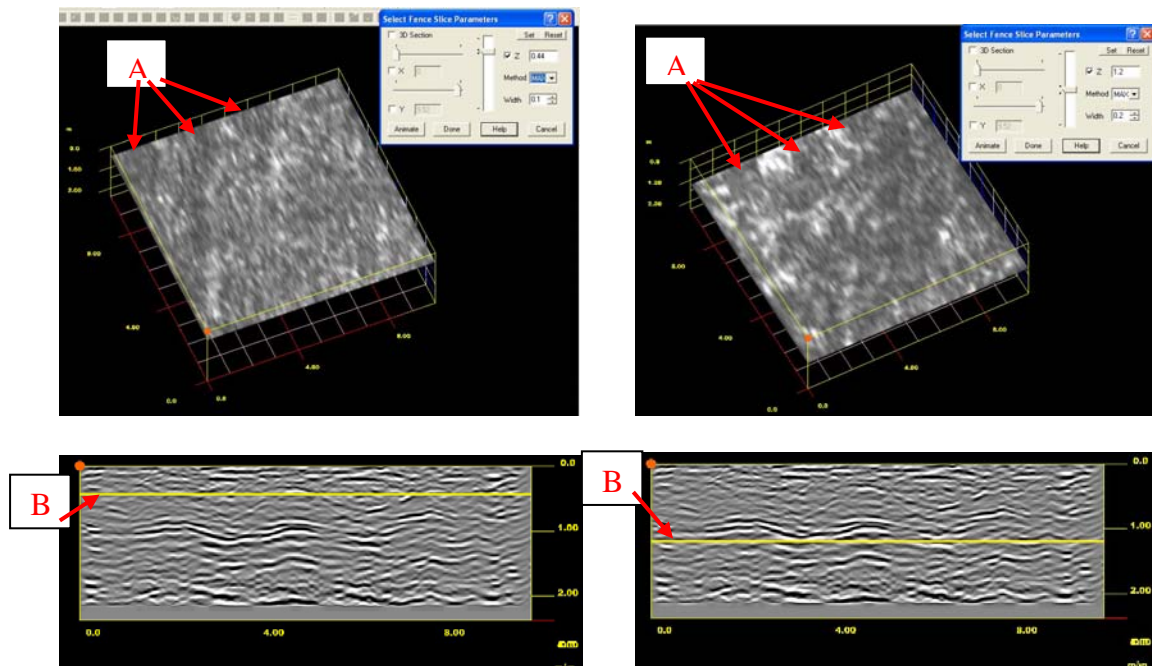


Figure 46. GPR plan views and vertical profiles detailing the pits of the pit-alignment and potential interpretation pitfalls. A. are the pit anomalies in the GPR plan views and B. shows the depth of the plan view at the position of the yellow line.

Note the image on the right in Figure 46 shows anomalies which appear below the level of the archaeological feature and could be misinterpreted.

The first clear map of archaeological features from the gravel survey is recorded in, or above, the ground coupling wave. Data have been processed so that time zero is at the very beginning of the first break to the positive peak of the coupling wavelet.

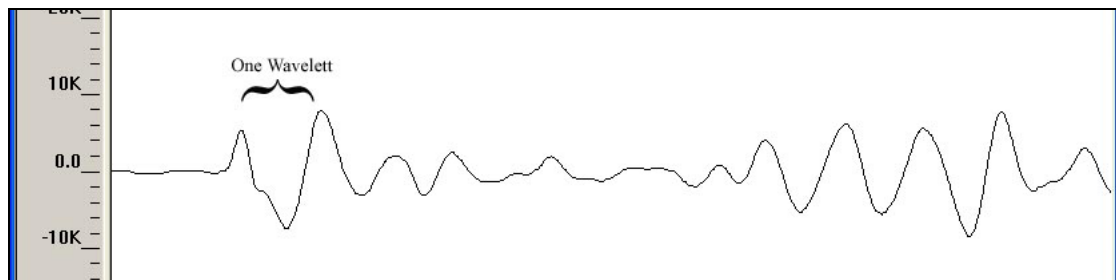


Figure 47. The ground coupling zone at the top of the GPR record measures approximately one wavelet.

The ground coupling zone, otherwise known as the ‘dead zone’, is believed not to record valid information of the survey near surface. In the case of the A1 gravel survey one wavelet is 4 ns, or approximately 0.17m. One would assume that approximately the top 0.17m of the GPR record would not provide valid data.

GPR data processing involves a number of nearly automatic steps during post-processing that include correction of time 0 (placing 0 at the true top of the survey surface) to filtering and gain adjustment. Typical work post-field includes spot checking of vertical profiles to make sure data are valid across the site then batch processing and creation of 3D cubes. Once the data are processed and in the 3D cube format data assessment begins.

Because of the nature of this project, data were viewed in the field daily both to assess data quality and to obtain information to help position further survey areas for the subsurface and 2m x 5m sub-area locations. During preliminary review data were not processed but just viewed in 3D cubes. The phenomenon of mapping through the direct coupling was discovered during this process.

Plans of each area with a 0.01-0.02 slice thickness at the very surface of the GPR record show changes in the direct wave amplitude due to variations of the surface dielectric (Chanzy 1996). This occurs because the very first (or top) part of the direct coupling is most sensitive as it is the superposition of the airwave and ground wave. When data were later adjusted to time 0 in post processing following normal time 0 guidelines, this detailed map of the archaeological record disappeared from the GPR data. Thus an adjustment was made to the time 0 process to include the direct wave amplitude, the difference not having a significant effect on the depth conversion for the rest of the data.

Though the true location of time zero is debated within the GPR community, the peak of the first positive lobe of the ground coupling wavelet is the standard time 0 position used in the concrete assessment industry (GSSI training manual).

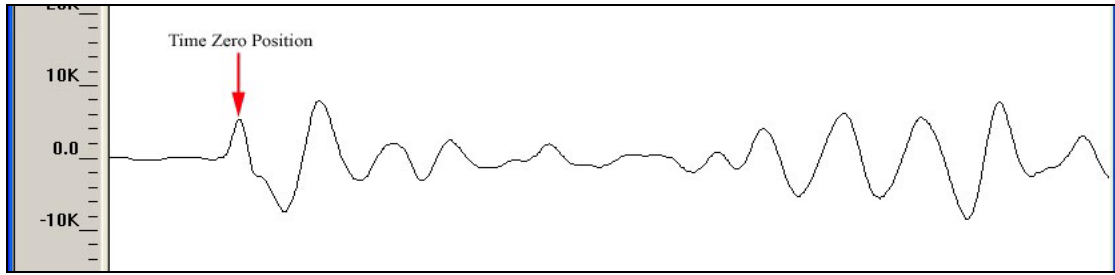


Figure 48. Time zero position for GPR trace.

Due to the new formatting of the SIR3000 GPR computer, the surface pulse is set down to 10% of the total selected range. This enabled the coupling image to be discovered.

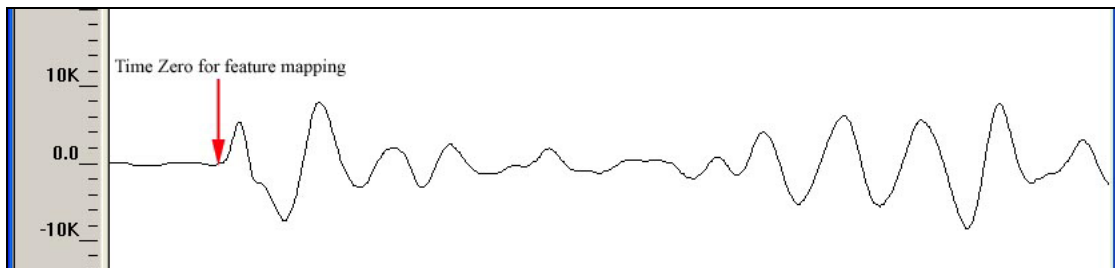


Figure 49. Adjusted time 0 setting to include the direct wave amplitude.

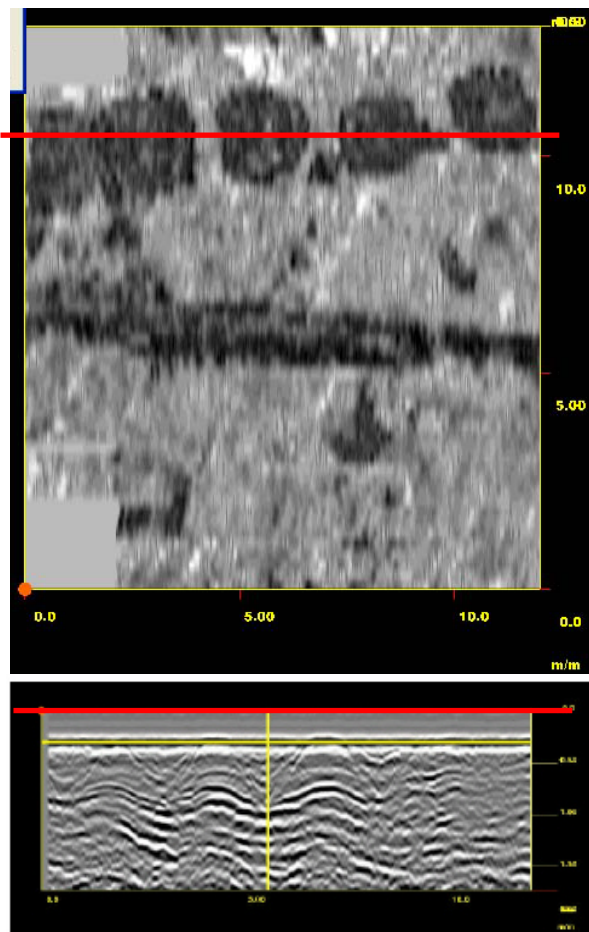


Figure 50. A1 GPR slice at time zero. The red line in the top image designates the position of the vertical profile at the bottom.

The results included at the very top of the scan in the data enables the generation of a map of surface dielectrics reflecting the details of the archaeological features. The first mapping of the pit-alignment was in the coupling wave of the radar survey, directly on the surface of the gravel as can be seen in the figure above. These data represent the moisture difference between the humic pit-fill and the sandy gravel background geology.

The second manner through which the pit-alignment pits were mapped was through the definition of the pit edges and changing velocities visible in the radar profiles and plan. Viewing the profiles adds further understanding to the plan and provides further detail of the archaeological features.

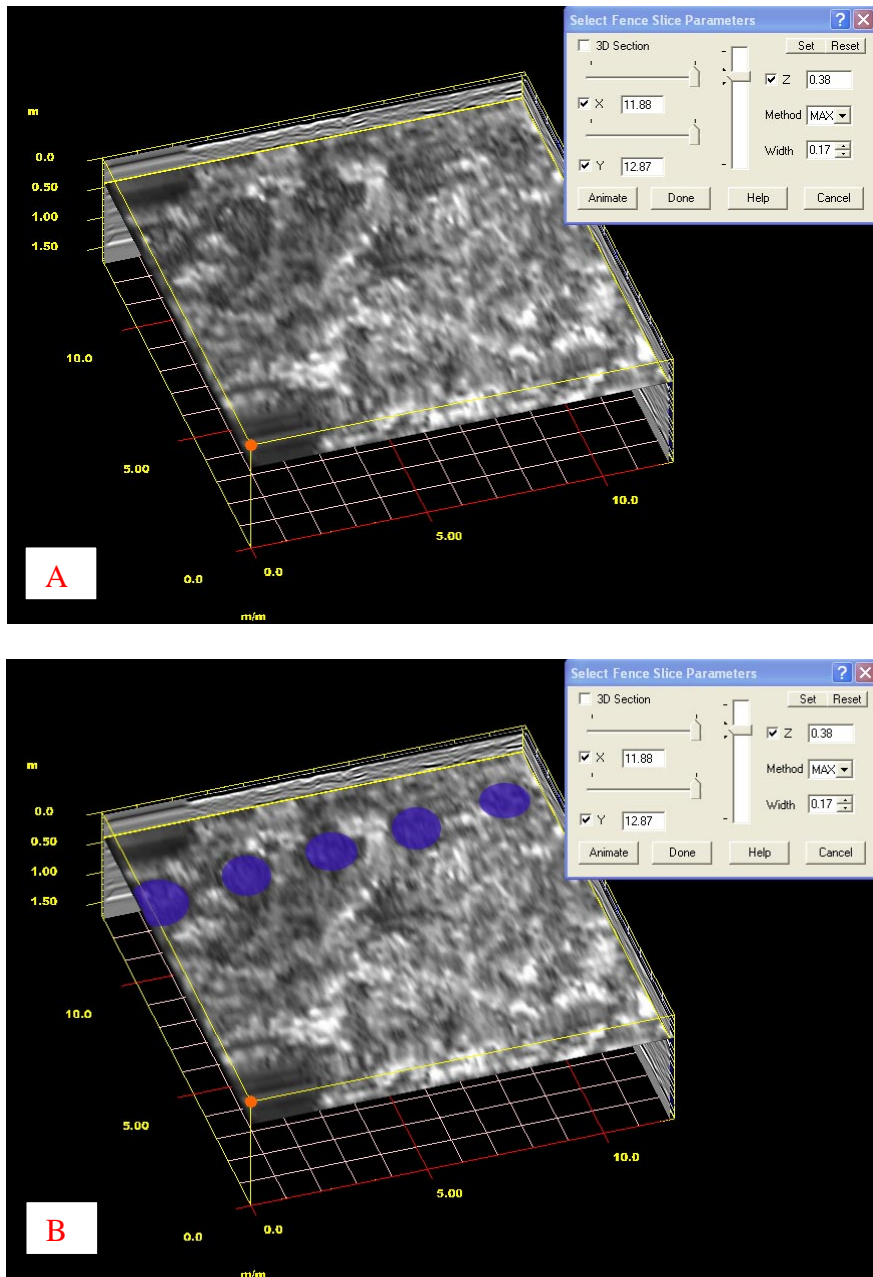


Figure 51. GPR plan map showing pit-alignment anomalies (blue) in A1.

Further details such as different deposits within the pits may have contrasting dielectric properties that are mapped in profile and through plan views. Detail on pit edges can be seen in profiles.

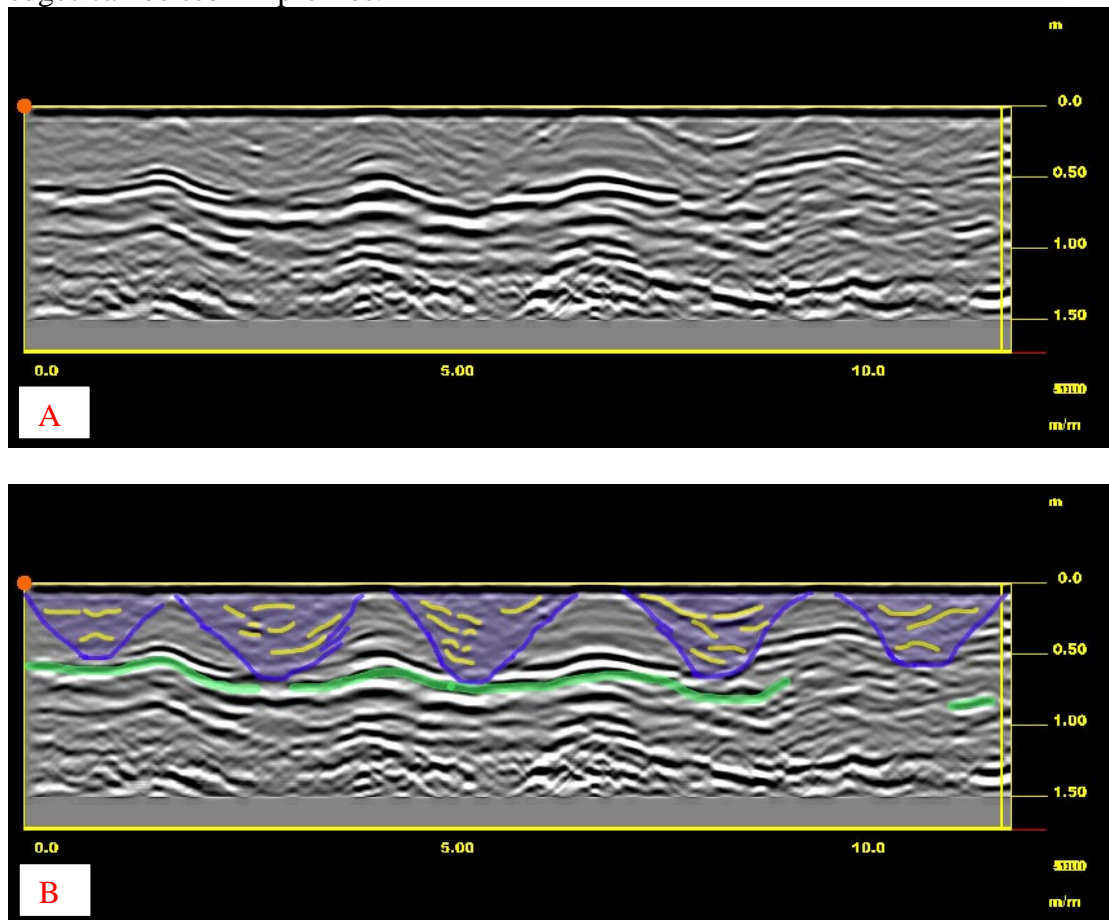


Figure 52. GPR profile across pit-alignment in A1. A is a processed profile and B is the same profile with preliminary interpretations.

Figure 52 presents a GPR profile across the pit-alignment. The top image (A) is processed data (time zero correction, horizontal background removal, migration) and the image on the bottom (B) has preliminary interpretations of the GPR anomalies in this profile. The green line represents the layer of stratigraphy that reflects the changing velocity of the radar wave due to the contrasting dielectric properties of the pit fill (a higher dielectric due to water content slows the signal down therefore creating a dip in the contrasting linear surface below) and the surrounding sandy gravel material. Blue areas define the pits and pit edges. The yellow lines define layers of materials within the pit features defined through contrasting dielectrics.

Further investigations into the pit fill materials with the integration of excavation records, other geophysical data responses (one 2m x 5m sub-area sectioned one of the pits) and the results from the soil sampling work should provide a more detailed picture of the actual structure of the pits and their fills.

5.1.5 A1 2m x 5m Sub-area

5.1.5.1 Magnetic Susceptibility

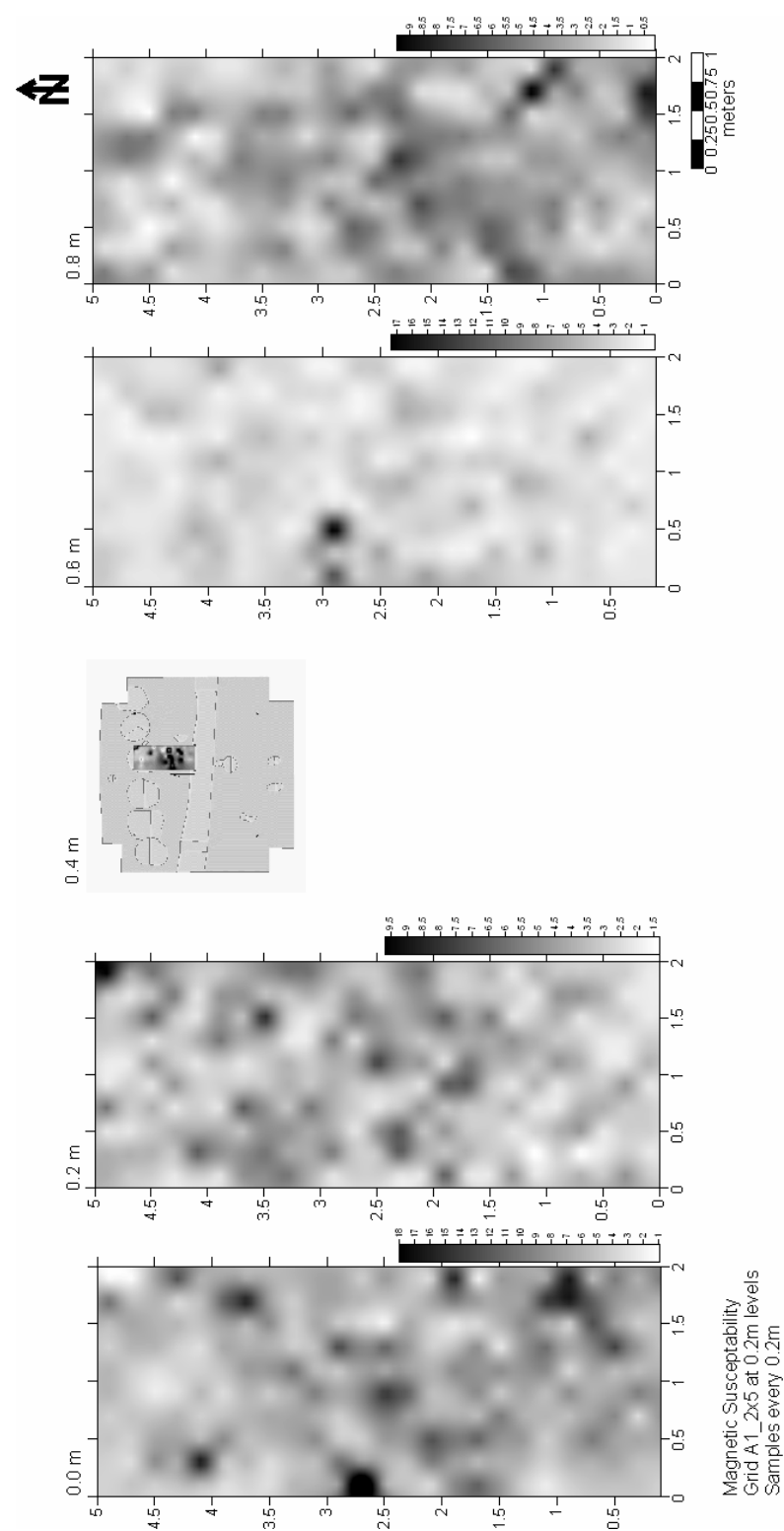


Figure 53. A1 2m x 5m magnetic susceptibility survey results.

The magnetic susceptibility maps do not reveal clear anomalies that can be related to the archaeology in A1.

5.1.5.2 Resistivity

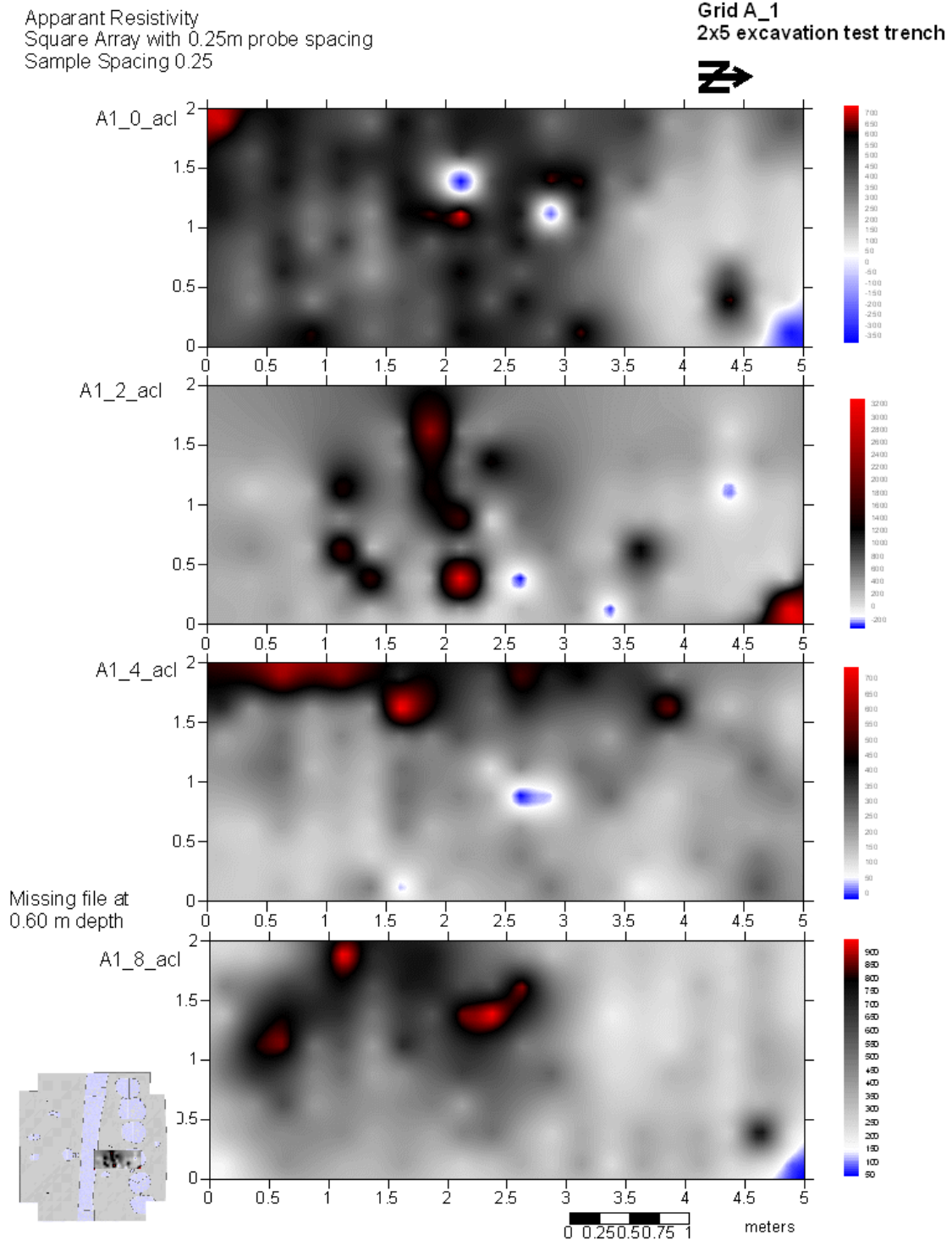


Figure 54. A1 2m x 5m sub-area resistivity survey results.

The apparent resistivity maps do not reveal clear anomalies that can be related to the archaeology in A1.

5.1.5.3 Dielectric Permittivity

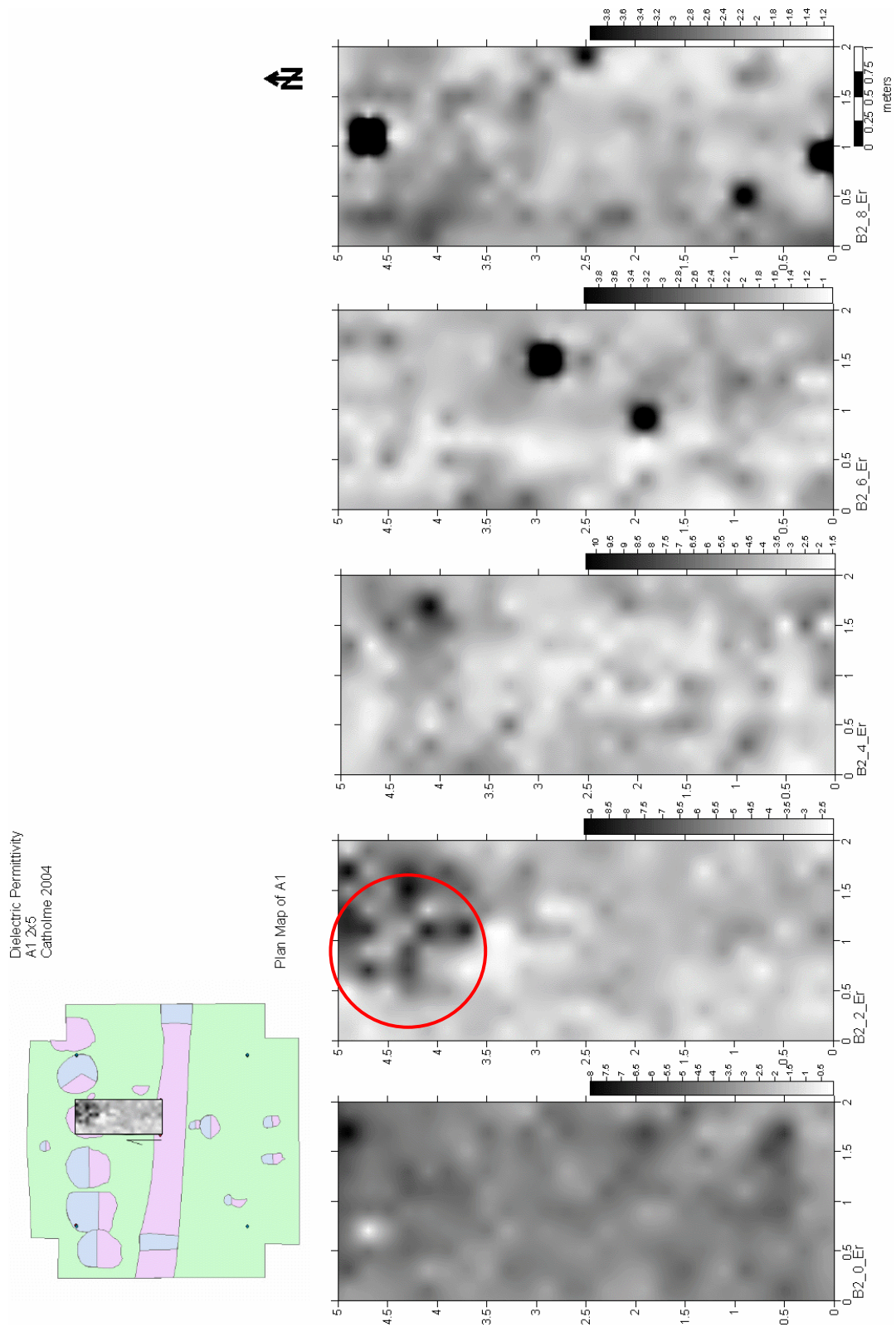


Figure 55. A1 2m x 5m sub-area dielectric permittivity survey results.

The best representation of the pit is mapped in the dielectric permittivity at 0.2m depth, outlined in red above.

5.2 Area A2

5.2.1 Magnetometry Survey Results

The G858 magnetometry survey on the surface of A2 mapped a number of anomalies. Initial review of the data grouped the majority of dipolar anomalies together as one of the possible rings of the 'Woodhenge' feature. With further consideration it was thought that magnetic signature of these anomalies may not be expected as post-pit fill. During post-processing viewing the excavation plan map overlain on the data confirmed the fact that the surface magnetic survey did not conclusively map the 'Woodhenge' feature.

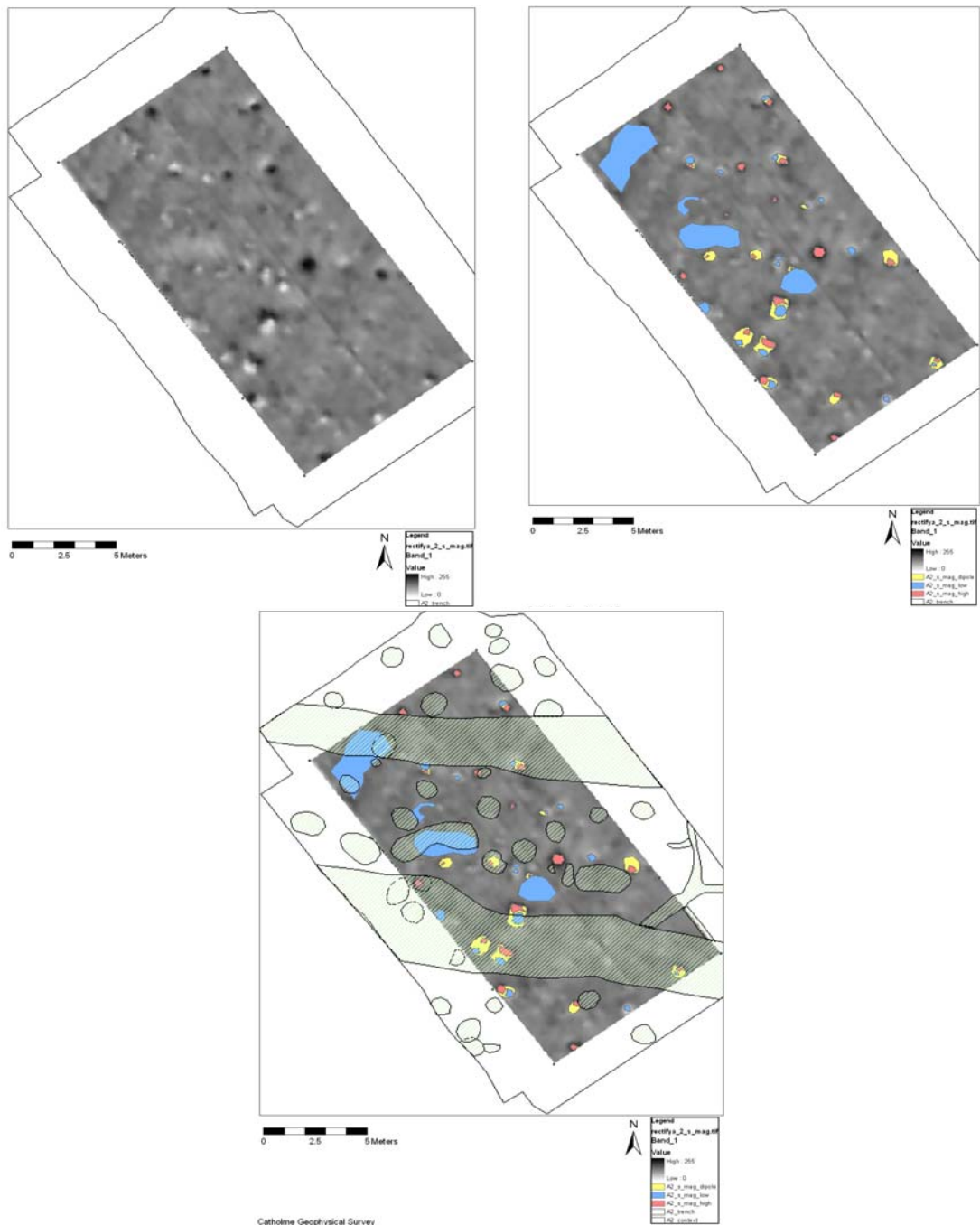


Figure 56. A2 surface magnetometry map (top left) with interpretations (top right) and overlain excavation plan (bottom).

After the removal of the topsoil, further magnetic survey with the G858 thoroughly mapped the archaeological features of the 'Woodhenge'. The images below mapped the pit-posts as medium-high magnetic anomalies with the large pit mapped as a very strong high magnetic anomaly.

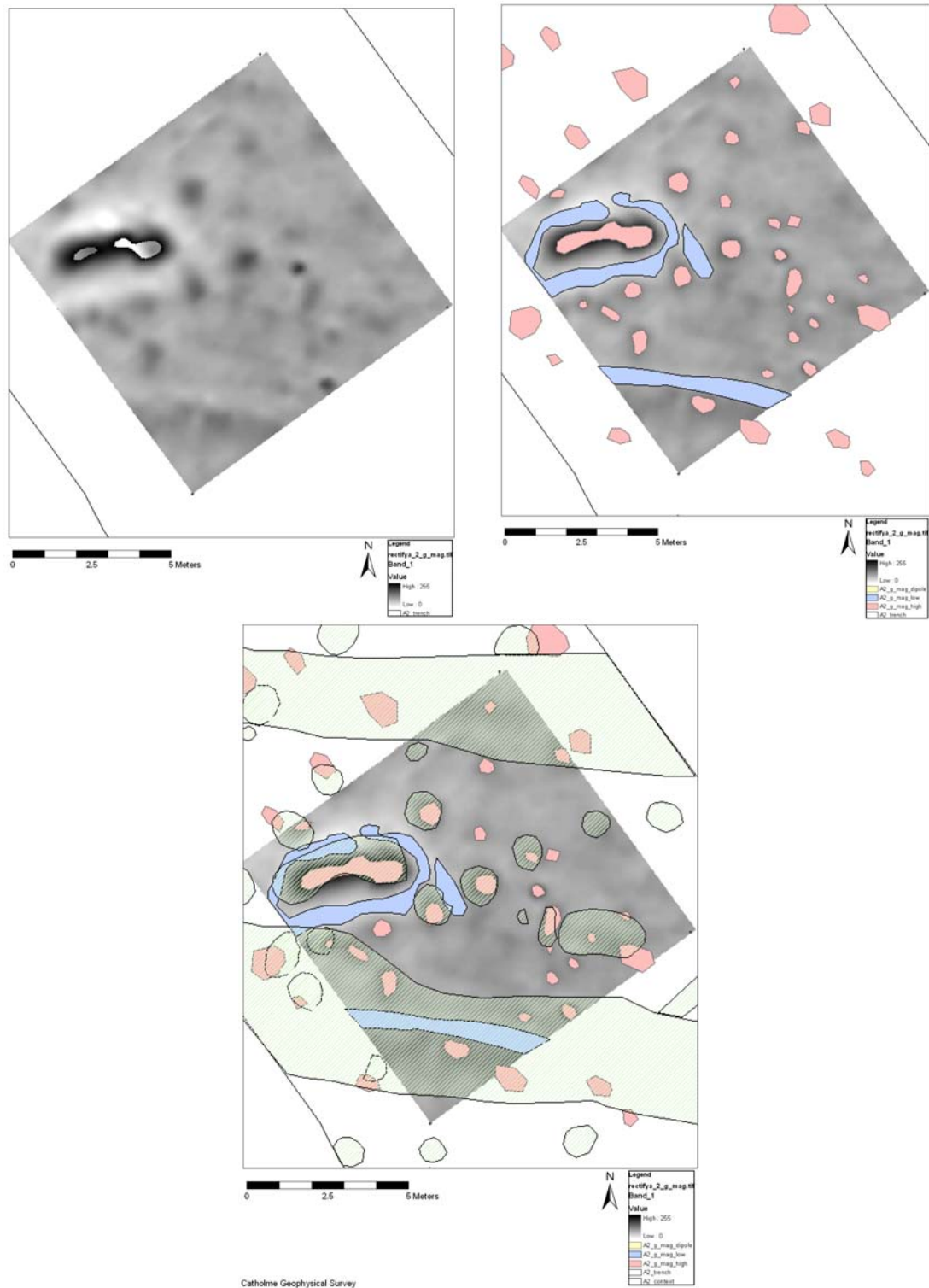


Figure 57. A2 gravel magnetometry map (top left) with interpretations (top right) and overlain excavation plan (bottom).

Because the results of the G858 magnetic survey so effectively mapped the archaeological features on the natural subsoil the FM256 was used to cover the entire area cleared in order to collect additional data for analysis. The FM256 provided a clear map of the archaeological features.

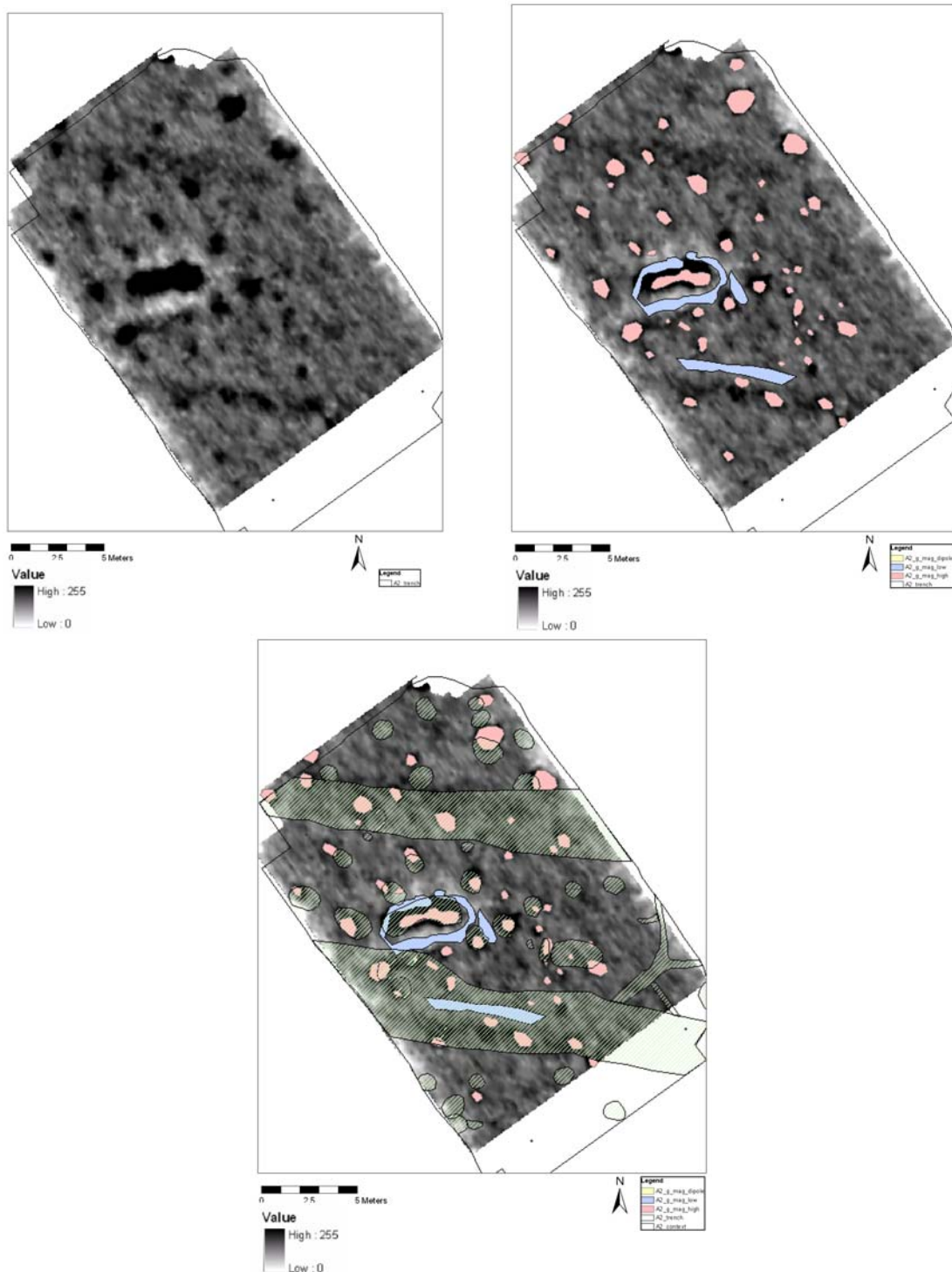


Figure 58. A2 gravel FM256 magnetometry map (top left) with interpretations (top right) and overlain excavation plan (bottom).

In both of the gravel maps the post-pits were mapped with a high magnetic signature in contrast to the background gravels. The large pit that appeared as a high magnetic feature surrounded by a slightly lower magnetic response was excavated and appeared

to be two pits excavated one into the other. The plough furrows crossing through the site were mapped as medium-high anomalies.

5.2.2 Magnetic Susceptibility Results

Results from the surface magnetic susceptibility survey showed the presence of the strong magnetic pit feature in the north eastern section of the survey area. Though a strong magnetic susceptibility anomaly was visible in the data, it does not correspond to the same orientation as the archaeological feature. This could be a result of ploughing in the area, elongating the central concentration of materials along the path of the plough furrows.

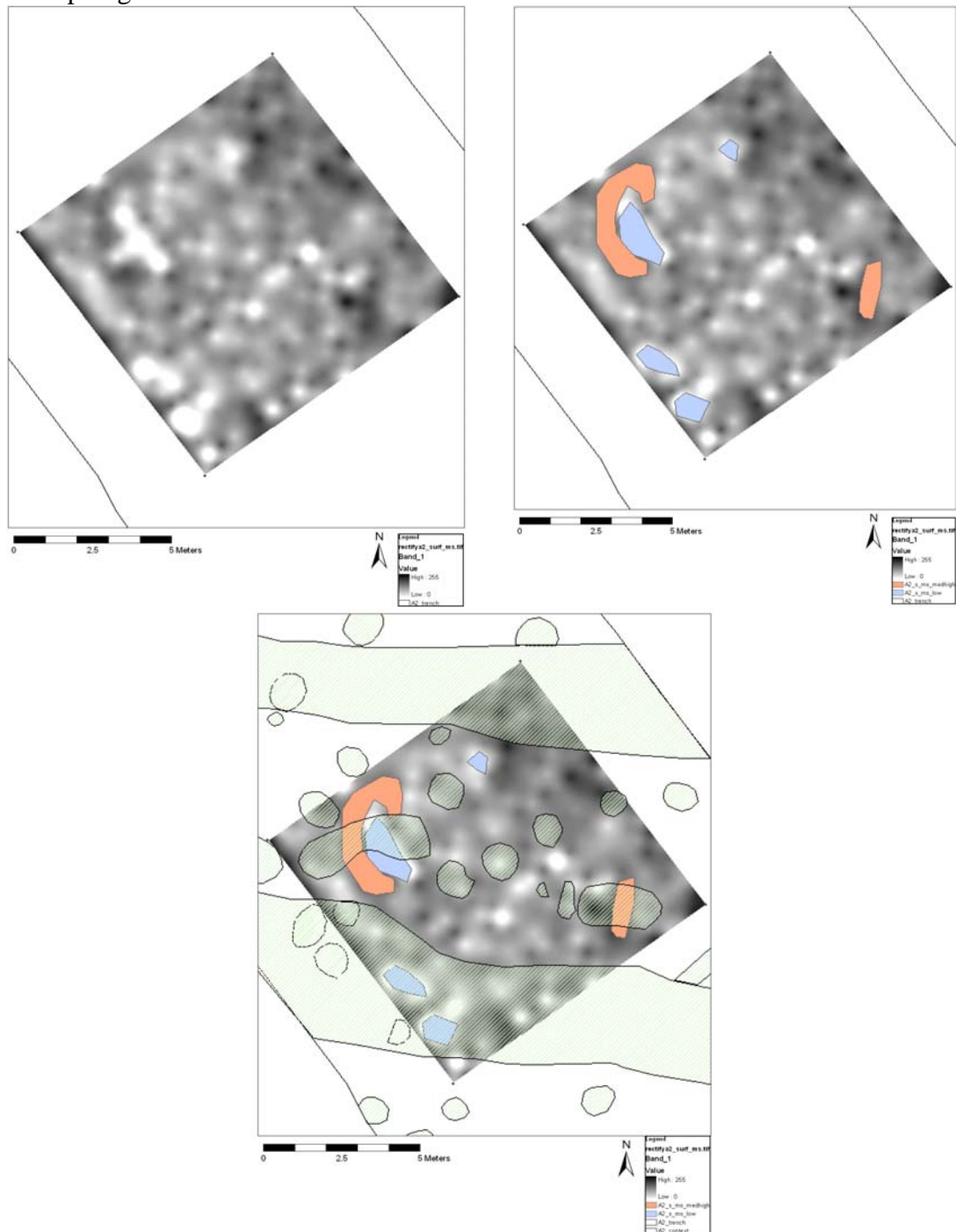


Figure 59. A2 surface magnetic susceptibility results (left) with interpretations (right) and overlay excavation plan (bottom).

5.2.3 Resistivity Survey Results

Area A2 covered the 'Woodhenge' monument where previous survey revealed no archaeological features. A few areas of high and medium-high resistivity appeared in the surface survey data but none provided conclusive evidence of the 'Woodhenge' monument. The example below shows the 0.25m resistivity plan map with highlighted anomalies followed by another image with the excavation plan map.

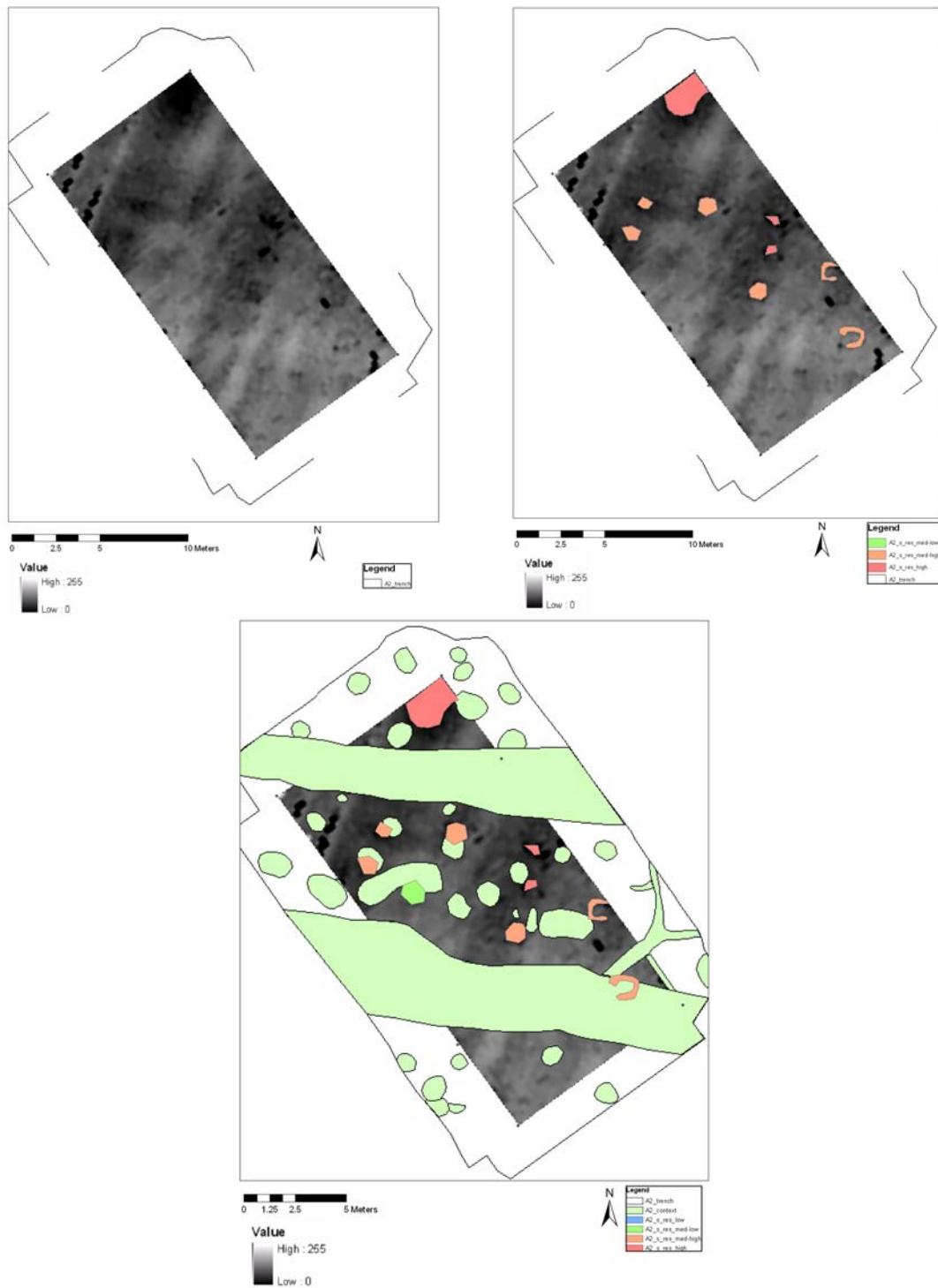


Figure 60. Area A2 resistivity survey map at 0.25m depth (left) with overlain highlighted anomalies (right) and excavation plan (bottom).

Though three anomalies identified in this instance at 0.25m appear to coincide with post-pits, they do not provide enough conclusive evidence for the mapping of the 'Woodhenge'. As in the case with area A1, one or two possible pit features do not constitute an archaeological feature interpretation.

These three anomalies at 0.25m depth in addition to a few other medium-high anomalies interpreted throughout the entire depth of the data do coincide with some of the archaeological post-pit features. Though previously stated that this would not define an archaeological feature such as the 'Woodhenge', these anomalies are important to investigate further. If they do in fact represent the post-pit features in the 'Woodhenge' it should be established why these and not others appear as weak anomalies in the surface survey. Suggested further methods of investigation include inversion and vertical profiling of the data and examination in a 3D format. Additional scrutiny of excavated materials from these post-holes compared to others that did not appear in the resistivity data and information from the soil sampling work would hope to better understand the reasons why some post-pits appear, though weakly, in the surface resistivity data.

Most of the post-pit features appeared as low resistivity anomalies in the gravel survey at the 0.25m depth. The overlain excavation plan showed positive identification of approximately 8 out of 9 or 10 mapped post-pits.

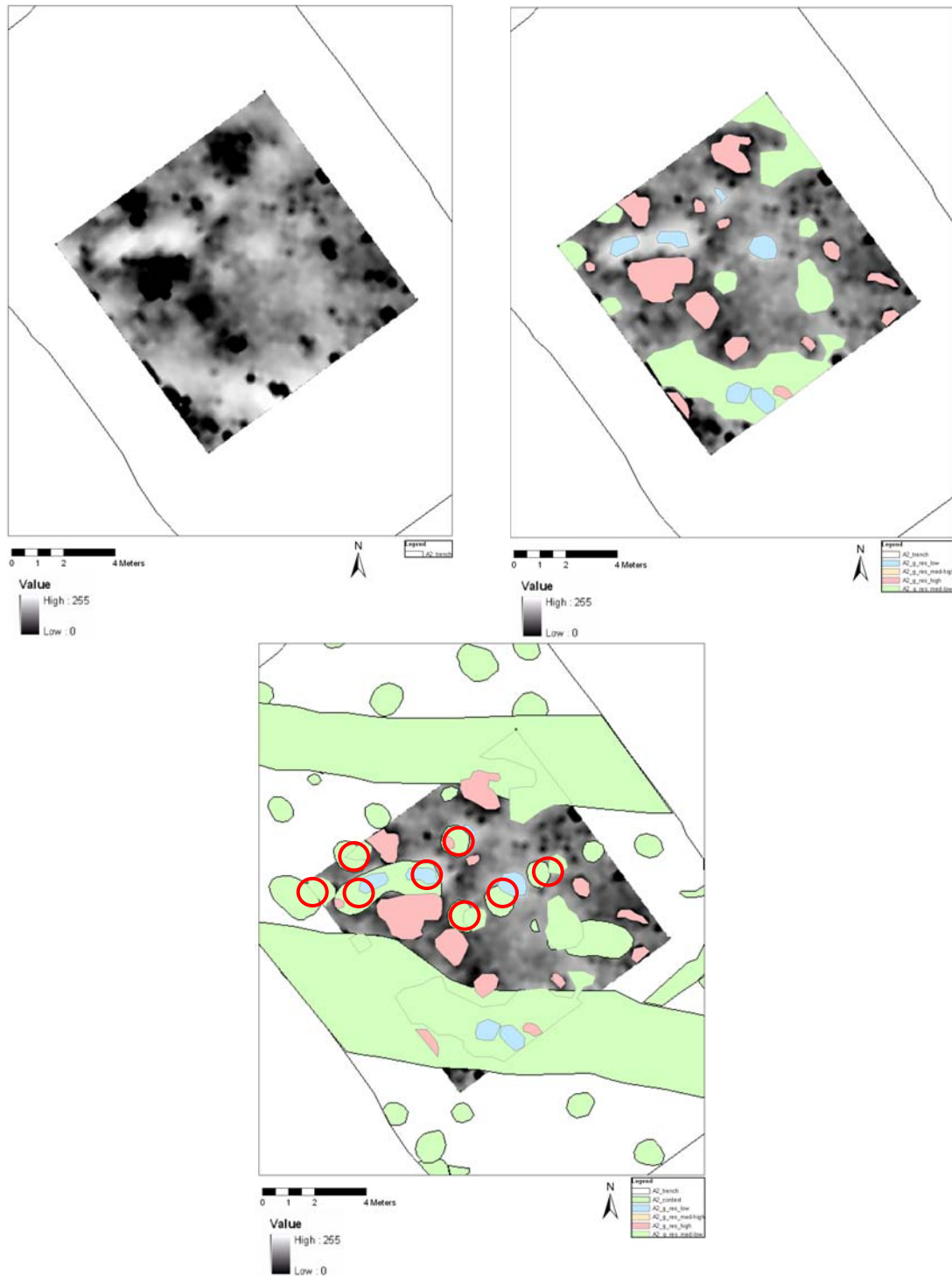


Figure 61. Area A2 resistivity (left) with identifications (right) and overlain excavation plan (bottom). Notice the high percentage of post-pits that have been mapped (circled in red).

Note: due to in-field mapping discrepancies, the archaeological plan map and geophysical maps do not perfectly align, but features overlap sufficiently to be positively identified.

Investigation of subsequent maps at 0.50 and 0.75m levels did not reveal strong anomalies defining the post-pit features. Instead the anomalies in the resistivity data appeared to be more geological and random in nature.

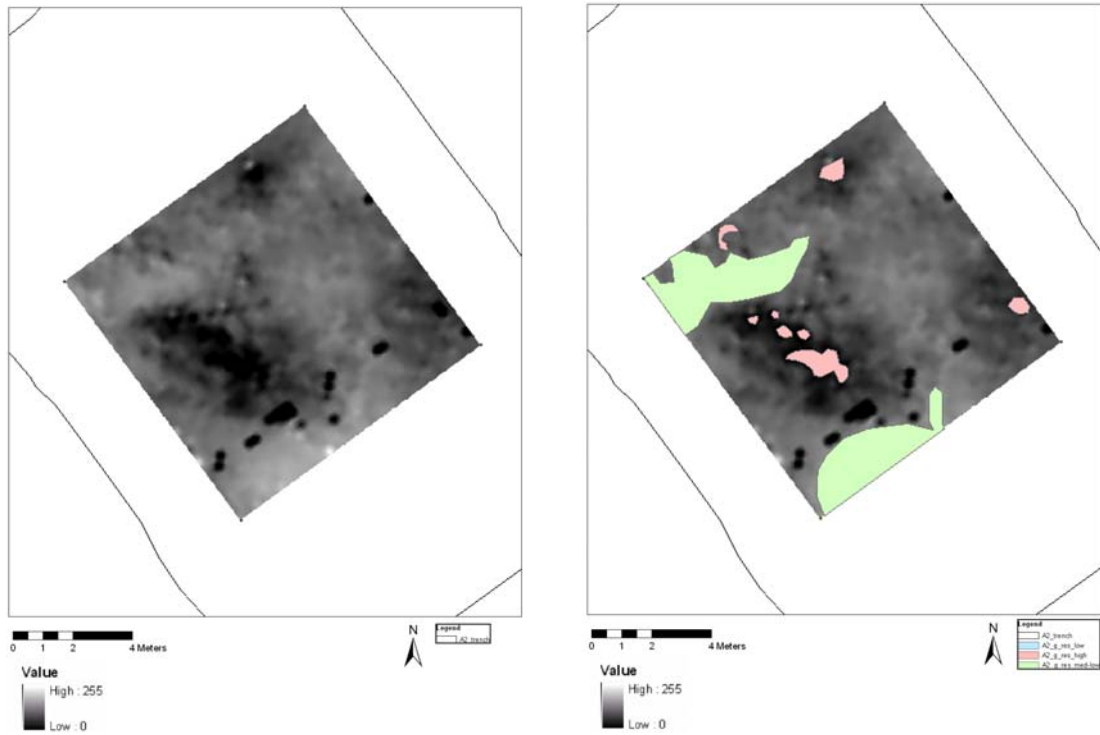


Figure 62. A2 resistivity gravel survey data at 0.50m (left) with interpretations (right). Note the lack of distinct post-pit anomalies.

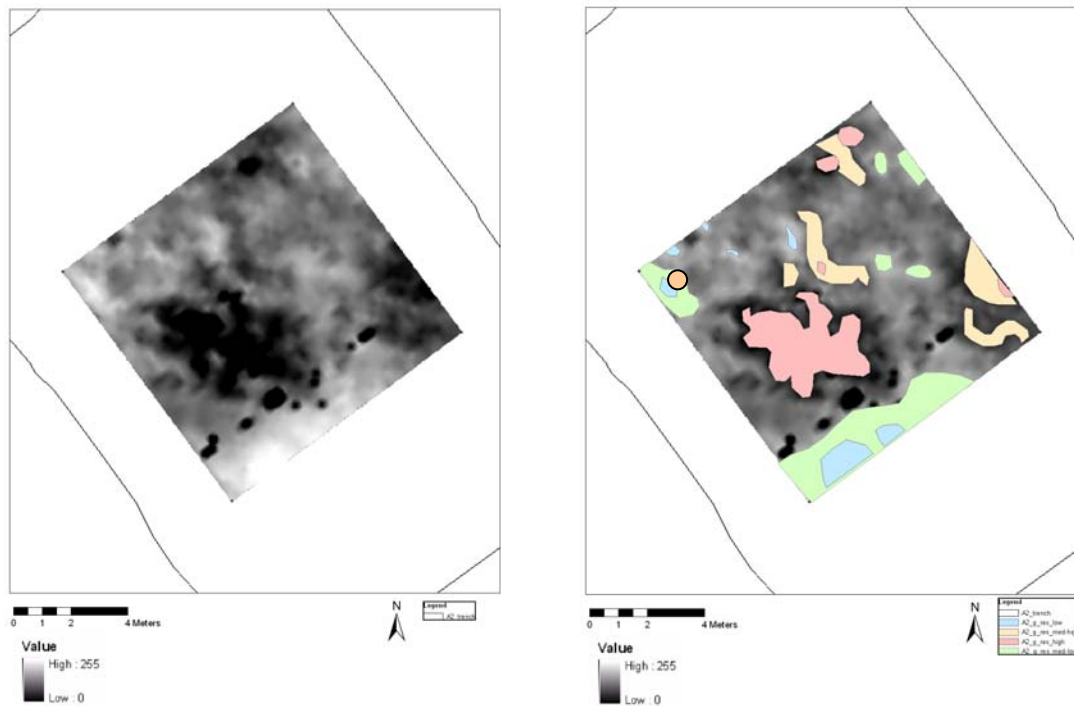


Figure 63. A2 resistivity gravel survey at 0.75m (left) with interpretations (right).

Though not entirely clear, the post-pit anomalies began to appear at 0.75m depth. This feature identification was done both on anomaly recognition and with the help of using excavation plans to look for anomalies that may not have been selected in the first round of data assessment.

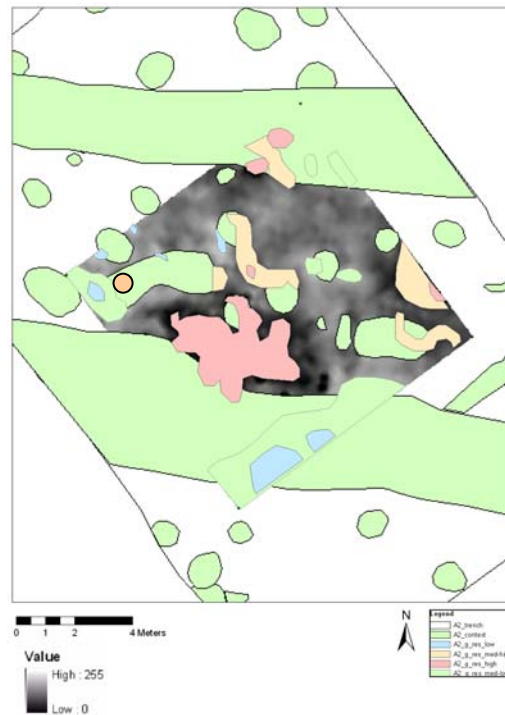


Figure 64. A2 resistivity gravel survey at 0.75m with interpretations and excavation plan.

The archaeological features become slightly more recognisable at 1m depth. This analysis was done however, with the aid of the excavation plan to interpret the anomaly map. The actual post-pit features appeared at this depth as predominantly medium-high to high resistivity anomalies, the opposite from how they were mapped on the surface of the survey area.

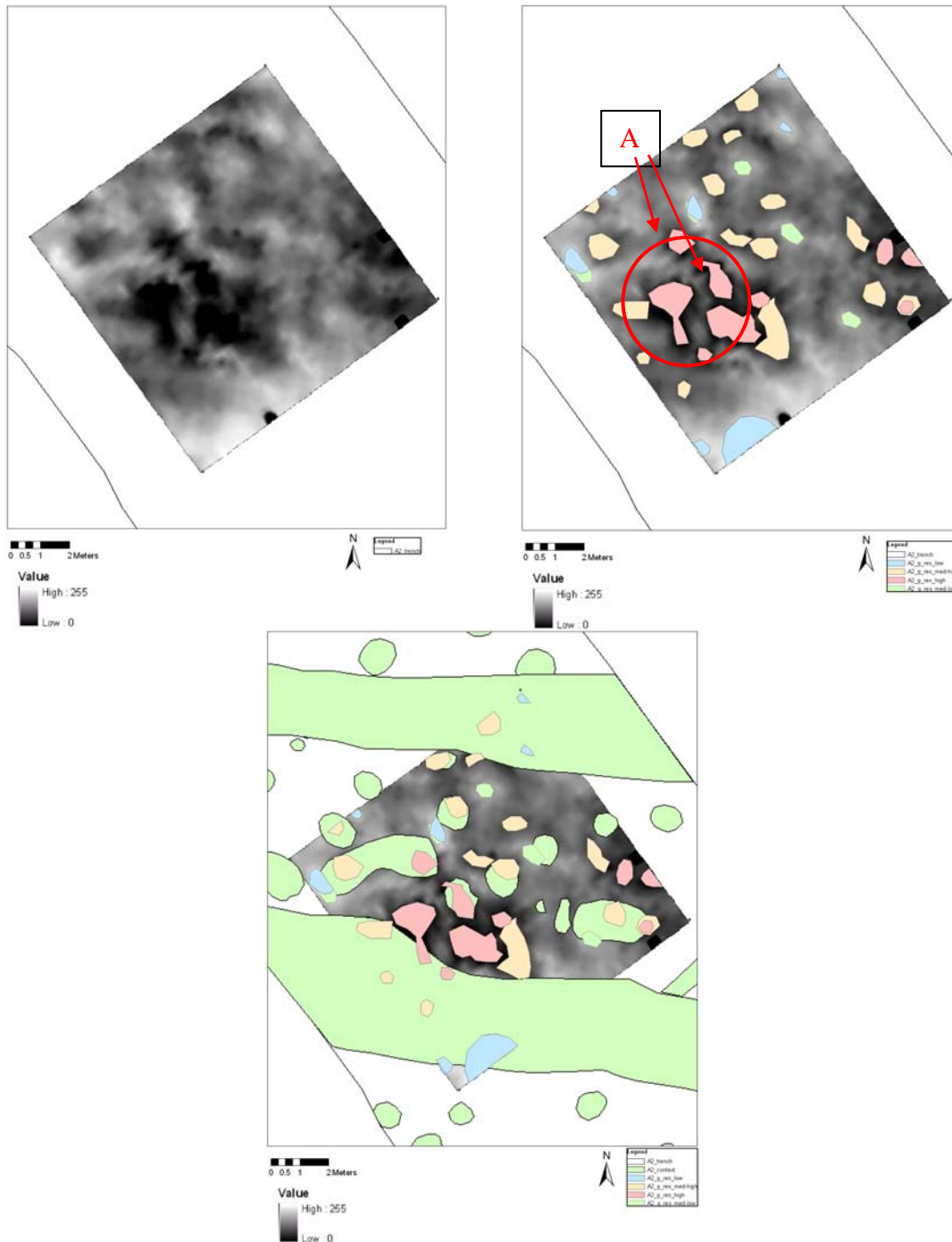


Figure 65. A2 resistivity gravel survey at 1m depth (left) with interpreted anomalies (right) and overlain excavation plan (bottom).

Note the predominant high resistivity anomalies clustered just west of the centre of the area (circled in red). Two of these features are post-pits A, in the figure above. The other, larger high resistance anomalies are a geological feature, most probably a deposit of gravel or other such well-drained material. It is instances like this that makes the interpretation between archaeological and geological anomalies very challenging. Another challenge presented to differentiation between archaeological and non-archaeological features at this point in the data is that the resistivity value of our target has changed from low to high. This prevents an across the board resistivity classification for the post-pit feature.

Presumably, the low resistivity anomaly at the natural subsoil was a response to the moisture maintained within the fill material of the post-pit feature. The feature was difficult if not impossible to reliably map between the 0.25 and 1m layers, which may be accounted for by a lack of contrasting fill material and moisture contained within the feature, so it appears the same as surrounding materials.

The geophysical character of this feature at a depth of 1m and deeper changed to high resistivity. One explanation for this may be that the bottom of the post-pit was being mapped through the contrasting moisture retained in the pit fill material and the gravel base that it was excavated into.

5.2.4 GPR Survey Results

The surface GPR survey initially appeared to map the ‘Woodhenge’ feature. A number of anomalies were interpreted in this data set; some correspond to the ‘Woodhenge’ post-pit features while others appeared to be natural. A gravel layer appeared in the data that was an obvious hydro-deposited gravel bank that slopes to the south

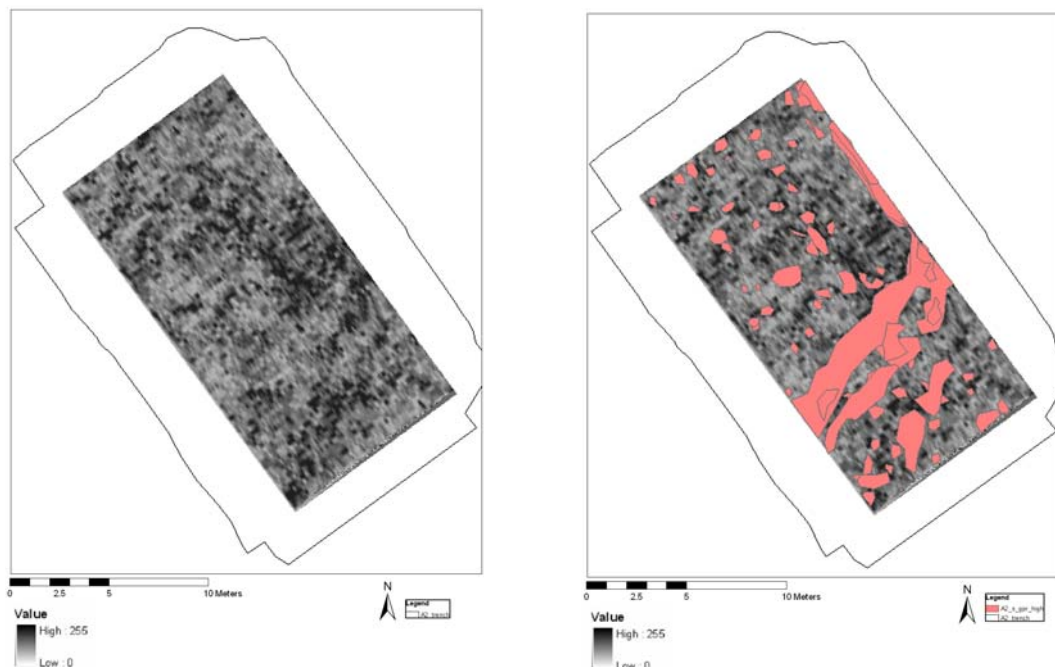


Figure 66. A2 GPR plan map at 0.75m (left) with interpretations (right).

The goal of this survey was to map the post-pit features of the ‘Woodhenge’ monument. During the interpretation process special attention was focused on identifying circular anomalies with similar appearances in the data. As can be seen in the image on the right of figure 66 a number of circular anomalies were identified. The second step in interpretation was to attempt to recognise patterns in the distribution of the circular anomalies that may reflect the concentric rings of post-pits visible in the cropmarks.

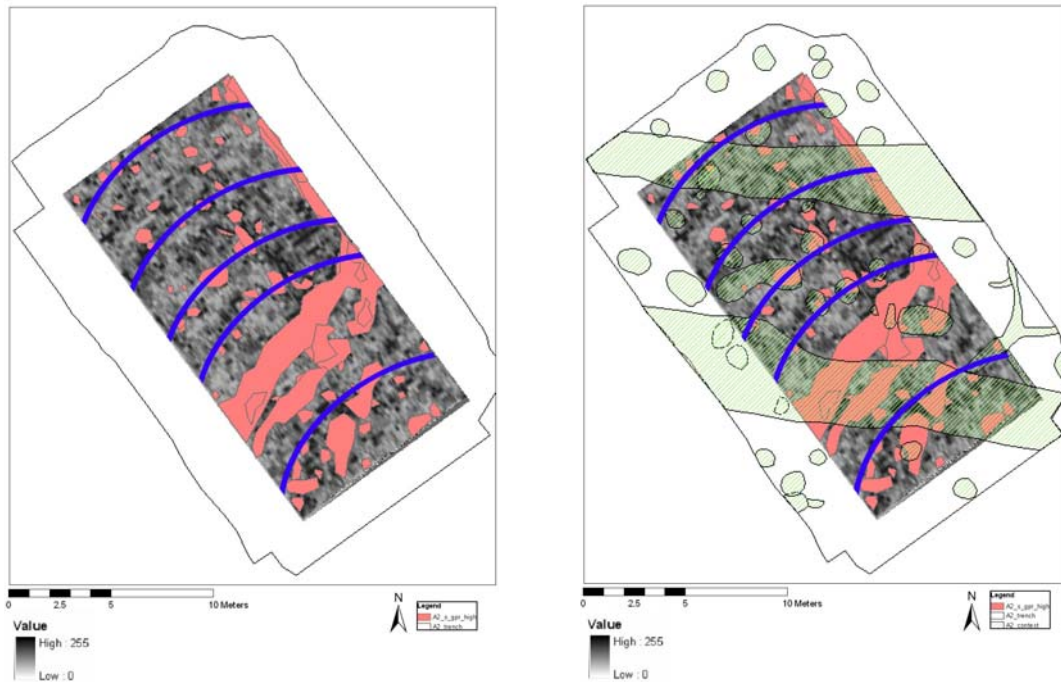


Figure 67. A2 GPR anomaly interpretation with overlain blue arcs at possible post-pit alignment (left). The image on the left shows the excavation plan mapping the position of post-pits.

This method of data interpretation identified the positions of post-pits of the ‘Woodhenge’ feature in the surface GPR survey, much to the surprise of the interpreter. Note that GPR anomalies were identified that lay beneath the broad plough furrows that cross the survey area (green hatched features in figure 67, image on the right). Some of these anomalies appeared to correspond to the arcs of pits in the plan map and may be post-pits. In this particular application, GPR appeared to be an effective survey tool to use to ‘see’ beneath other features that may block visible identification.

Very important to this identification process for the GPR data was the fact that the interpreted anomalies were not all in the same plan map, but instead they were distributed throughout the first 1.25m of the GPR data. Only through intensive assessment of individual plans (one every 0.05m) were the anomalies able to be grouped together to present a larger picture of the nature of the information within the GPR data. The fact that these data are in a GIS and each anomaly interpreted has an assigned depth provides a format for further investigations into individual features and their appearance or not, in the GPR data.

GPR survey on the natural subsoil provided detailed information on the archaeological features. Post-holes appeared mostly between approximately 0.30 to 0.40m in the GPR record as low amplitude anomalies. In a few instances, additional anomalies appeared at 0.55m depth.

As with the GPR survey in area A1, a detailed map of surface features was recorded in the ground coupling wave and provided a clear picture of the archaeological features of the ‘Woodhenge’. But in the case of A2, the best plan of the archaeological features was seen at approximately 0.55m depth.

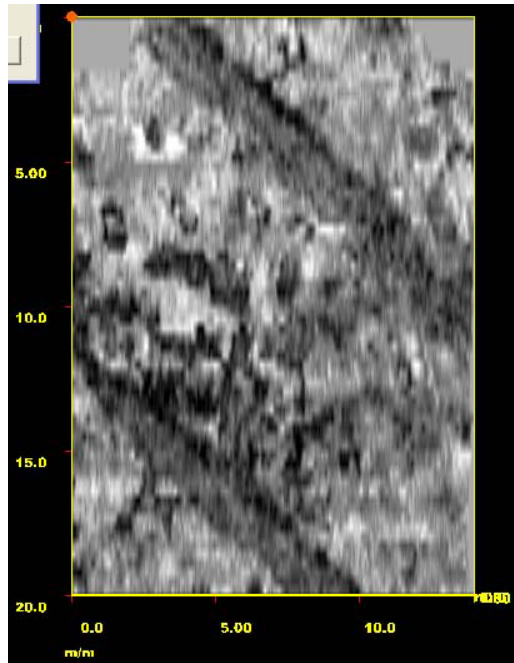


Figure 68. A2 GPR natural subsoil plan map at the ground coupling position.

Nearly all of the post-pit features were identified in the GPR data. Note the slight offset of the maps below, this is due to mapping inaccuracies and data rectification. Despite the offset, the anomalies identified can be related to the archaeological features. Post-pits located beneath the plough furrows were even more clearly mapped than in the surface GPR survey.

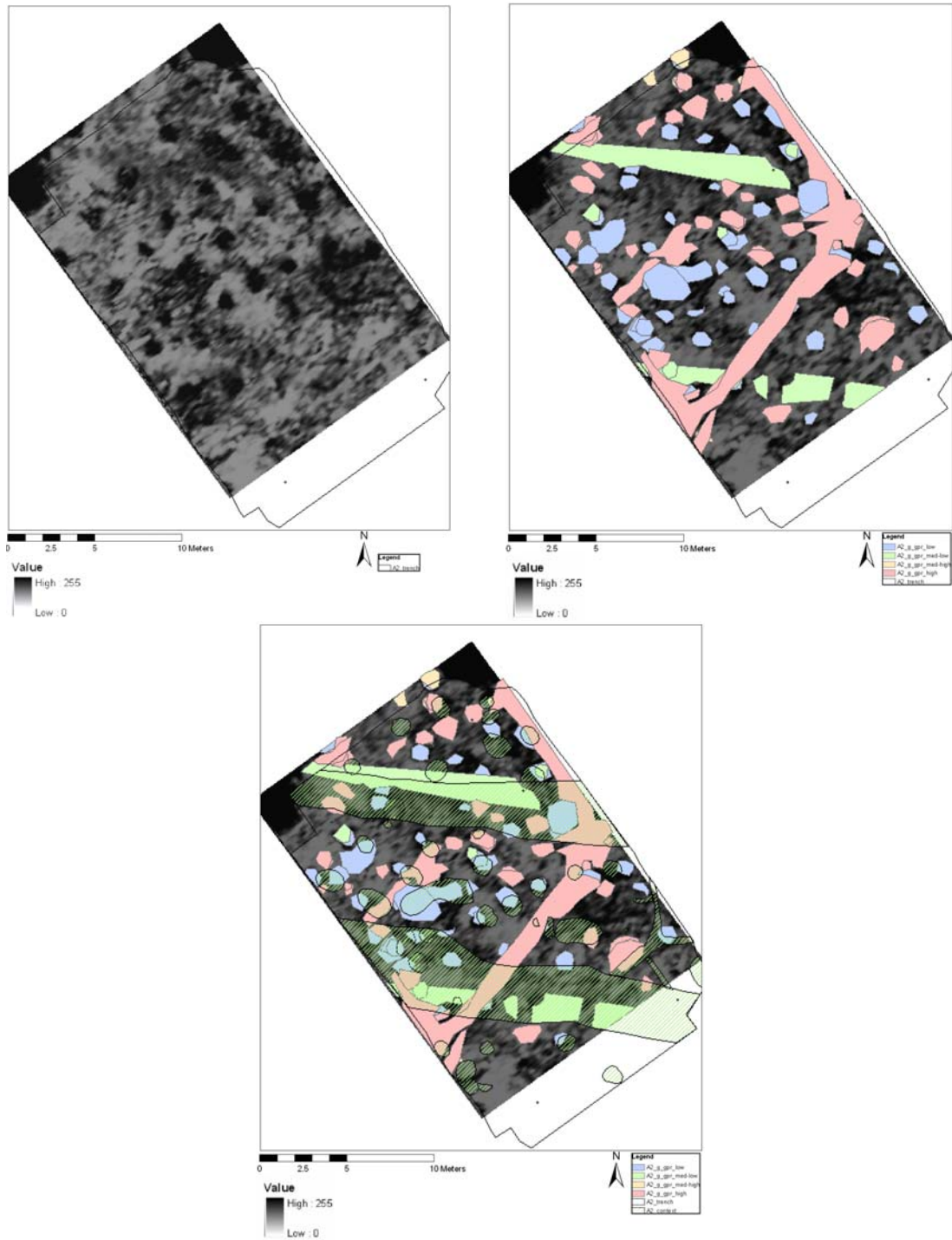


Figure 69 A2 GPR natural subsoil at 0.55m depth (left) with interpretations (right) and overlain excavation plan (bottom).

At 0.65m we began to see a gravel bank that first appeared on the northeastern edge of the area and crossed over just below the middle of the survey area. This feature appeared as a linear high amplitude anomaly and was traced across the site with increasing depth as it travels to the south. In this gravel bank, one post-hole was clearly seen to be excavated down into the gravel, revealed very distinctly in the data. The area of this excavation was smaller than, presumably, the same anomaly identified closer to the surface. In this instance we saw the GPR data provided not

only positional information on the archaeological feature, but depth and diameter as well.

The actual post-pit anomaly did not appear in all of the GPR plan. Instead, we saw it at the very surface of the survey and at the bottom of the feature but not in between. On the surface we saw the contrasting dielectric values of the pit fill and the surrounding materials and at the base of the feature we probably saw the contrasting properties of the pit fill and the underlying gravels. The reason why we did not see the feature clearly between these two stages is probably related to the geometry of the GPR radar wave pattern and the structure of the feature in its surrounding context.

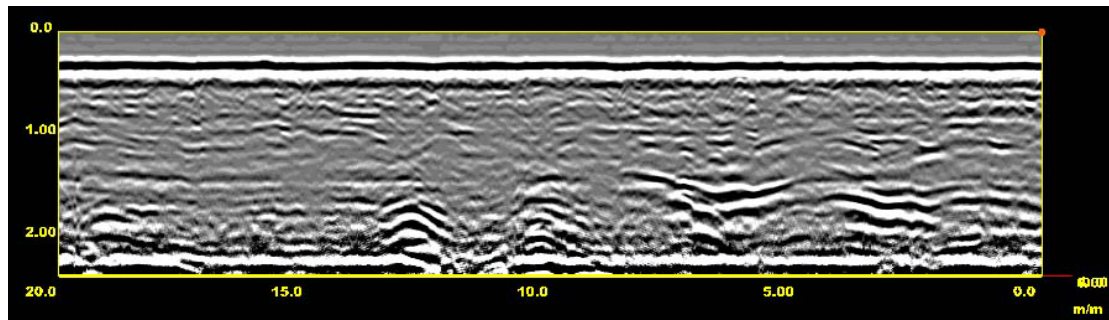


Figure 70. A2 GPR profile across post-pit features.

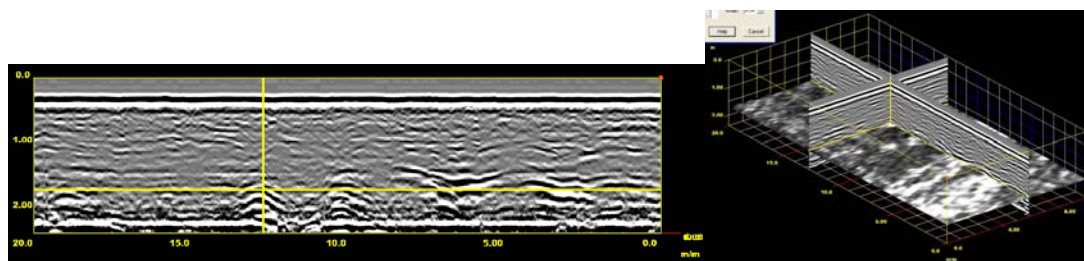


Figure 71. A2 GPR profile across post-pit features with yellow crosshair identifying position of post-pit in the plan map.

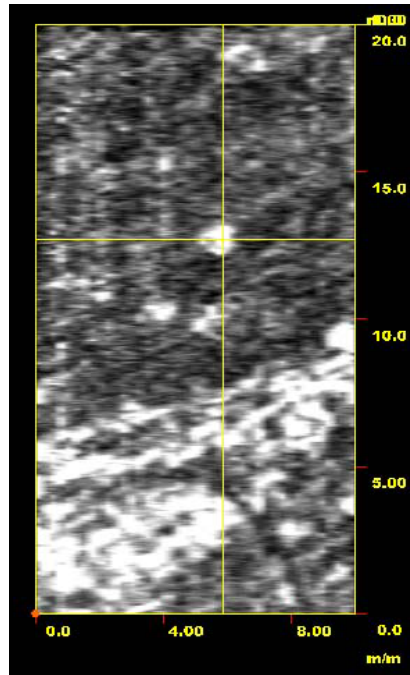


Figure 72. A2 GPR plan map at approximately 0.65m depth.

The identification of post-pit features in the vertical GPR profiles was difficult compared to the pits of Area A1. The most effective mapping of the post-pit feature was through the plan view maps.

5.2.5 A2 2m x 5m Sub-area

5.2.5.1 Magnetic Susceptibility

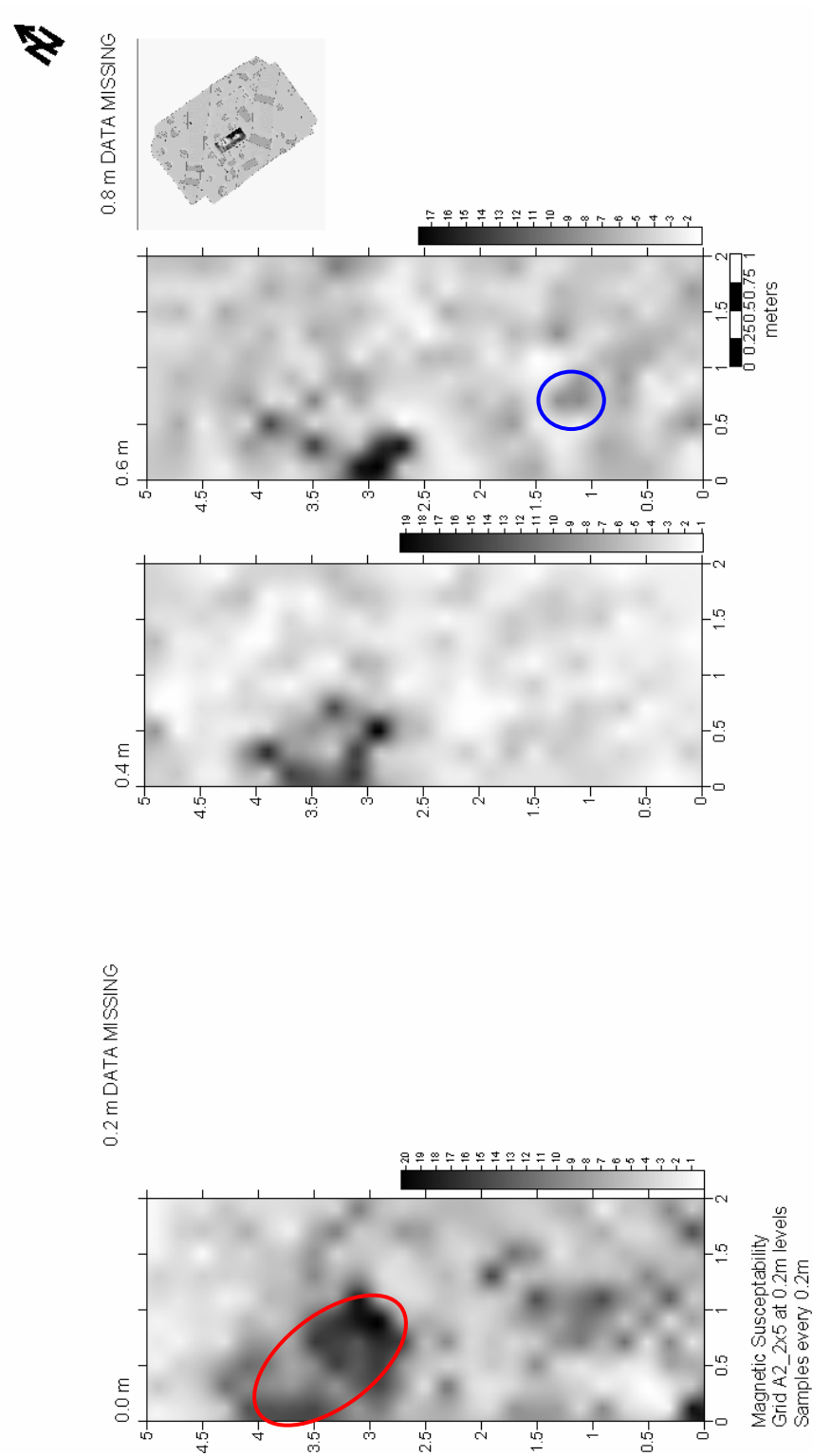


Figure 73. A2 2m x 5m sub-area magnetic susceptibility survey results.

The magnetic susceptibility maps showed the large pit feature (circled in red in the top layer) throughout all levels surveyed. The anomaly outlined in blue may represent the post-pit in the bottom of the sub-area.

5.2.5.2 Resistivity

Apparant Resistivity
Square Array with 0.25m probe spacing
Sample Spacing 0.25

Grid A_2
2x5 excavation test trench

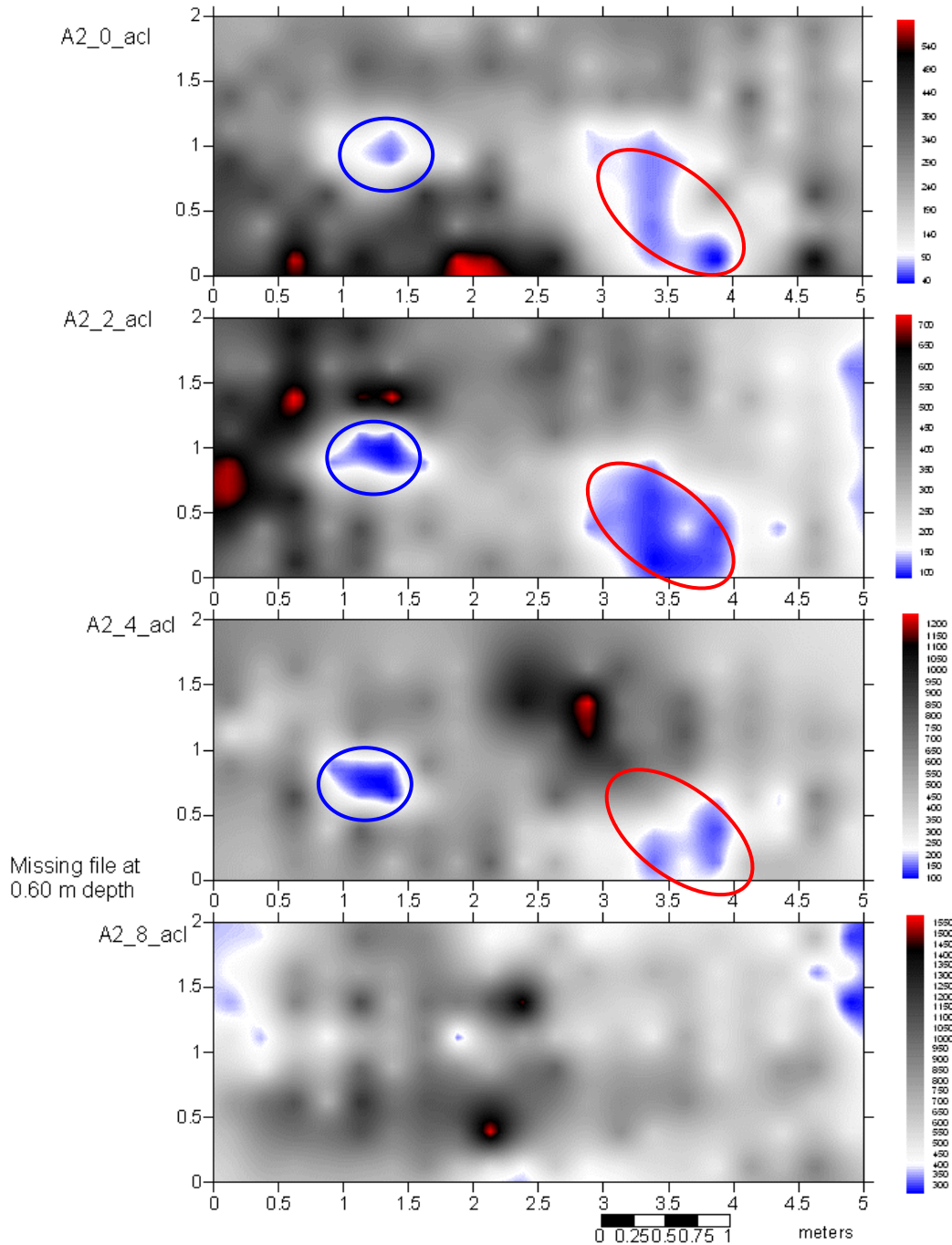


Figure 74. A2 2m x 5m sub-area resistivity survey results.

The apparant resistivity maps may show evidence for the large pit feature circled in red and the same post-pit that was mapped in the magnetic susceptibility survey, circled in blue.

5.2.5.3 Dielectric Permittivity

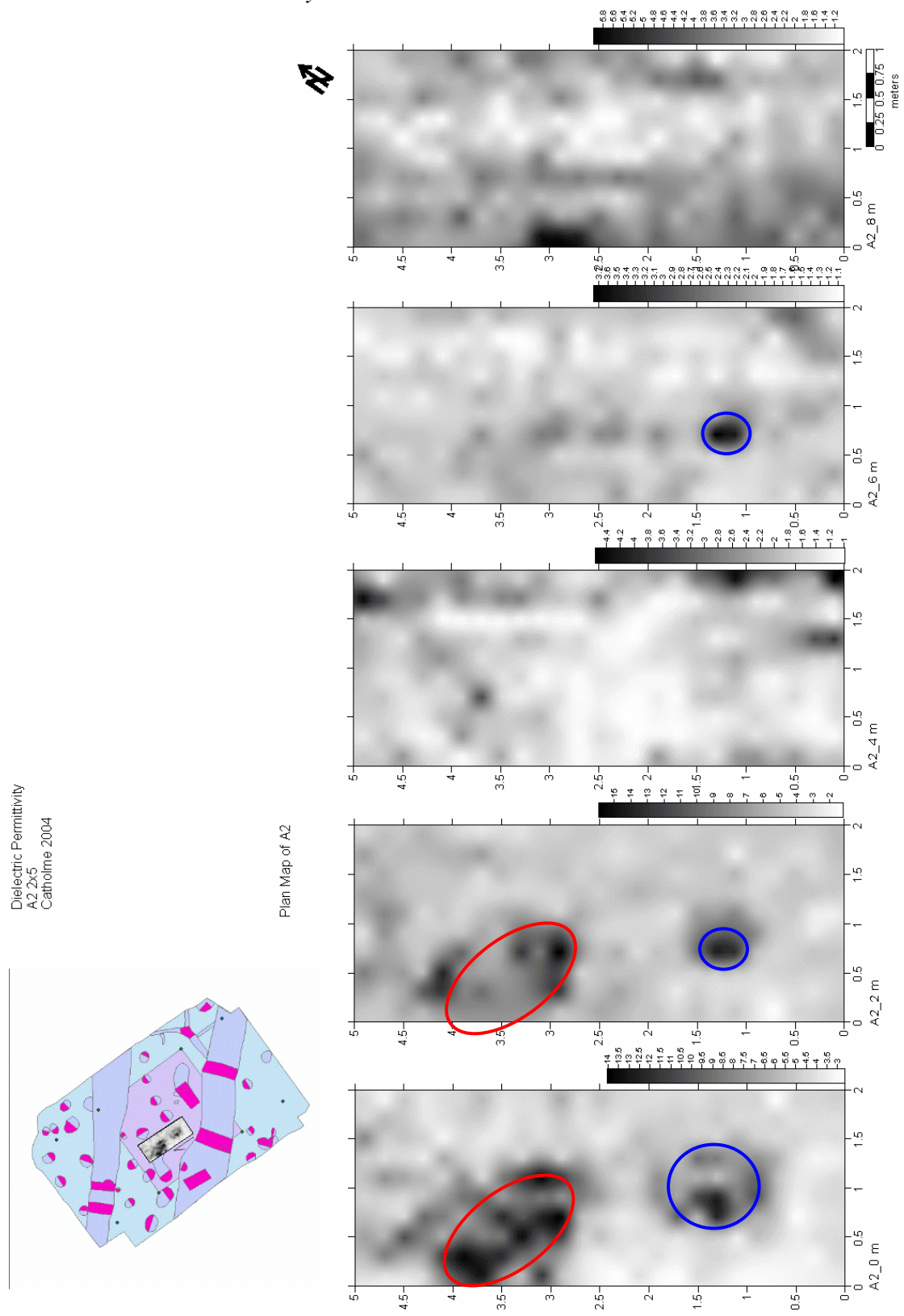


Figure 75. A2 2m x 5m sub-area dielectric permittivity survey results.

The dielectric permittivity maps showed evidence for the large pit feature circled in red and the same post-pit, circled in blue, that was mapped in the magnetic susceptibility and resistivity surveys.

5.3 Area B2

5.3.1 Magnetometry Survey Results

The surface magnetometry survey with the G858 was the best surface magnetic map for the entire Catholme surface survey in terms of positively identifying the underlying archaeological features. In this map the ring ditch (A), central burial (B) and area with *in situ* burning (D) are easily identified in figure 76.

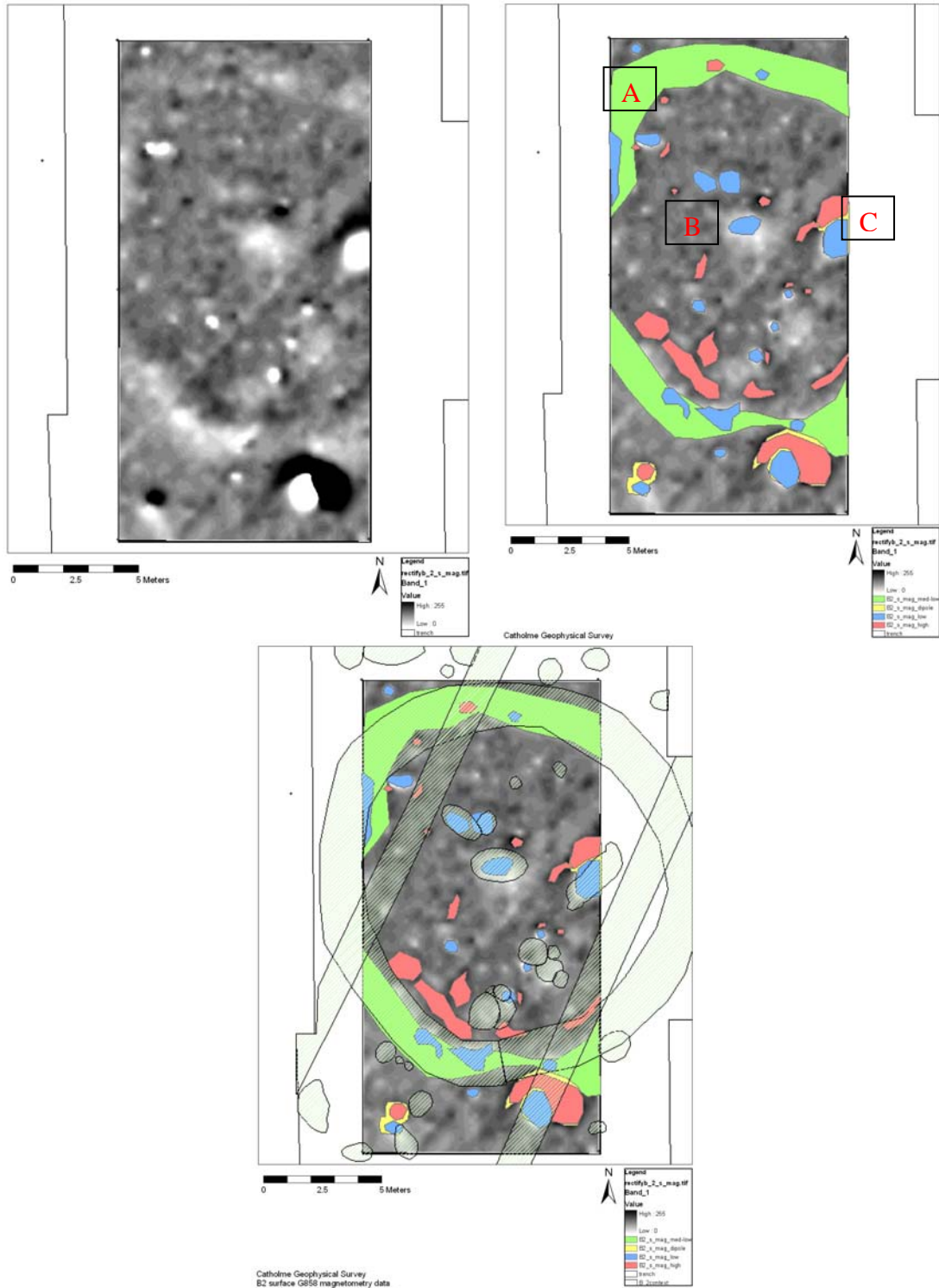


Figure 76. B2 surface magnetometry map (top left) with interpretations (top right) and overlain excavation plan (bottom left).

Re-survey after the removal of the topsoil provided a detailed and sensitive map of the magnetic properties of the archaeological features with little variation in the background material. The image below shows the detail of the magnetic field strength that defines each feature.

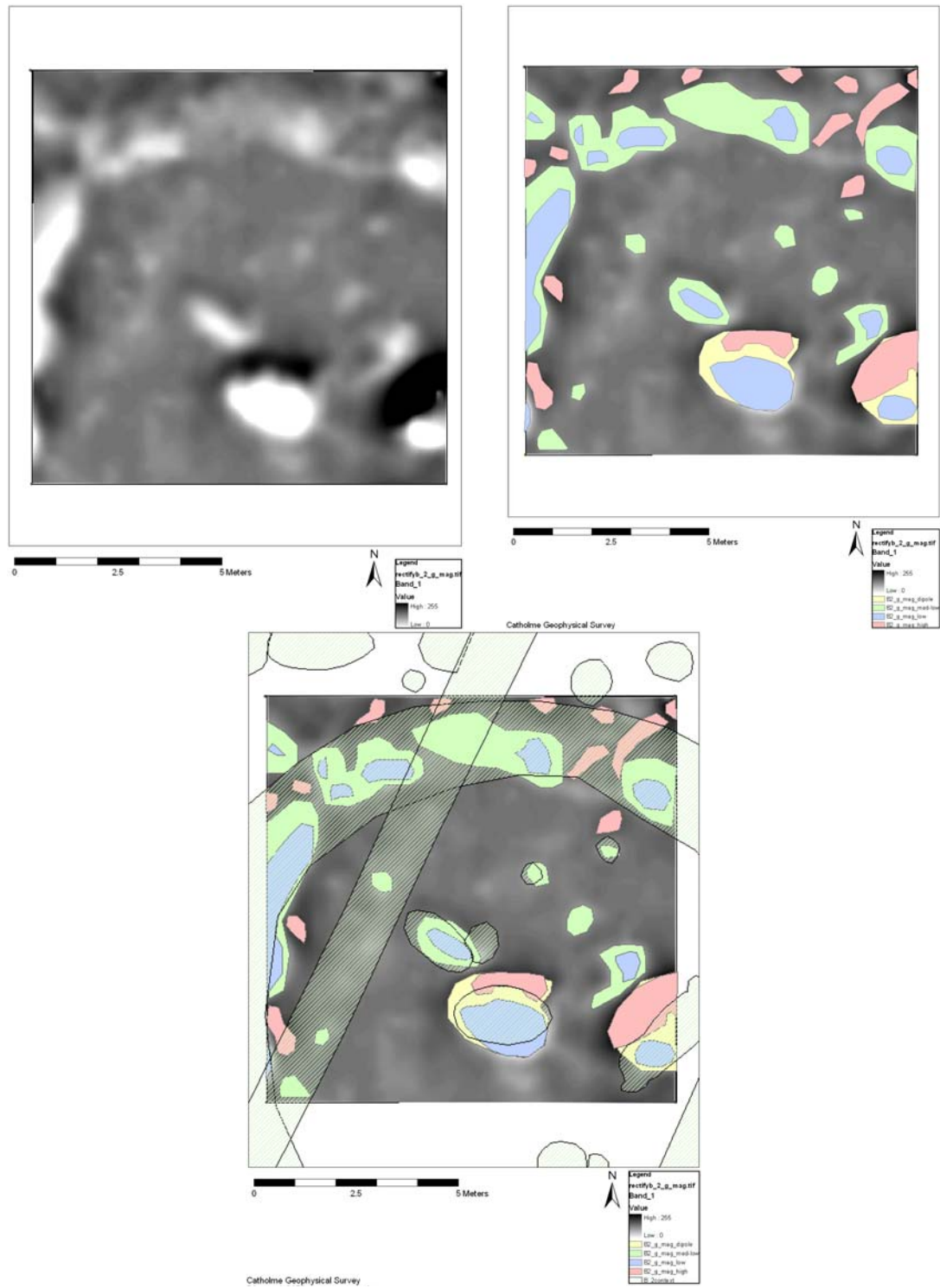


Figure 77. B2 gravel magnetometry map (top left) with interpretations (top right) and overlain excavation plan (bottom).

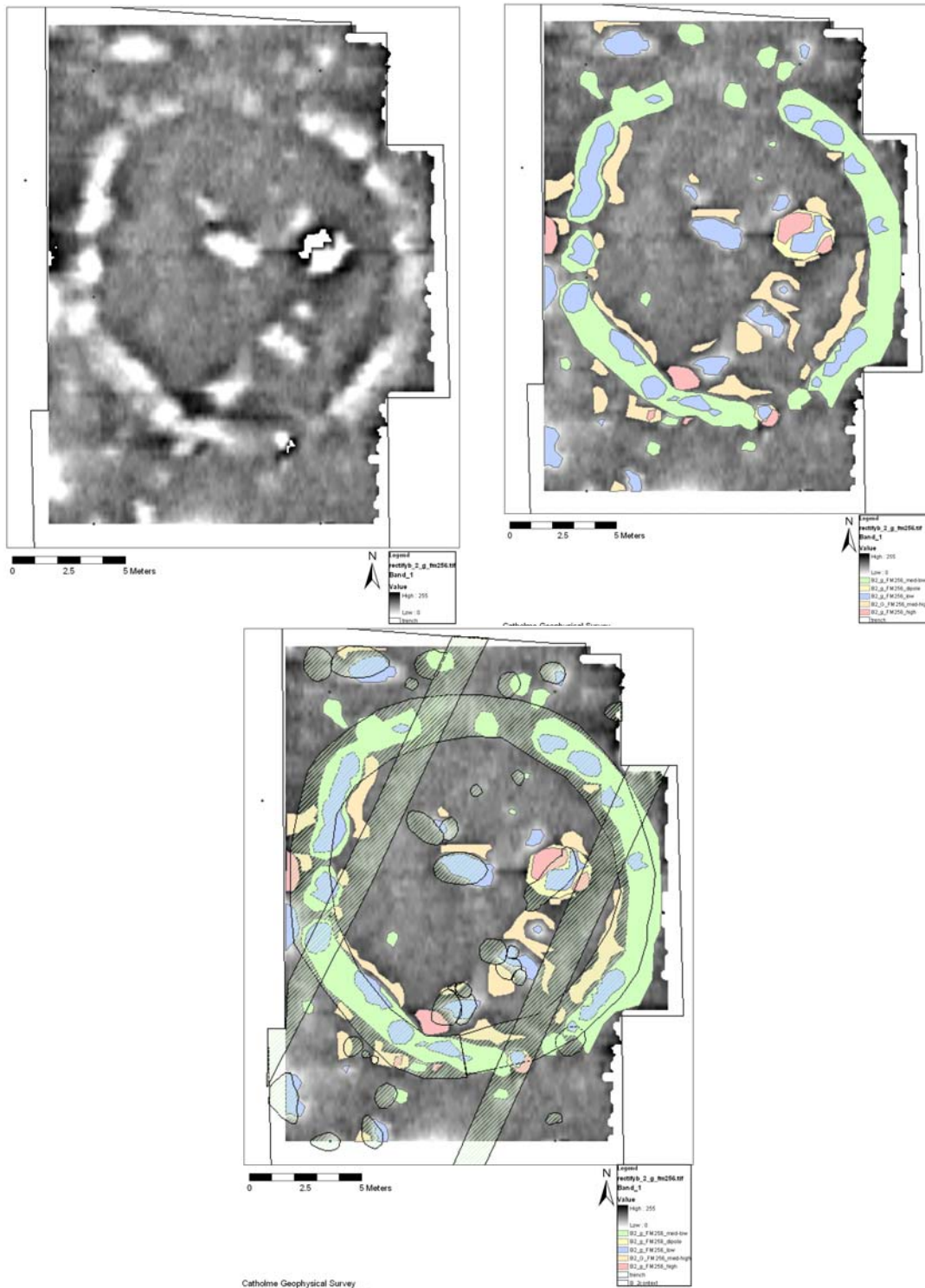


Figure 78. B2 gravel FM256 magnetometry map (top left) with interpretations (top right) and overlain excavation plan (bottom).

The natural subsoil magnetic surveys with the G858 and the FM256 (entire area survey) provided high quality magnetic maps of the ‘Sunburst’ feature. The irregular magnetic signature of the ring ditch suggested areas with concentrations of materials that have a lower magnetic value than the background. The features mapped through the magnetic survey include: the ring ditch, pits, post-holes, *in situ* burning, the central burial and detail into the magnetic structure of some of these anomalies.

Further integration of these maps with excavation results and other soil analysis methods should provide the background for a detailed understanding of the magnetic properties of the archaeological features and their relationship to the surrounding materials.

5.3.2 Magnetic Susceptibility Results

The magnetic susceptibility survey from the surface level of B2 did not reveal anomalies that could be identified as archaeological. The image below shows a random distribution of magnetic susceptibility properties.

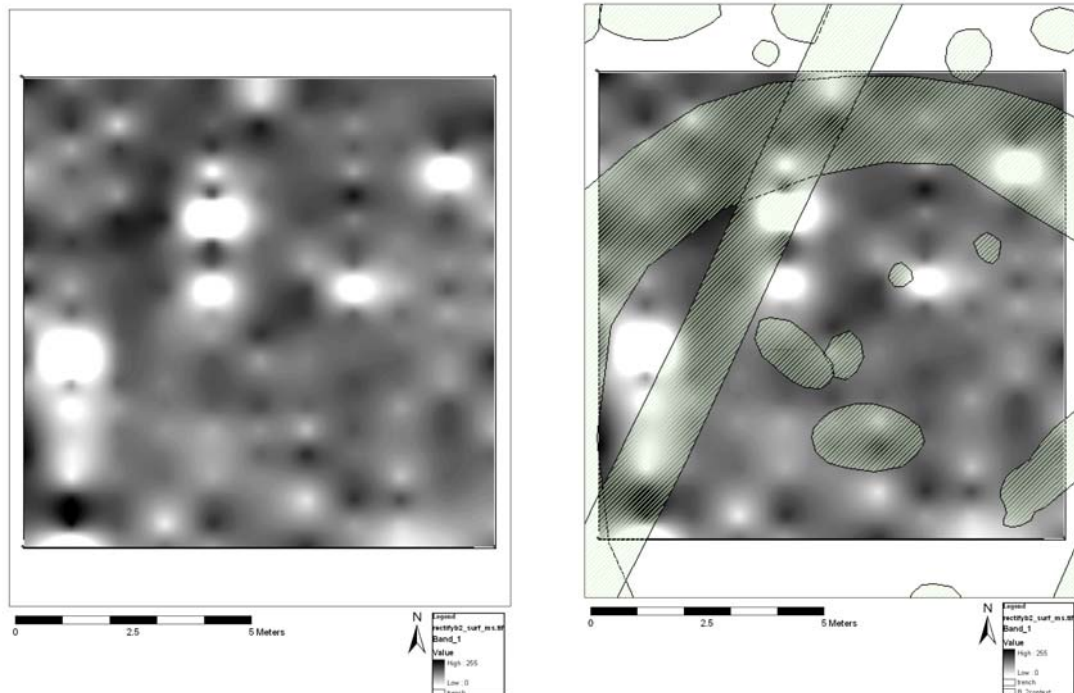


Figure 79. B2 surface magnetic susceptibility results (left) with overlain excavation plan (right).

The magnetic susceptibility map from the natural subsoil of B2 clearly delineated the ring ditch as a medium low feature with three separate areas of low susceptibility. The central burial also appeared clearly as a low susceptibility feature. The square-appearing white anomaly in the northeastern part of the area is most likely an artefact introduced through data interpolation.

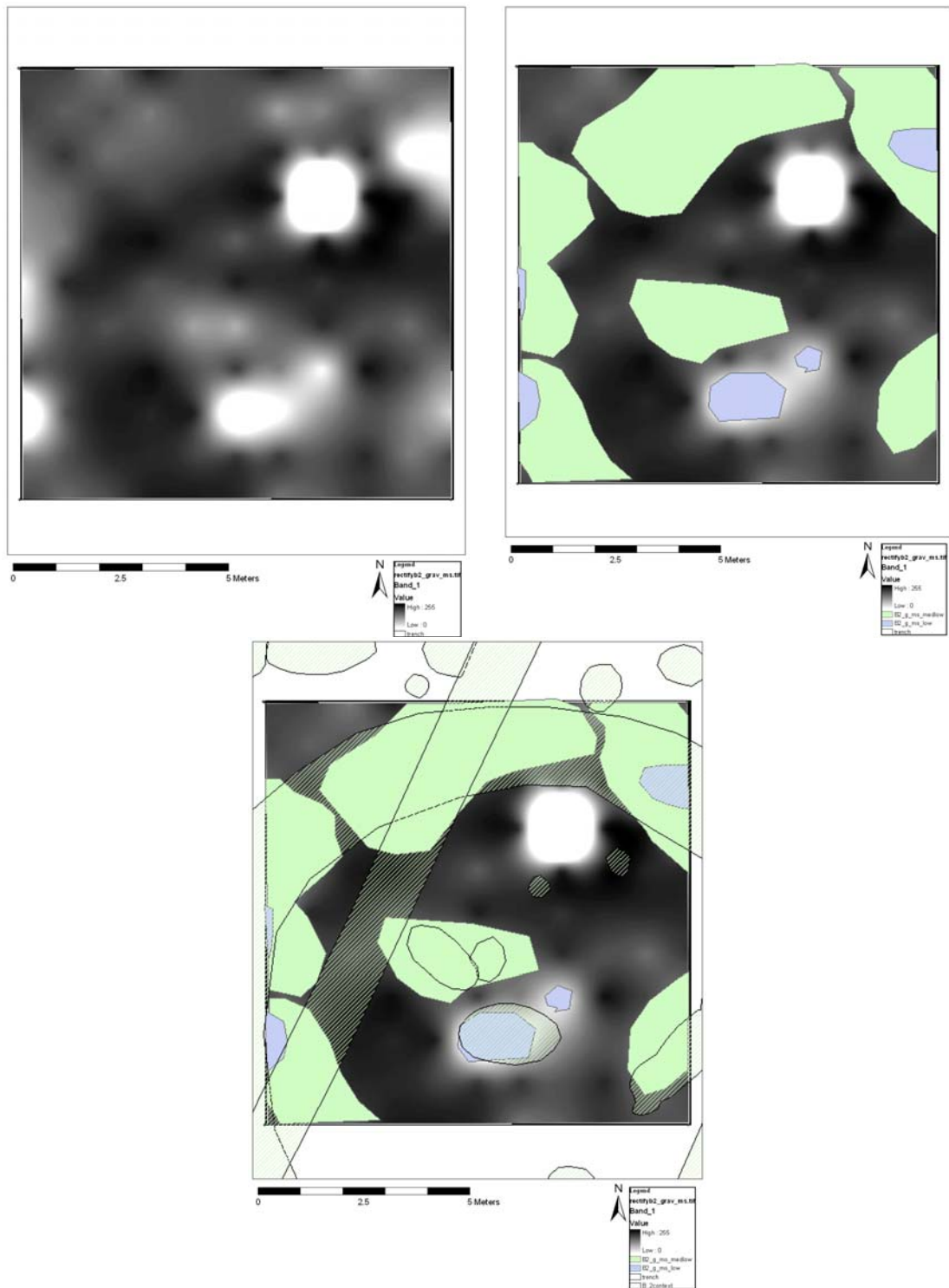


Figure 80. B2 gravel magnetic susceptibility results (left) with interpretations (right) and overlay excavation plan (bottom).

5.3.3 Resistivity Survey Results

The surface resistivity survey of B2 was not strongly affected by effects of ploughing (like surveys in field F and A1) but revealed more about the geological background of the area versus the archaeological features.

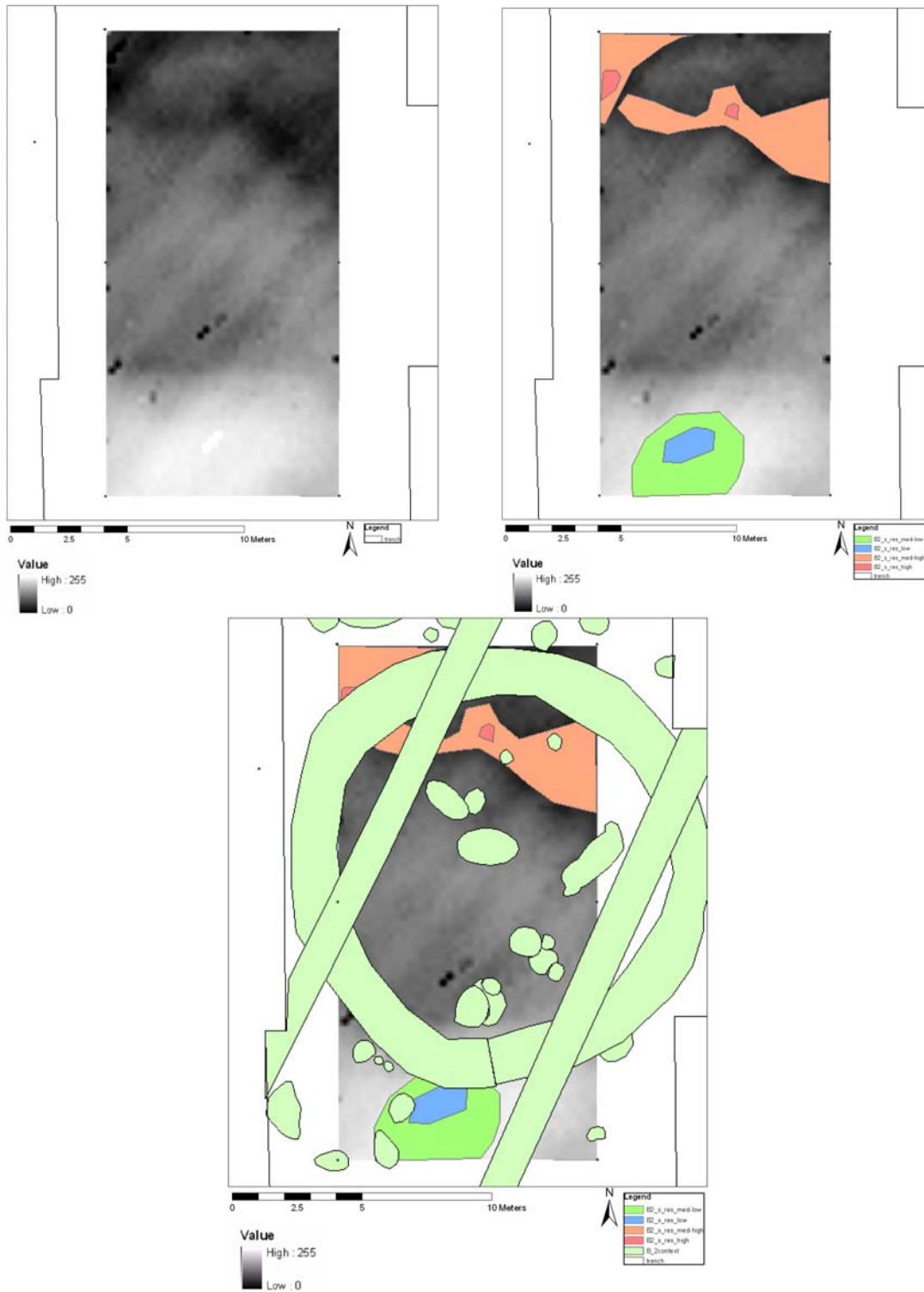


Figure 81. B2 resistivity surface survey (left) with interpretations (right) and overlain excavation plan (bottom).

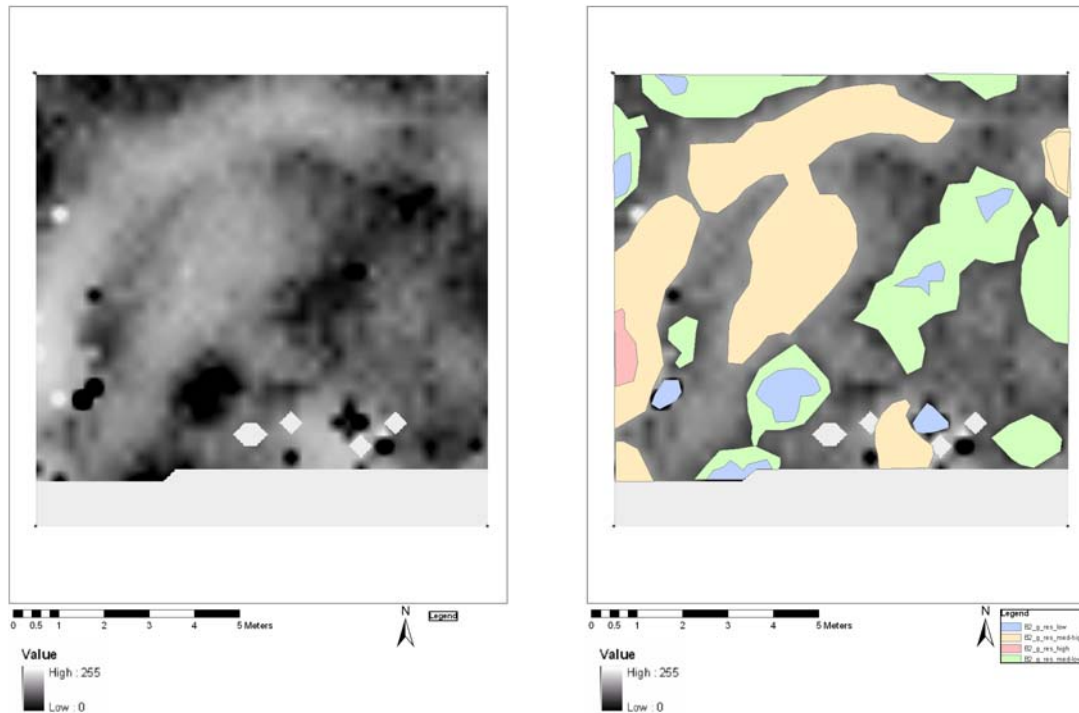


Figure 82. B2 resistivity gravel survey at 0.25m (left) with interpretations (right).

The gravel survey provided a good map of the archaeological features. The ring ditch was identified as a medium-low anomaly with one area of lower resistivity. Other pits and post-holes appeared, but did not coincide exactly with the archaeological plan. This may be attributed to issues with mapping discrepancies, the data collection method, or the fact that since they do not correspond with mapped features, some anomalies may simply represent variation in the background material resistivity.

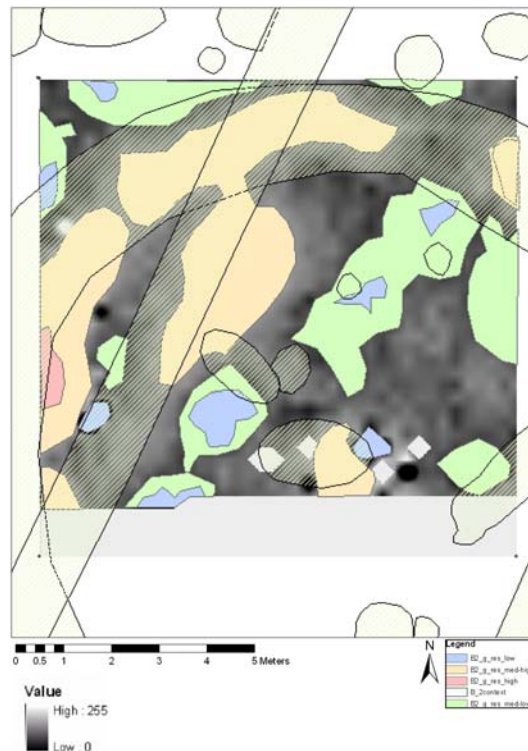


Figure 83. B2 resistivity gravel survey at 0.25m with interpretations and overlain excavation plan.

As depth increased the character and definition of the archaeological features changed so that at 1.25 and 1.50m depth the ring ditch properties inverted from low resistivity to medium-high. At this point however it is necessary to reiterate the issue of pseudosection inversion discussed in the A1 Resistivity Survey Results section before drawing detailed conclusions as to data interpretations.

5.3.4 GPR Survey Results

Surface GPR survey mapped the ring ditch clearly beginning at approximately 0.20m from the surface down to approximately 0.65m. The pit fill appeared as a low amplitude reflector in contrast to the slightly stronger reflection from the surrounding sandy gravels. Distinct areas of high amplitude reflectors appeared throughout the data from near surface to the bottom of the trace (approximately 2.25m deep). The distribution of these patches of high amplitude reflectors were clustered mainly within the area delineated by the ring ditch. The clustering of these anomalies helped identify the position of the ring ditch and geometric pattern suggested human impact in this area. Once the ring ditch no longer appears in the GPR data, at approximately 0.65m, the areas of high amplitude were more evenly distributed across the survey area and suggested a natural geological cause.

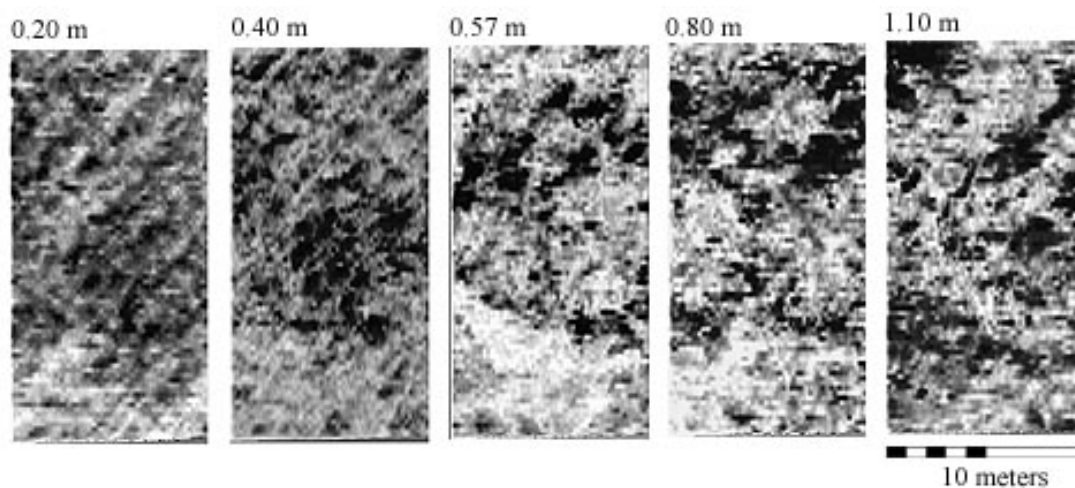


Figure 84. B2 surface GPR plan views showing the appearance of the ring ditch.

Though the ring ditch was visible it is not a distinct circular looking anomaly. The central burial was not clearly visible in the data nor were the pits that are present in the survey area. This may be a result of the GPR not being able to distinguish between the topsoil and the pit fill materials.

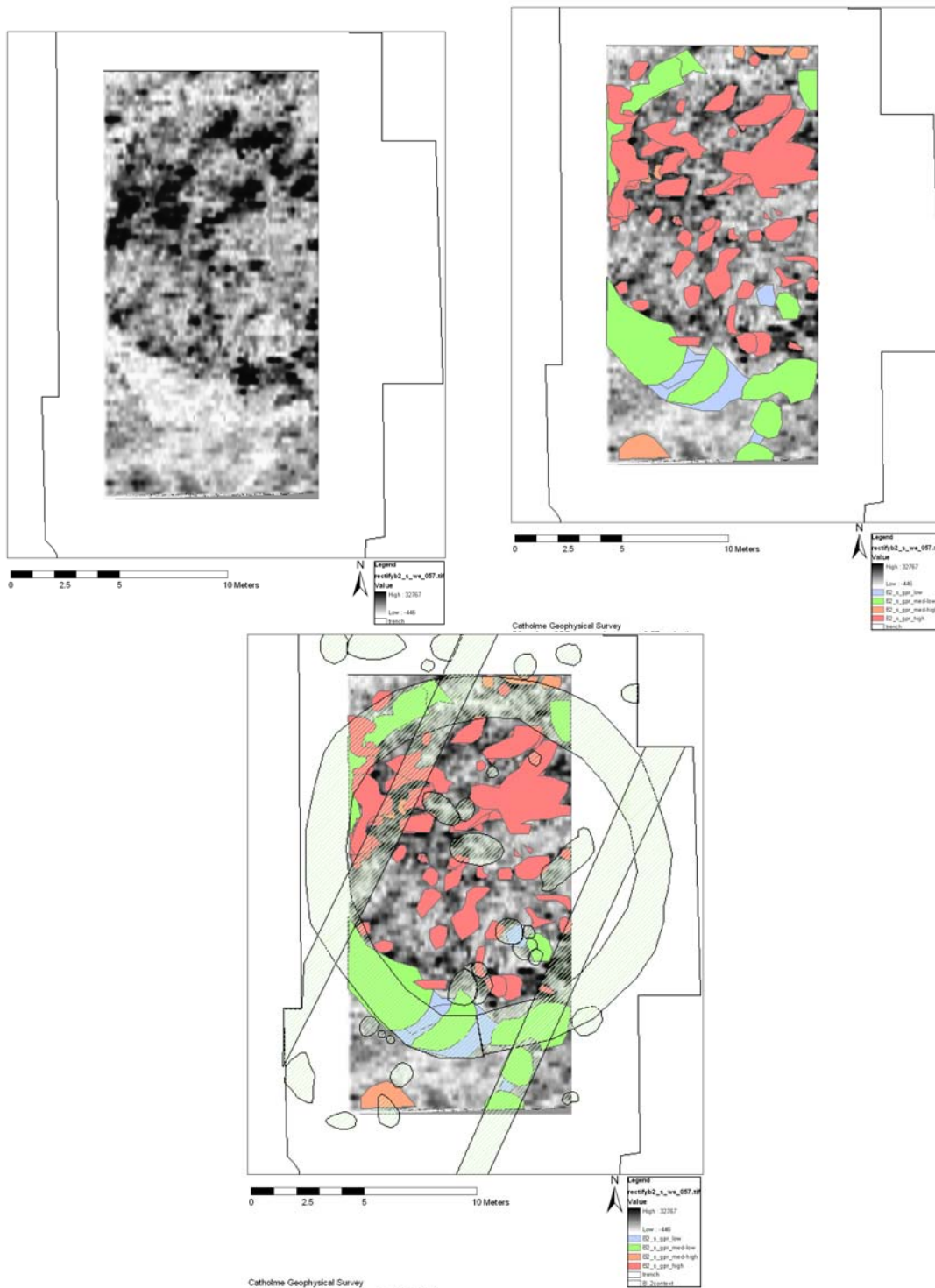


Figure 85. GPR surface survey plan map at 0.57m (left) with interpretations (right) and excavation plan (bottom).

The ground coupling map of the B2 gravel survey clearly delineated all of the archaeological features visible. The map also contains additional information that reflected the geological nature of the surface.

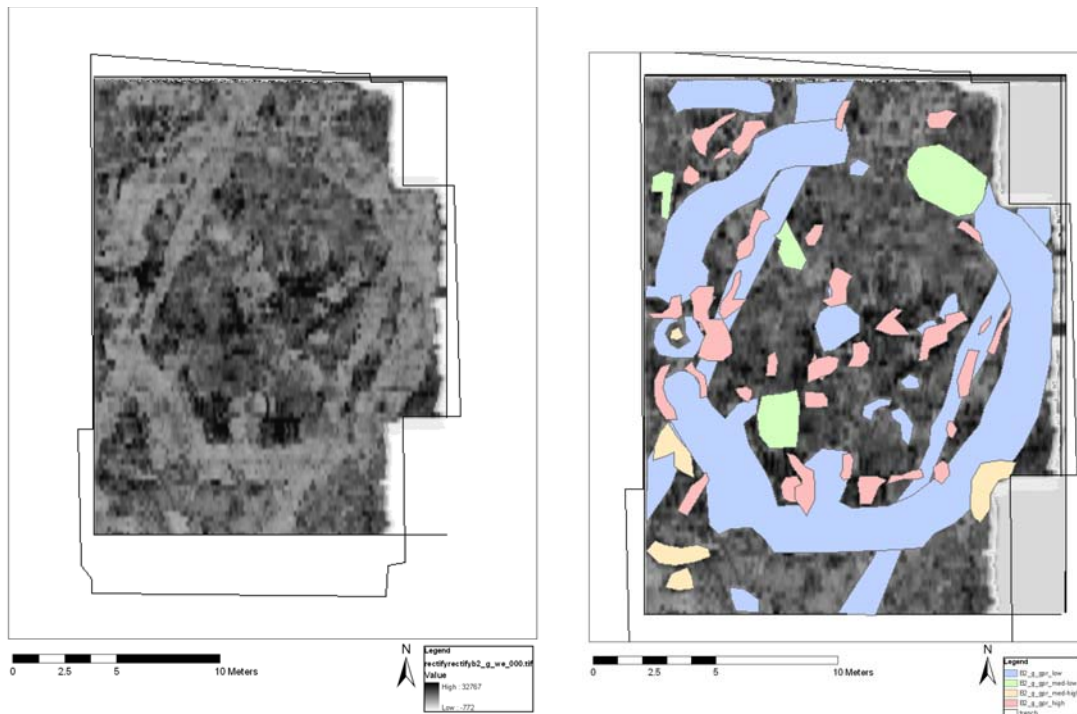


Figure 86. B2 'Sunburst' Monument. GPR record from the ground coupling signal (left) with interpreted archaeological and geological features (right).

Below the coupling zone, the archaeological features were not clearly delineated until approximately 0.3m depth. In this instance, the ring ditch was apparent, but may be difficult to identify without background knowledge of both the archaeological feature and GPR.

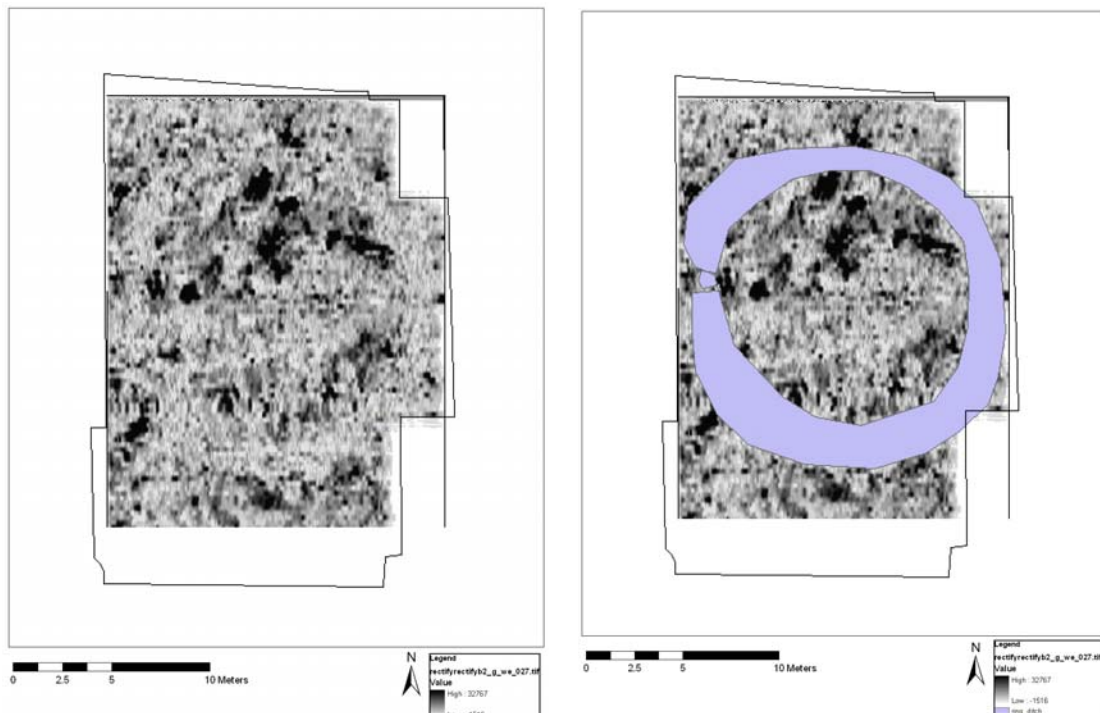


Figure 87. B2 'Sunburst' Monument ring ditch in GPR data.

As can be seen in the data above, the ring ditch was defined by a low amplitude reflector at this depth. Better definition of the ring ditch can be seen at approximately 0.4m depth with a distinct contrast between ditch fill and the background sandy gravel in material. This appears only in some sections of the ditch while in others, the definition of the ring ditch was lost because of the lack of contrasting properties between the ditch fill and surrounding materials.

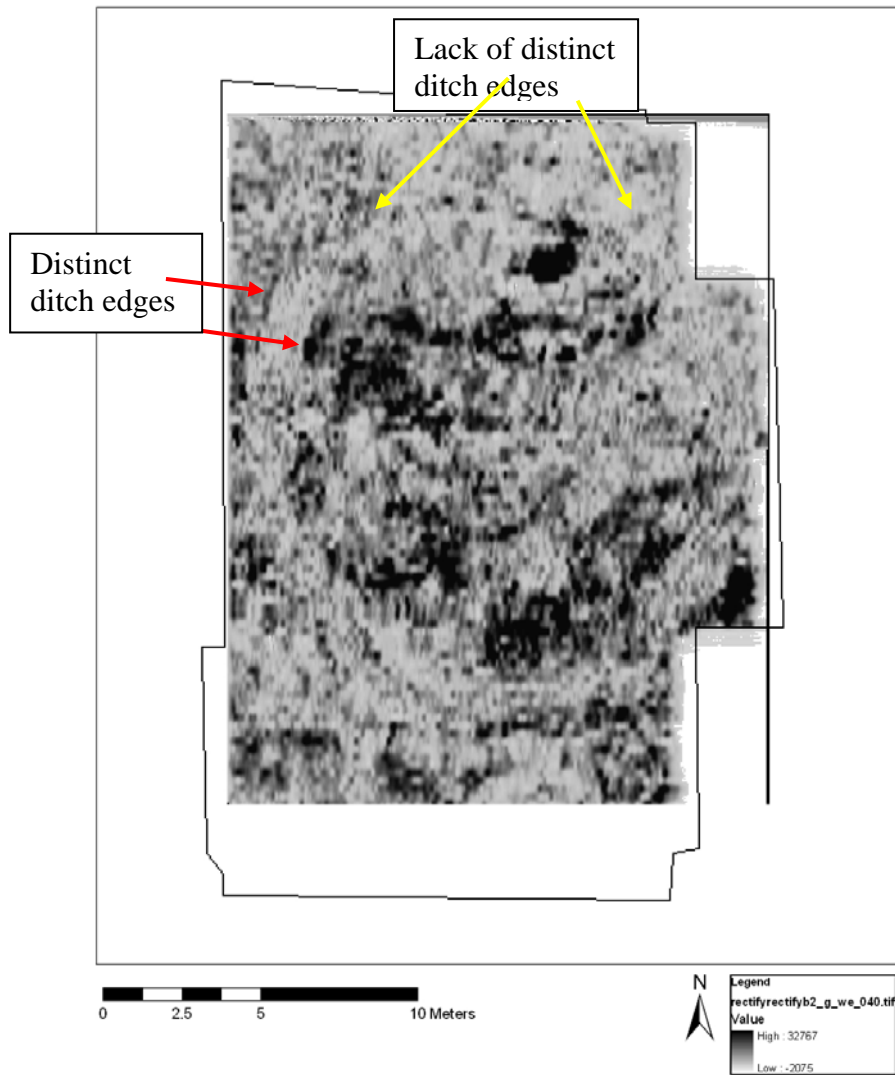


Figure 88. B2 'Sunburst' monument GPR data at 0.4m depth showing distinct ring ditch property contrasts with background material (red arrows) and the lack of contrast and ditch definition (yellow arrows).

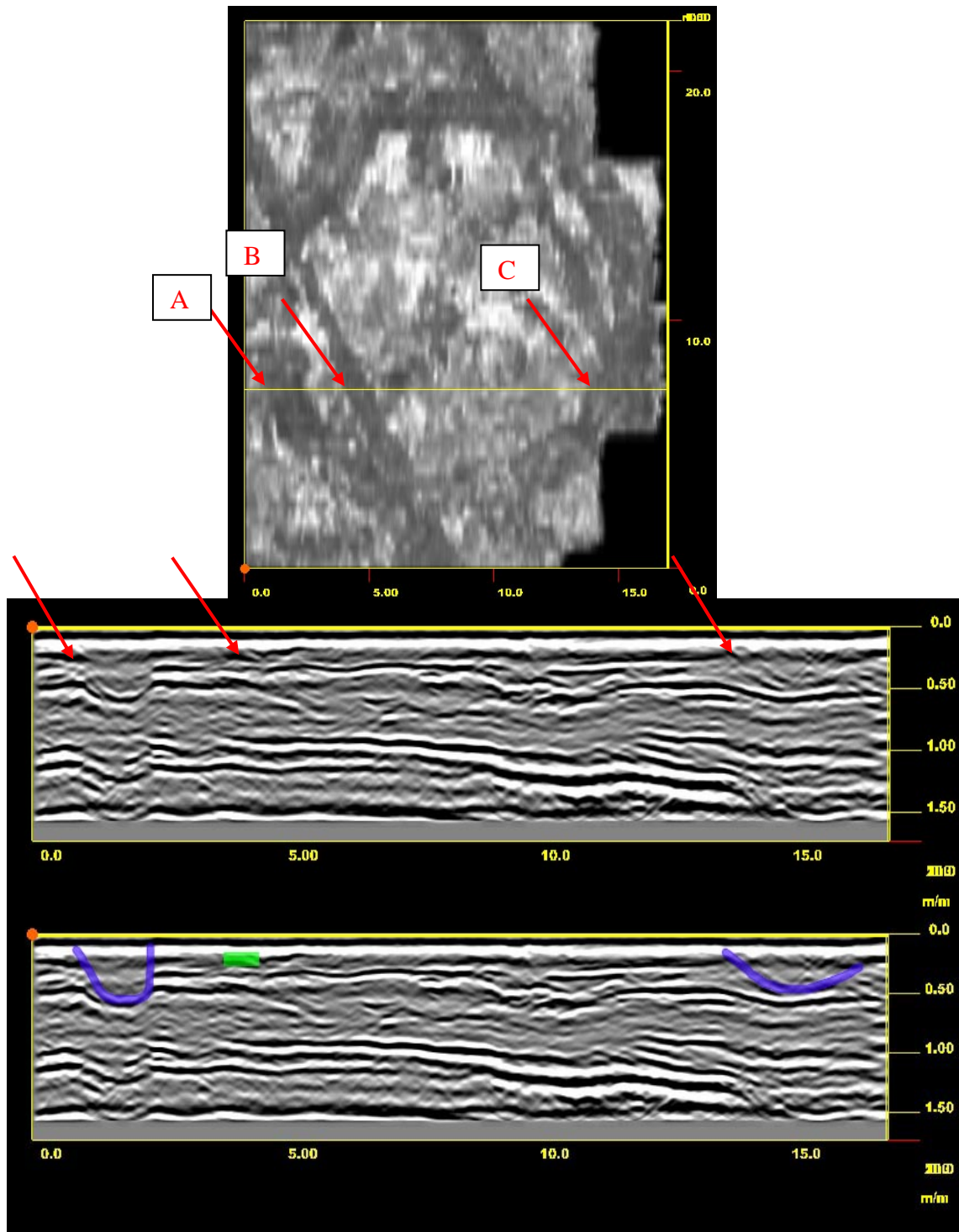


Figure 89. B2 GPR image of profile through ring ditch. A and C are the ring ditch (blue) and B is one of the plough furrows (green) passing through the ring ditch.

The ring ditch has many variations in structure. The example in figure 89 shows two sections of the ring ditch that have different constructions. The western side, A, is a deep, well defined anomaly where C on the eastern side is not as well defined and could be challenging to interpret as a ring ditch if supplementary information was not available. The plough furrow running through the ring ditch barely appears in the GPR profile, and would not be recognisable in this format. As with the pits in A1, examination of the GPR profiles can provide additional detail and information on the

structure and possible fill characteristics of archaeological features such as the ring ditch.

Another GPR profile provides a cross-section of a pit that appears on the western side of the ring ditch situated between two terminus points of the ditch. This profile also crosses over the burial anomaly, the ditch with the *in situ* burnt wood, the plough furrows and the eastern edge of the ring ditch.

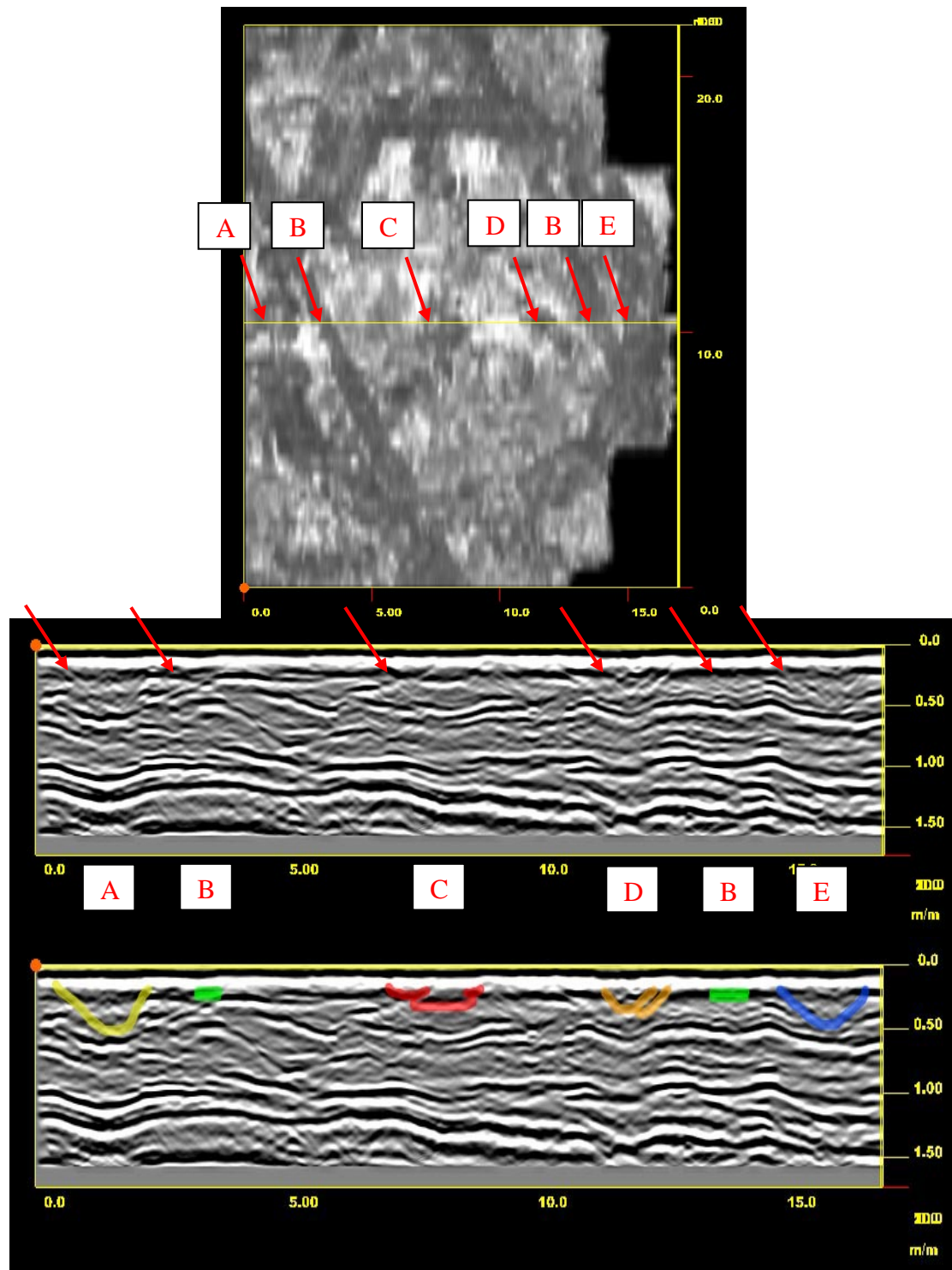


Figure 90. B2 GPR profile through archaeological features: A - pit, B- plough furrow, C- burial, D- pit with *in situ* burning, E- ring ditch.

Figure 90 shows a profile of GPR data cutting through the centre of the ring ditch passing through different types of archaeological features including: A – pit, B – plough furrow, C – burial, D – pit with *in situ* burning and E – the ring ditch. All the features have been highlighted in the bottom image of the figure. As with the example in Figure 89 above, the pit and ring ditch have similar appearing anomalies. This is not surprising as, taken in profile, theoretically they should have a similar form. The plough furrows are difficult to recognise in the data; the one to the east is not visible at all even as a slight disturbance in the radar profile. The plough furrow at these points is not recognisable in the radar profile. The pit with the *in situ* burning can be identified, as can the burial, but both of these features would be difficult to discern as archaeological in nature without previous knowledge of feature positions. Due to the background structure of the survey area with inter-bedded sands, gravels and silts it is difficult to extract the more ephemeral anomalies and to then interpret them as archaeological features from vertical profiles. Consideration of both the vertical profiles and plan views provides the most effective interpretation for the archaeological nature of the GPR data in B2.

5.3.5 B2 2m x 5m Sub-area

5.3.5.1 Magnetic Susceptibility

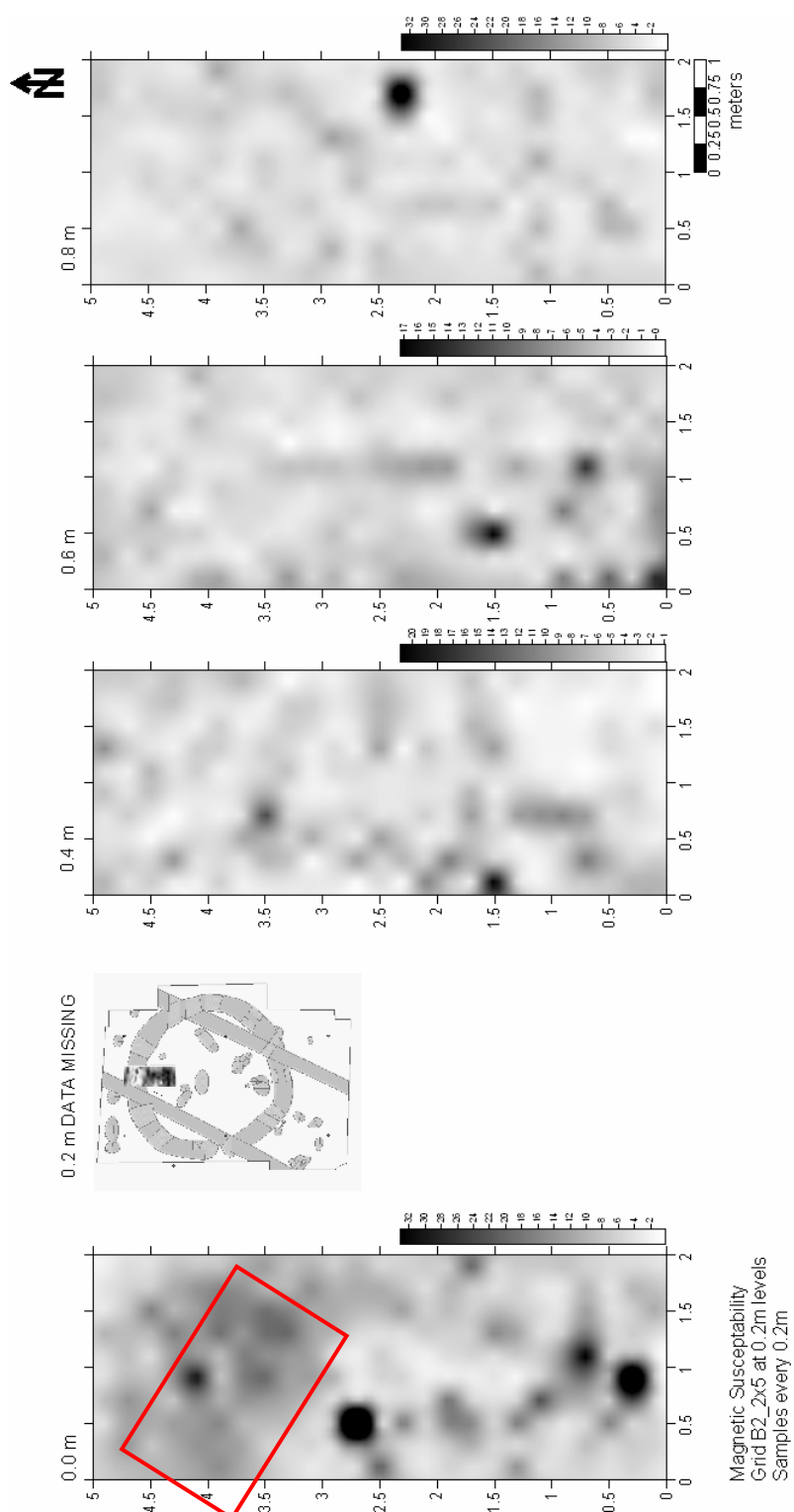


Figure 91. B2 2m x 5m magnetic susceptibility survey results.

The natural subsoil magnetic susceptibility survey mapped the ring ditch, as is outlined in red.

5.3.5.2 Resistivity

Apparant Resistivity
 Square Array with 0.25m probe spacing
 Sample Spacing 0.25

Grid B_2
 2x5 excavation test trench

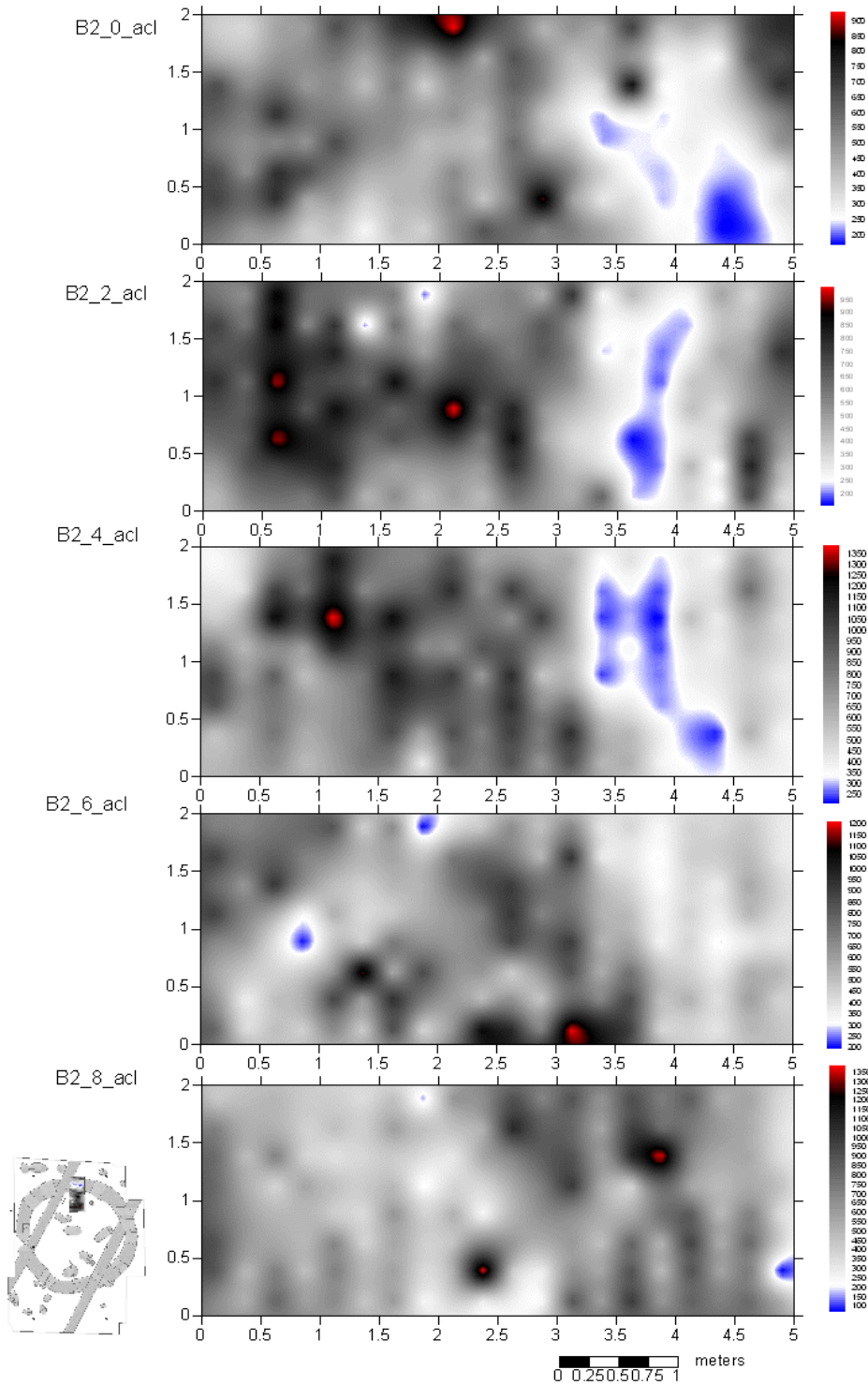


Figure 92. A1 2m x 5m resistivity survey results.

The resistivity results mapped the ring ditch down to 0.6m as a low resistivity anomaly (blue).

5.3.5.3 Dielectric Permittivity

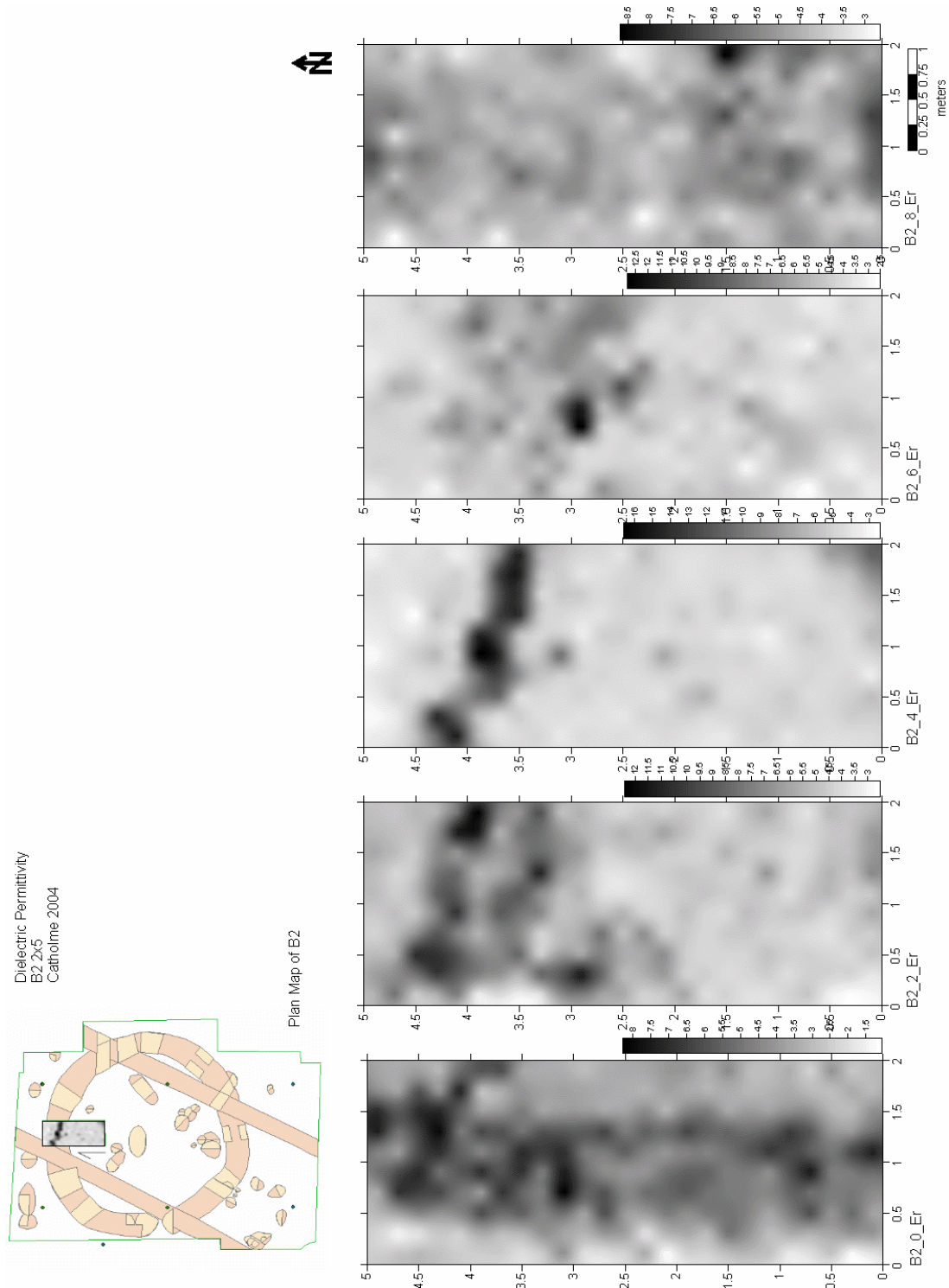


Figure 93. B2 2m x 5m dielectric permittivity survey results.

The results from the dielectric permittivity survey mapped the ring ditch from the ground surface through to 0.6m depth. The dielectric permittivity was mapped as a strong (high) feature that represents the moisture maintained within the ditch fill. The pattern that this follows of a relatively narrow line that defines the ditch was probably related to the shape of the feature and the rate at which it was drying with removal of the topsoil and each subsequent level.

5.4 Area F1

5.4.1 Magnetometry Survey Results

The surface magnetometry survey of area F1 did not reveal any archaeological information. The interference from data spikes that were probably ferrous material in the topsoil overshadowed any weaker underlying magnetic anomalies.

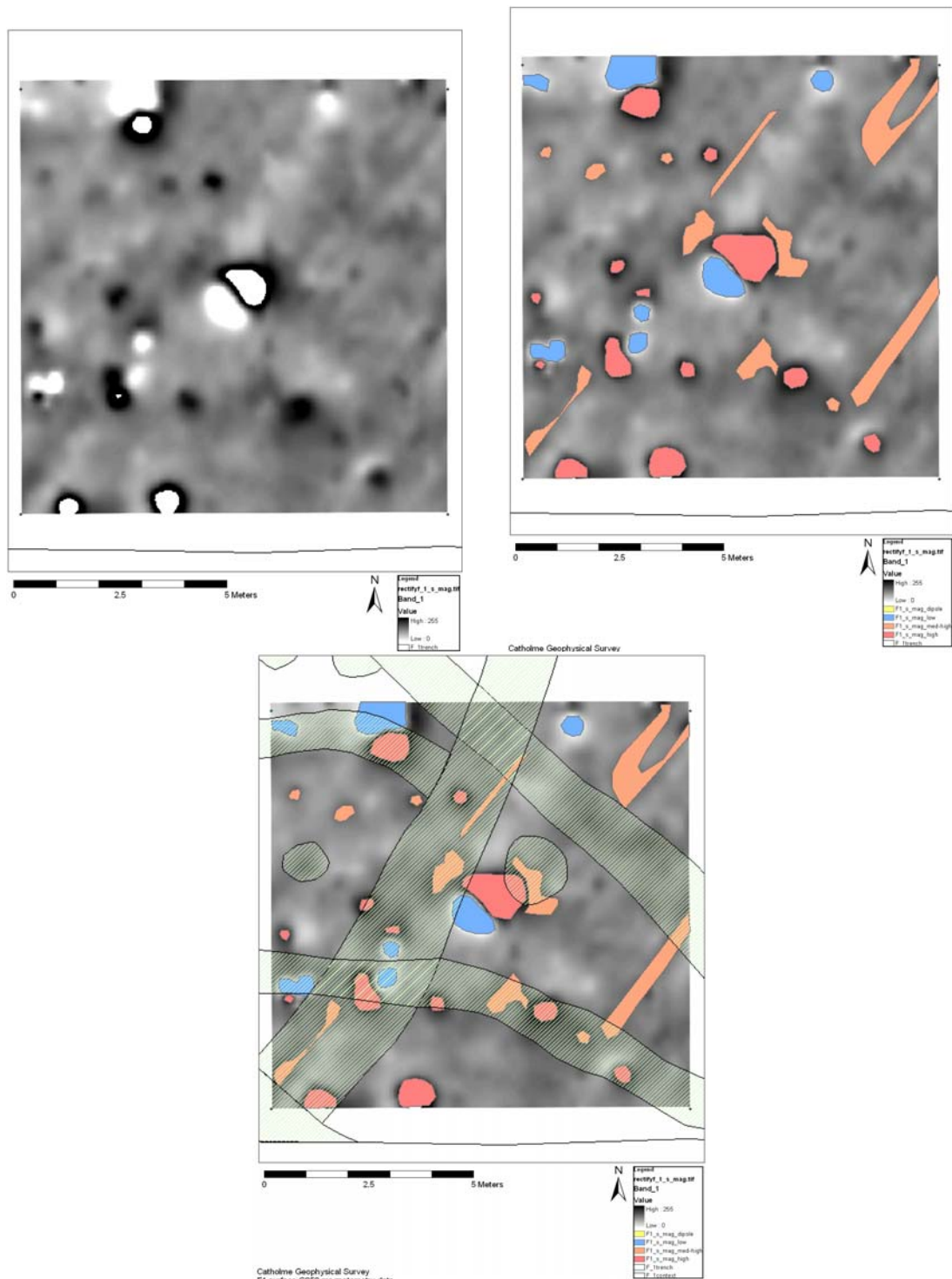


Figure 94. F1 surface magnetometry map (top left) with interpretations (top right) and overlain excavation plan (bottom).

After the removal of the topsoil the magnetic survey clearly mapped the visible archaeological features including the ring ditch, pits and the linear features that extend to the east of the ring ditch. Further correlation of this data to other geophysical results, excavation information and results from further soil analysis should produce a better understanding of the nature of the archaeological features.

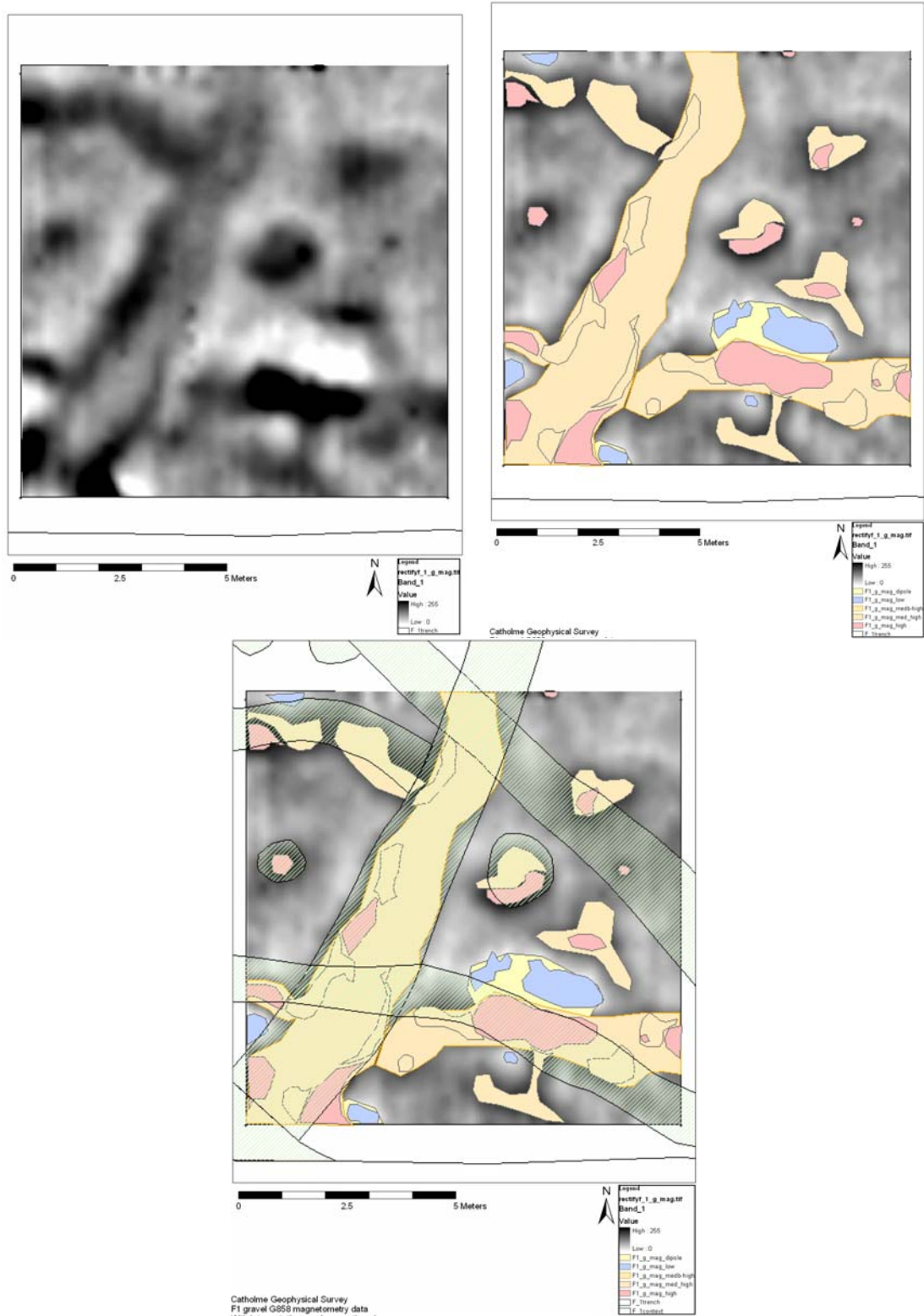


Figure 95. F1 gravel magnetometry map (top left) with interpretations (top right) and overlain excavation plan (bottom).

5.4.2 Magnetic susceptibility Results

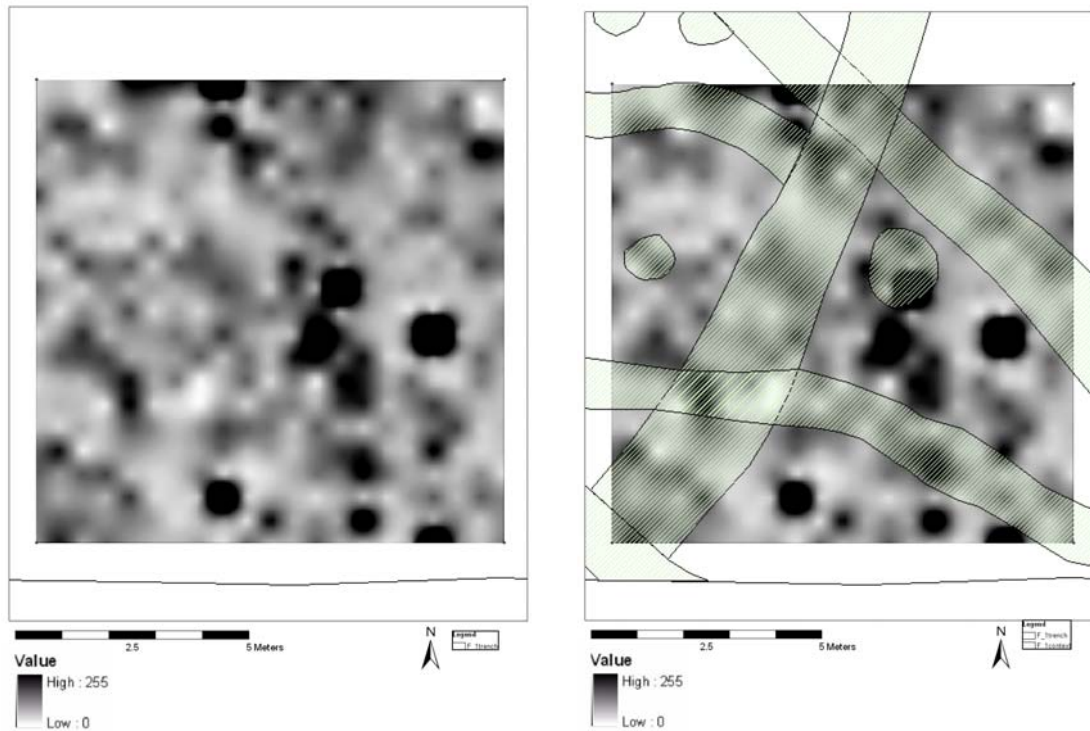


Figure 96. F1 surface magnetic susceptibility results (left) with overlain excavation plan (right).

Results from the F1 surface magnetic susceptibility survey did not present recognisable archaeological anomalies.

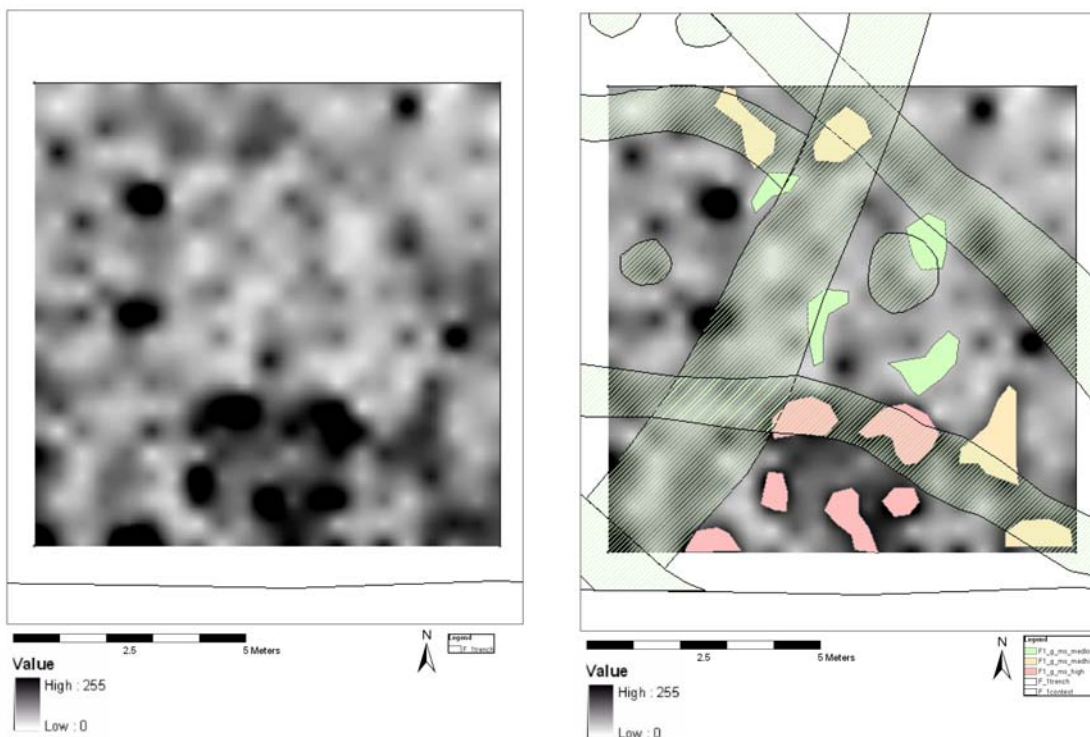


Figure 97. F1 gravel magnetic susceptibility results (left) with overlain interpretations and excavation plan (right).

Results from the F1 gravel magnetic susceptibility survey did not present recognisable archaeological anomalies.

5.4.3 Resistivity Survey Results

The resistivity results from F1 were strongly influenced by recent ploughing activity that can be seen in data as diagonal lines oriented northeast to southwest. Effects from this ploughing were seen throughout all of the surface resistivity survey files. It is important to keep in mind while examining this data that the pseudo-sections, or vertical profiles of data, have not been inverted and thus artefacts are present in the data that are caused by surface features.

The surface survey resistivity data had one linear anomaly that crossed through the survey area from the northwest to southeast and was visible in the 0.25 and 0.50 depths. Comparison to the archaeological plan shows a similar feature less than a metre to the east of the anomaly. This survey was in the area where the two extending linear features cross the large ring ditch. The geophysical survey from Phase I investigations showed numerous anomalies in this area.

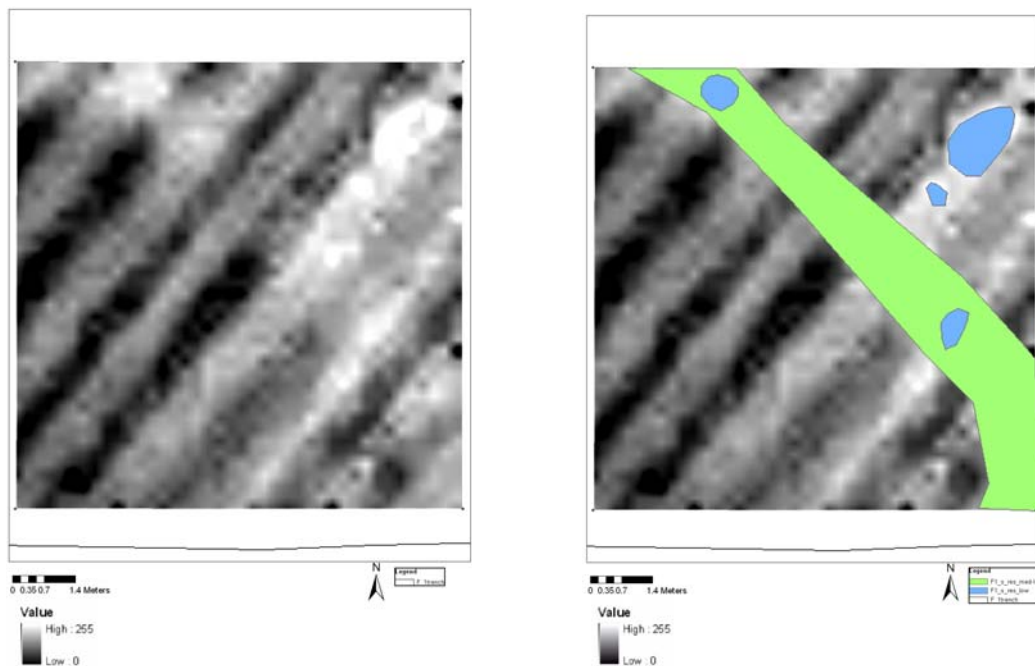


Figure 98. F1 resistivity map at 0.25m depth (left) with interpretations (right).

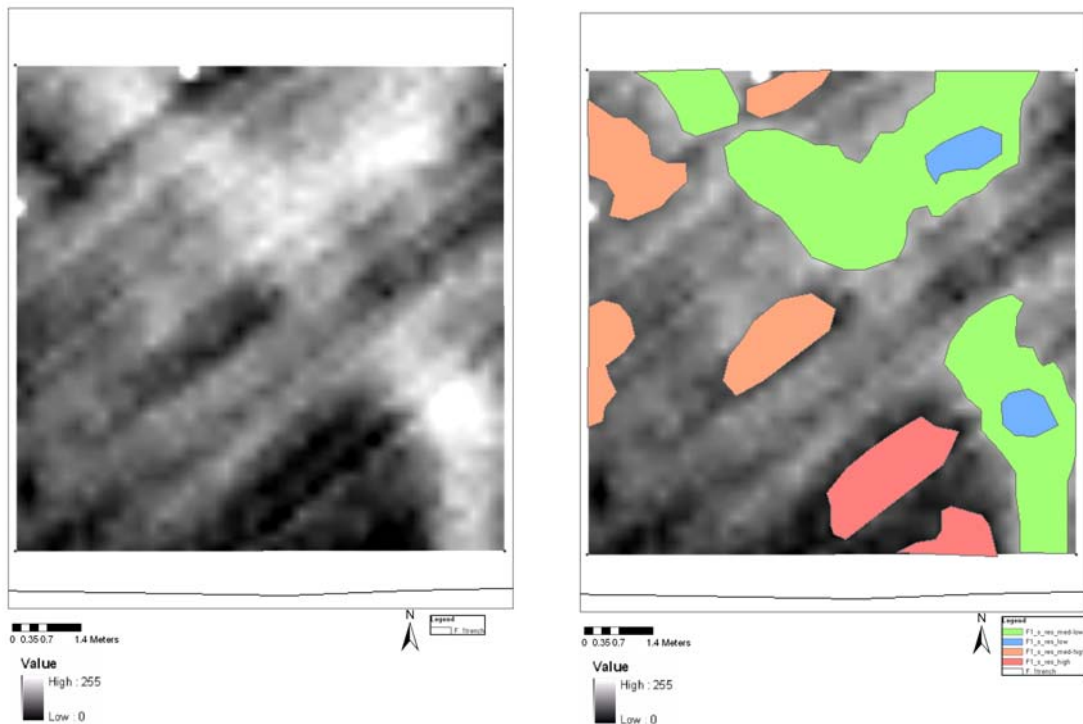


Figure 99. F1 resistivity map at 0.50m depth (left) with interpretations (right).

The linear feature that appeared near to the surface in the resistivity survey did not appear to correspond with the ring ditch, but it may be part of the linear features extending from the ring ditch. The image below overlays the excavation plan on the interpreted anomalies.

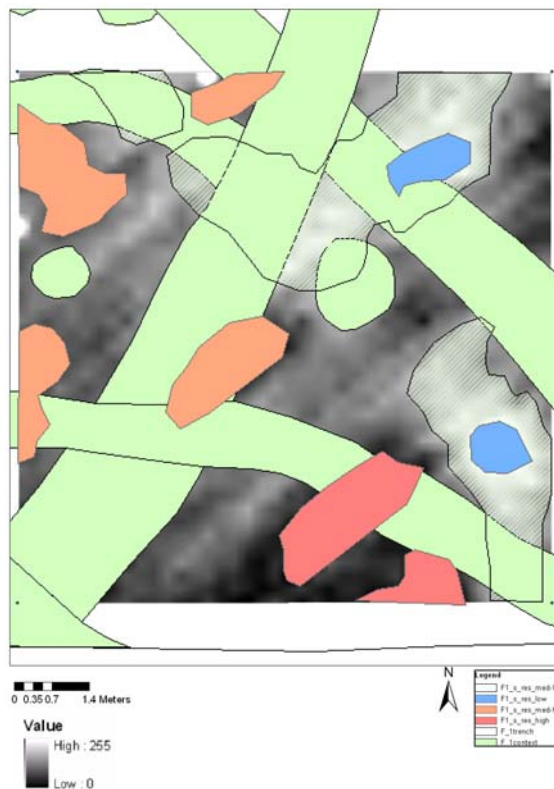


Figure 100. F1 resistivity survey at 0.50m depth with overlain interpretations and excavation plan.

The gravel resistivity survey revealed the same linear anomaly as the surface survey, crossing the area northwest to southeast. A second linear anomaly may define the ring ditch, though the west edge of the anomaly follows closely along the plough furrow orientation and may be an artefact related to the ploughing. The first evidence of other probable archaeological features appeared at 0.75m and remained in the data to the bottom of the profile (1.50m). The two additional features are interpreted as a pit in the middle of the survey area and the second linear extension feature that appears to the south of the first.

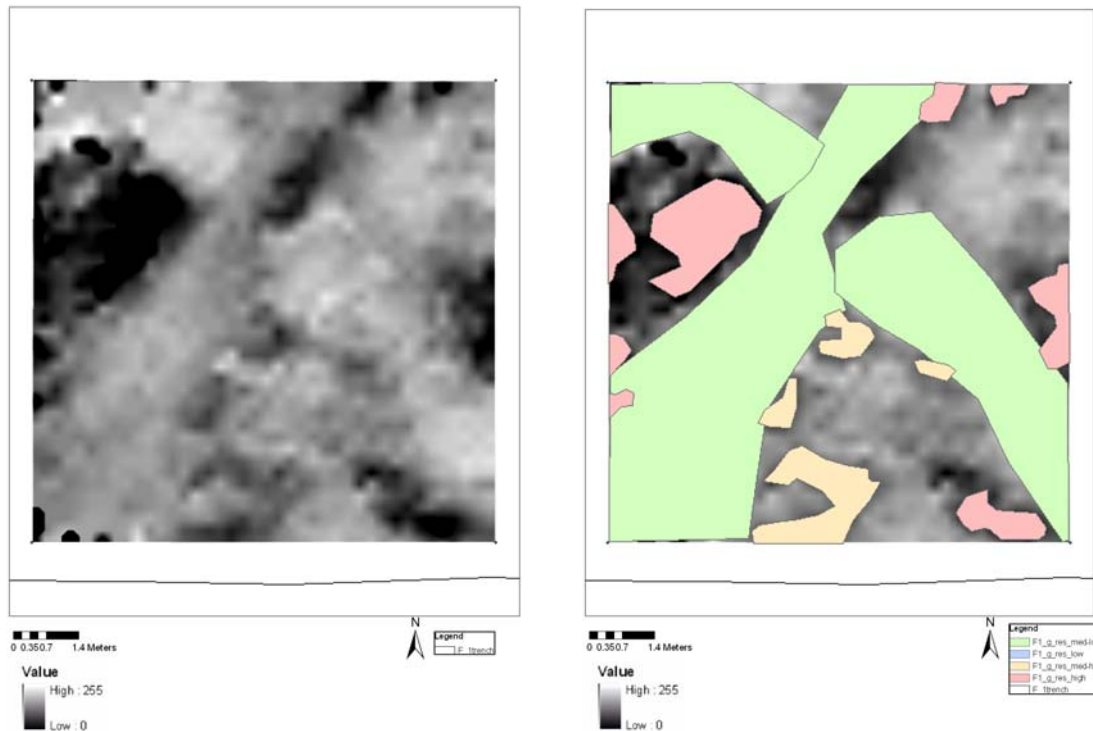


Figure 101. F1 resistivity gravel survey at 0.50m (left) with interpretations (right).

This survey area contained a complex grouping of potential archaeological features as can be seen in the archaeological record. Features are a mix of a substantial ring ditch, that barely appears in the resistivity data; 2 linear features that extend from the ring ditch enclosure, both are identified archaeologically as ditches and both appear in the resistivity data with different signatures and at different depths; and one of the main pits in this area can be seen in the resistivity data beginning at 0.75m depth.

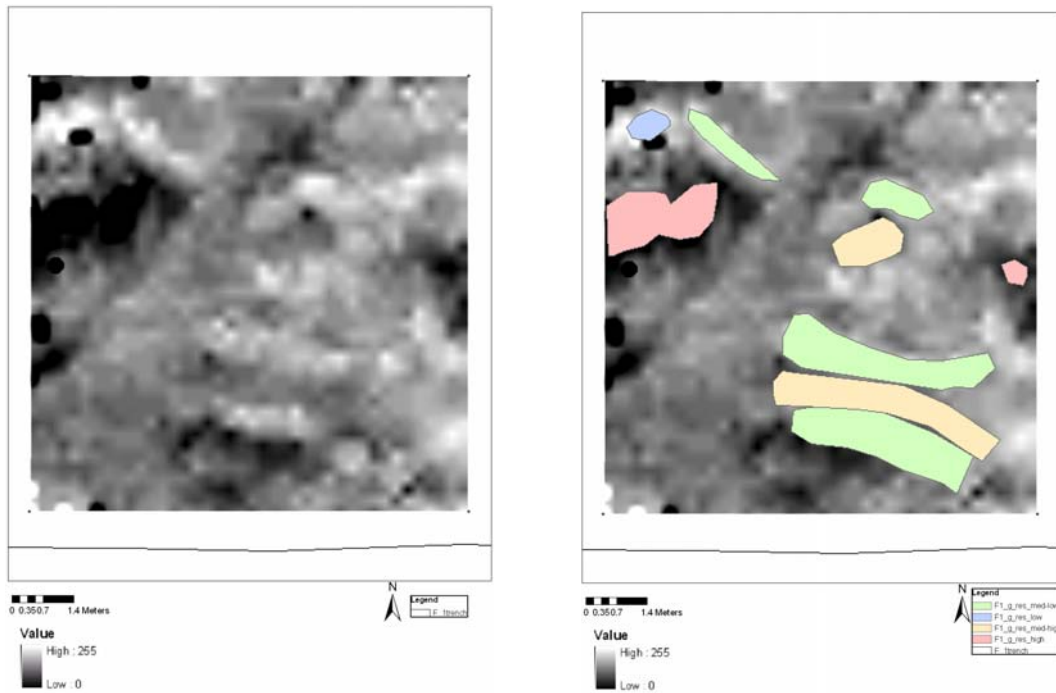


Figure 102. F1 resistivity gravel survey at 0.75m depth (left) with interpretations (right).

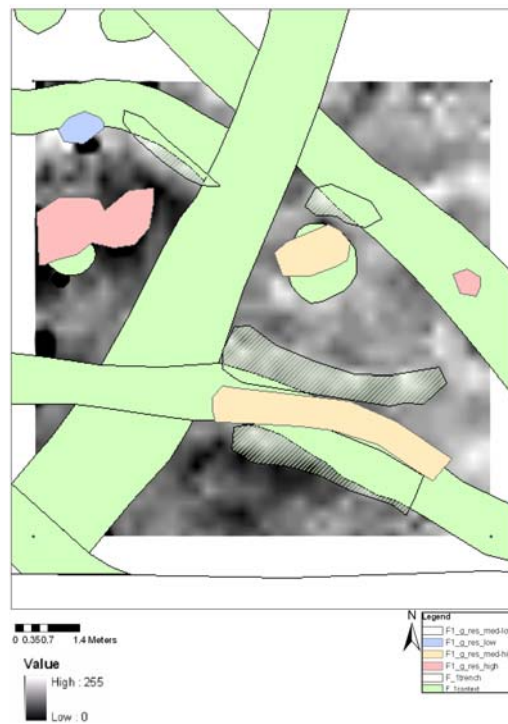


Figure 103. F1 resistivity gravel survey at 0.75m depth with interpretations and excavation plan.

The ring ditch was the weakest geophysical anomaly that appeared as a medium-low resistivity anomaly that gradually increases in resistance with depth. The strongest feature was the possible northern linear feature that extended from the ring ditch. This feature appeared in the surface survey as well as the gravel survey. In the surface survey the feature appeared as a low resistivity anomaly. In the gravel survey the northern linear feature began as a regular low resistivity anomaly but with

increasing depth discrete areas began to increase in resistivity suggesting the presence of possible pits or other such deposits of contrasting materials.

The southern linear extension appeared only at 0.75m in the gravel survey and was defined as a medium-high resistivity anomaly that was flanked on either side (north and south) by high resistivity values that may suggest this was a ditch feature excavated into a lower resistivity background material.

The identification of the anomaly in the centre of the survey area as a pit was possible with comparison with the excavation plan. When the pit appears at 0.75m depth the basic character of the resistivity map changed to reveal a more irregular record with areas of high and low resistivity that were difficult to interpret archaeologically. For example, the pit located just 5m directly west of the central pit feature did not seem to appear in the data. However, the data where the pit is located was an area of high resistivity that did not vary greatly in character from the ground surface to 1.50m depth.

5.4.4 GPR Survey Results

Effects of modern ploughing were evident throughout the surface GPR survey in Area F1. The first few plan views to a depth of approximately 0.6m exhibited regular plough furrow striping with continued effects of particularly deep furrows throughout the entire data set. It is necessary to bear in mind, however, that this does not mean the field was ploughed to the depth of 1.6m (the recorded depth of the GPR survey), but that the strong reflection and uneven surface of the plough furrows had contributed significant noise to this particular data set. No trace of archaeological features was seen in the surface GPR survey.

As with the other natural subsoil surveys, detailed archaeological information was mapped in the radar wave coupling zone. The ring ditch, pits and the linear cropmark features were all evident in the GPR data.

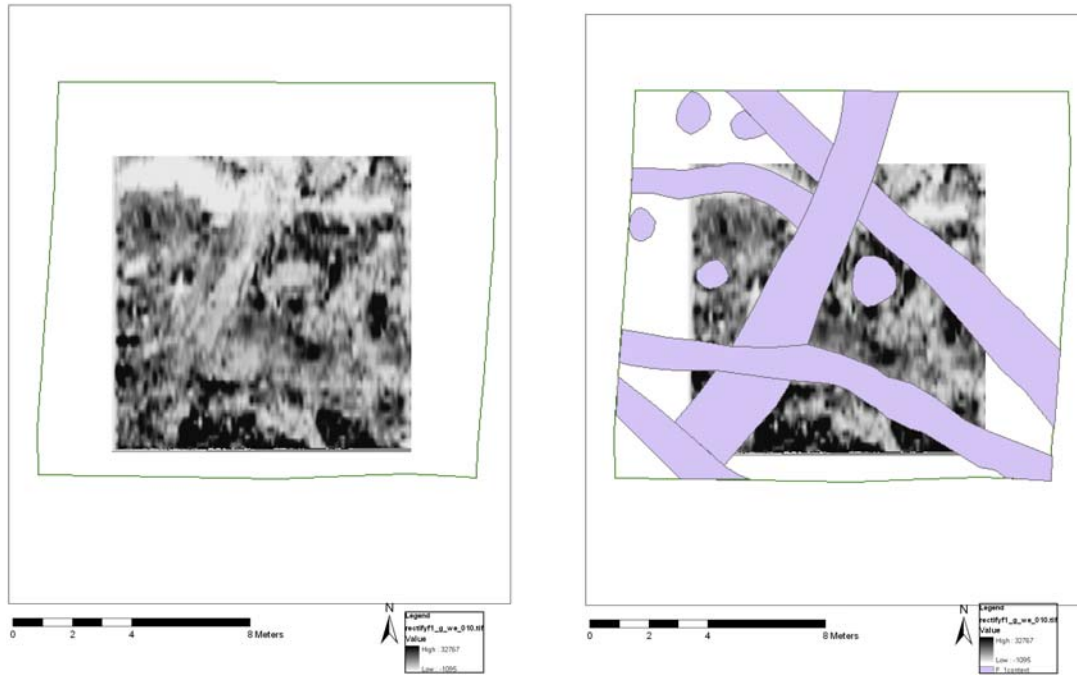


Figure 104. Ground coupling GPR map of gravel survey surface F1 over the Large Ring Ditch with extensions. The map on the right has the excavation features mapped that correspond with the GPR information.

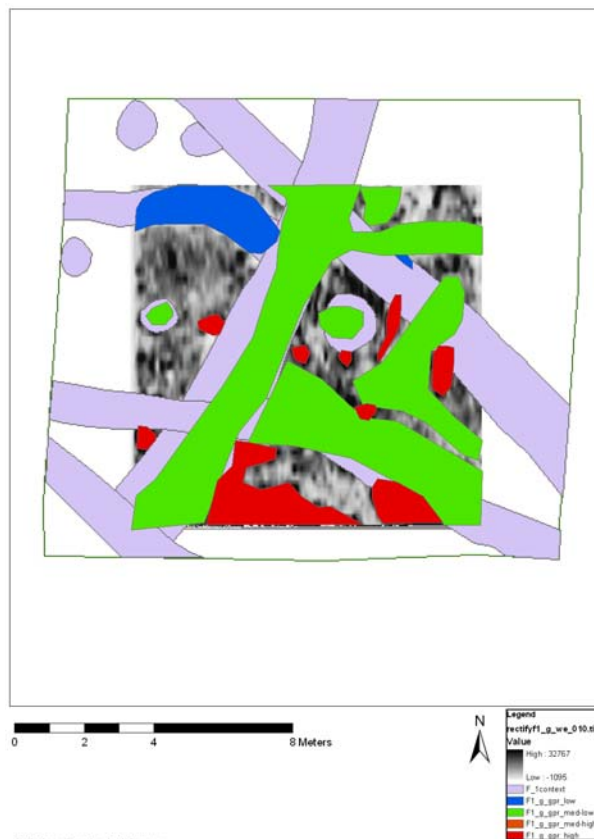


Figure 105. GPR interpretations from the surface of the GPR gravel survey area F1.

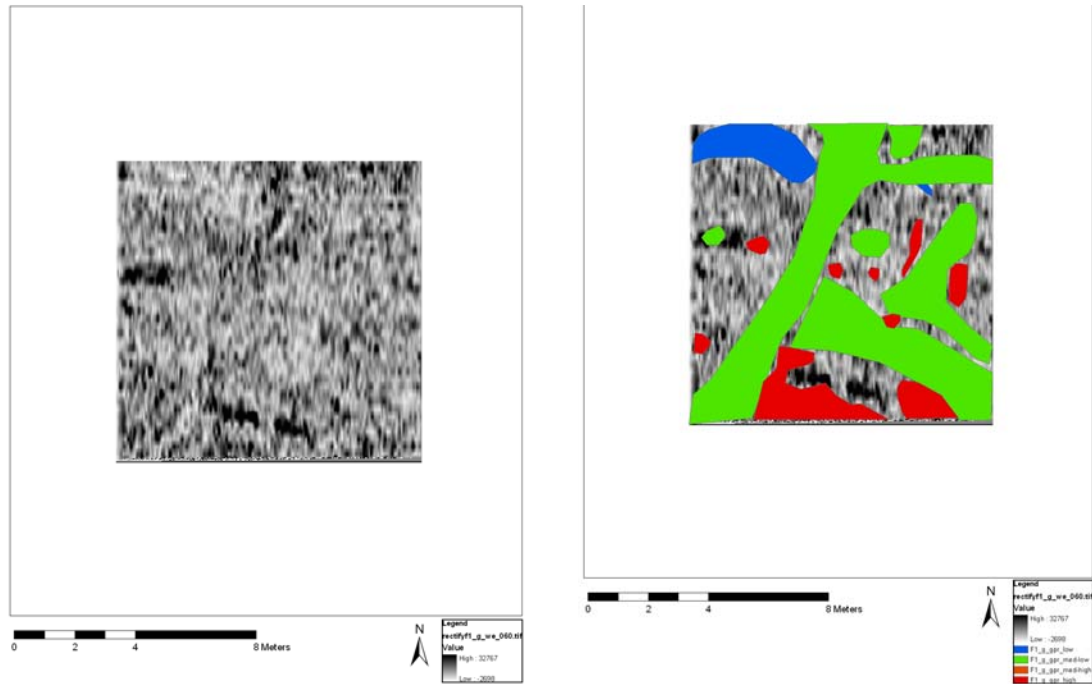


Figure 106. F1 gravel GPR data at 0.6m depth (left) with overlain interpretations (right).

With increasing depth the archaeological features appeared to disappear, as can be seen at approximately 0.6m. However, the nature of GPR survey and actual data collection does not necessarily map the entire feature on every level as depth increases, as was seen in A2. The complex nature of the geometry of the radar wave propagation enables us to see or not to see features as they appear in the ground. The very base of the ring ditch and part of one of the associated larger linear features could be seen as high amplitude reflectors at a depth of approximately 0.9m. This high amplitude reflection was most likely the strong contrast between the dielectric properties of the ditch fill and the background area materials of sand and gravel. Archaeological anomalies did not appear below 1.0m depth in the GPR data.

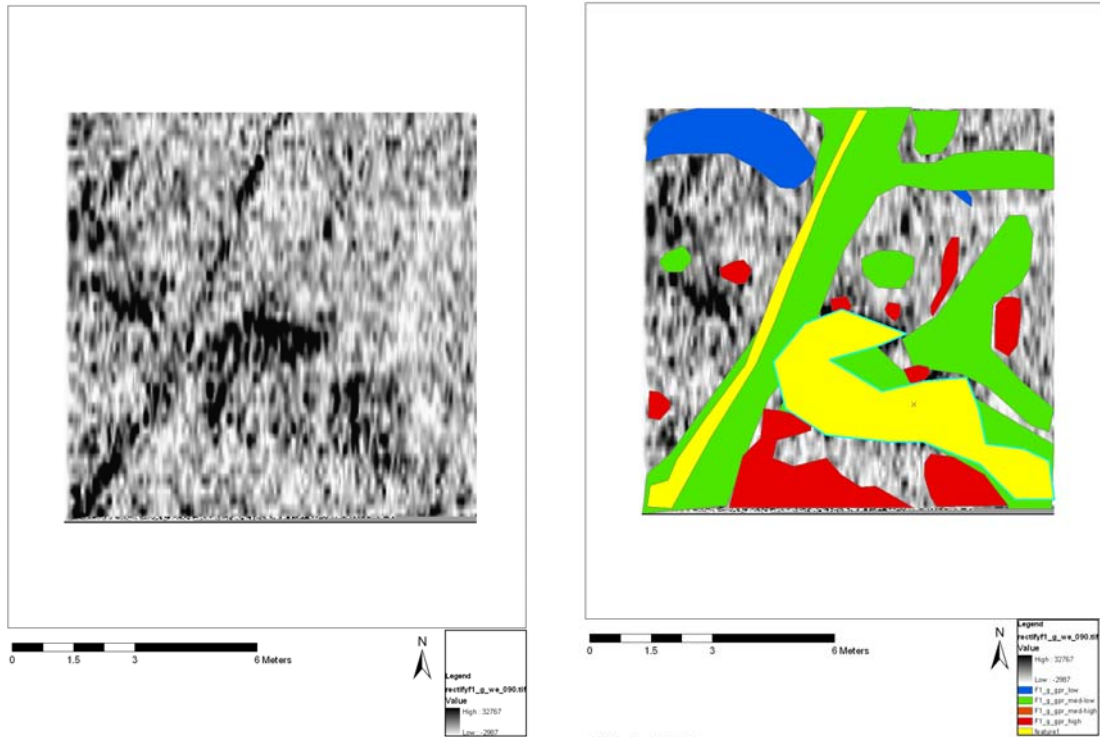


Figure 107. F1 ring ditch feature defined by high amplitude reflection at approximately 0.90m depth (left). The image to the right highlights in yellow the response of the GPR to archaeological features at 0.90m depth, this anomaly is overlain on previous GPR interpretations.

5.4.5 F1 2m x 5m Sub-area

5.4.5.1 Magnetic Susceptibility

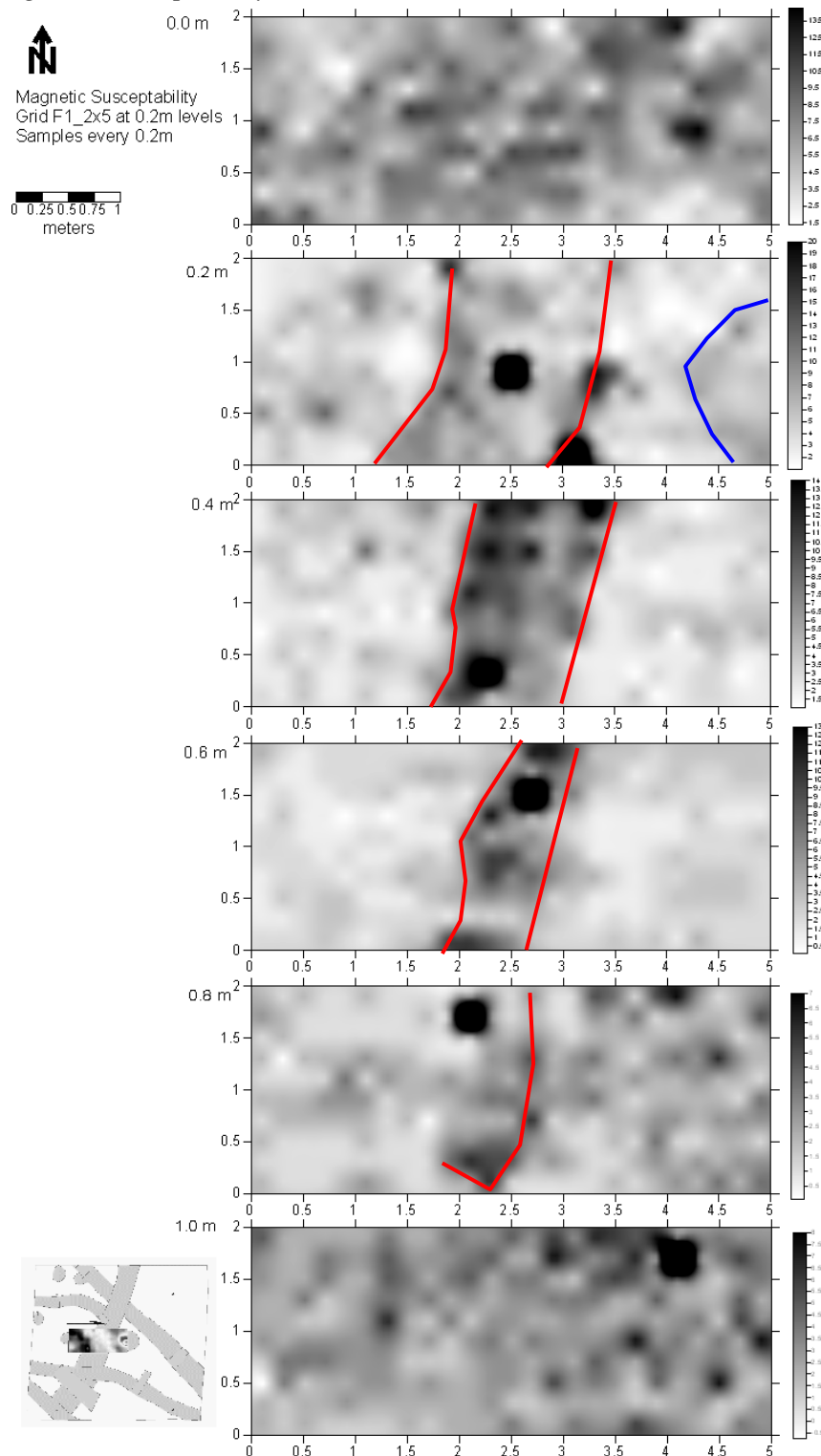


Figure 108. F1 2m x 5m magnetic susceptibility survey results.

The ring ditch and western pit appeared in the 0.2m level of magnetic susceptibility survey data. The ring ditch could be traced down to 0.8 m, but the pit appeared most clearly only in the 0.2m layer (with a vague shadow on the ground surface).

5.4.5.2 Resistivity

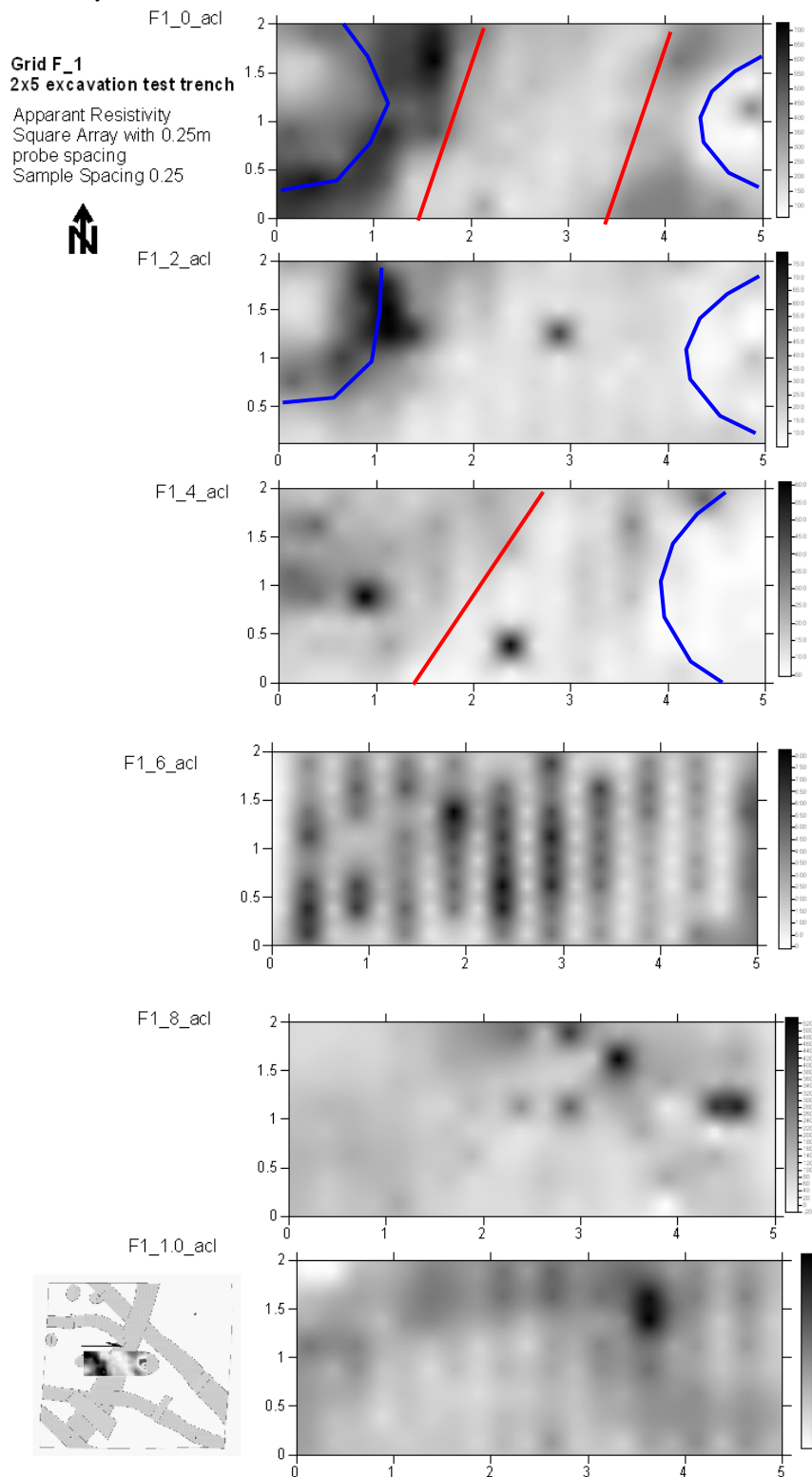


Figure 109. F1 2m x 5m resistivity survey results.

The resistivity survey showed the two pit features and the ring ditch in the upper few survey levels. Level 0.6m survey had an error in data order seen in the striped pattern in the data.

5.4.5.3 Dielectric Permittivity

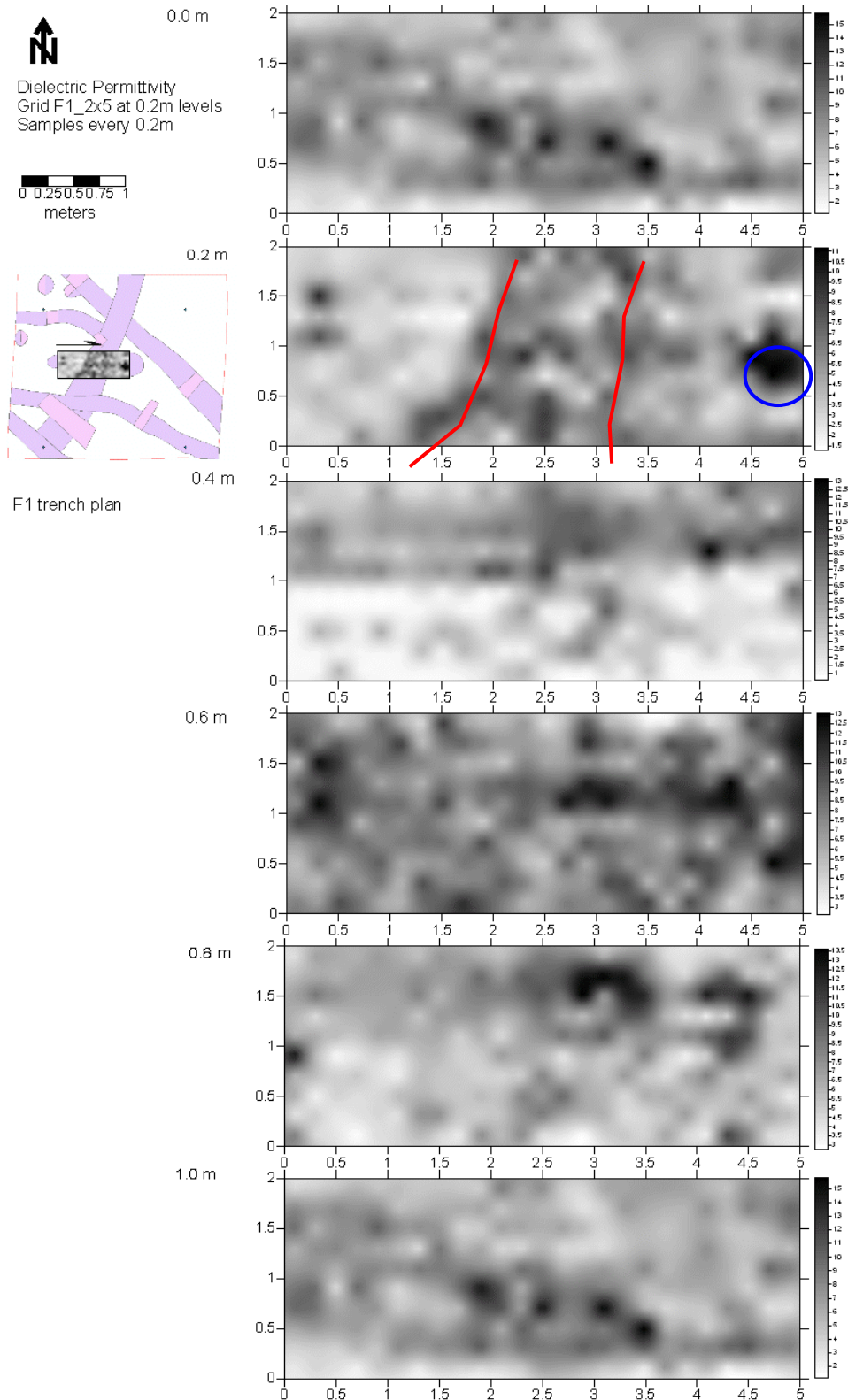


Figure 110. F1 2m x 5m dielectric permittivity survey results.

The western pit and ring ditch were well defined in the 0.2m level of the dielectric permittivity survey data. The features did not clearly appear in the remaining survey data.

6.0 Conclusions and Recommendations

6.1 Comments

6.1.1 Geophysical Survey

Phase II of investigations provided an extensive data base for analysis. Three main high density survey stages were conducted, the first on the topsoil surface, the second on the natural subsoil after the topsoil was removed, and the third in 2m x 5m sub-areas.

The first stage, on the topsoil surface, sought to assess our ability to detect buried archaeological features. Resulting geophysical images provided good information on some areas of the 'Catholme Ceremonial Complex' monuments. Each geophysical method performed differently in its response to archaeological features and presented a number of questions which it was hoped would be answered at the second stage of investigations.

Stage two, on the surface of the natural subsoil, was conducted to obtain a record of how the archaeological features and background geology of the survey areas were mapped through various geophysical methods. Resulting geophysical data and maps provided a base guideline of how the archaeological anomalies appeared in order to provide background knowledge for a re-examination of the results of the topsoil surface survey. In addition to a background for surface survey consideration, the natural subsoil survey provided detailed information of not only the geophysical properties of the archaeological features, but also additional information contributing to the formation and content of the archaeological features themselves. Results from this stage of survey should be integrated with data from the excavations, the archaeological record and the additional soil analysis results in order to provide a better comprehension of the archaeological nature of the site.

The aims of this project reached beyond mapping archaeological features and sought to achieve a better understanding of the processes of site formation and the influence of the geological background on the archaeological features. The feedback from this level of survey contributes to a better understanding of geophysical survey results. 2m x 5m sub-areas were excavated over different archaeological features in A1, A2, B2 and F1 with geophysical survey conducted at depths of 0.2m until the base of the archaeology was reached. This survey was conducted in tandem with an investigation into the magnetic properties and geoarchaeological nature of both the natural and archaeological deposits.

Further assessment of each geophysical technique should be undertaken at every stage of survey in order to assess how features are being recorded with each technique. Once this is completed results from the soils analysis should be integrated into the whole. This process should provide a more comprehensive understanding of how the geophysical techniques responded to the properties of the archaeological features and their surrounding environment.

All of the geophysical techniques used in the project performed well. It is clear that this suite of tools effectively mapped the archaeological features of the 'Catholme Ceremonial Complex'. The challenge, however, is in putting together a recommended survey strategy for future work on similar sites, and in fact also on dissimilar sites.

Approximately 1½ years have been spent on the geophysical survey section of the WRM project. Out of this time 9 months were spent in the field collecting data and 6 months were spent on data processing, interpretation and reporting. The amount and complexity of the data in the geophysical database alone was staggering. Challenges encountered in this process included the regulation of data collection over a period of varying weather conditions and survey personnel, accurate and methodological data storage, methodological data processing, database assembly and backup. The facilities available for this project ensured there was sufficient data storage space and multiple up-to-date, dedicated software programs.

After thorough study and consideration of the geophysical data, it is clear that the data contain significantly more information than could be analysed in this report. A broad statement can be made that GPR may be the most effective mapping tool of the three main techniques utilised. Not only did it map the 'Sunburst' monument (Field B) and the large ring ditch (Field F), it also mapped the 'Woodhenge' monument (Field A) from the topsoil surface survey. GPR therefore mapped all three main targets and provided important supplemental information related to the structure, form and depth of buried archaeological features and the impact of contemporary land use on the archaeological resource.

It is important to note that the GPR information which contributes to this report was not easily attained. Only after careful data collection, processing, imaging and consideration was it able to be extracted. Subsequently too, only through careful consideration of all of the project data will we be able to provide an integrated and effective survey strategy which could be suitable for use in commercial projects.

6.1.2 Resistivity Profiling

Preliminary analysis of resistivity pseudosections in Area A1 provided definitive evidence for the necessity of inversion. The nature of resistivity data recording along a vertical profile introduced artefacts into the results from deeper levels of mapping. In order to have the best presentation of resistivity properties as a whole from the site the data should be investigated through pseudosection inversion. Subsequent data can be assessed and considered for further 3D modelling.

6.2 Recommendations

6.2.1 Continuation of the WRM geophysical survey

Topsoil Surface Survey Requirements:

- To assess the data sampling intervals which are necessary for mapping the archaeological features.

- To achieve closer integration of environmental conditions, such as the impact of weather conditions and ploughing activities, with project results.

Natural Subsoil Surveys:

- Data should be compared to topsoil survey data in order to establish the influence of the topsoil on the effectiveness of geophysical mapping.
- A rigorous examination of geophysical survey results should be conducted to assess the relationship of different geophysical techniques and their sensitivity to the archaeological features.

2m x 5m survey sub-areas:

- Different data should be compared such as: resistivity to the dielectric permittivity.
- Data from the 2m x 5m should be compared to the natural subsoil survey and the topsoil surface survey data to see the differences in values with increasing depths and distance from the topsoil.
- Data should be compiled in vertical format in order to study the effects of the changing shape of archaeological features and increasing depth into the ground.
- The 2m x 5m geophysical survey data should be analysed in conjunction with the results of the soil analyses.

Phase I geophysical survey results should be re-examined in the light of Phase II data integration and assessments. It may prove to be the case that further archaeological features were in fact mapped in the Phase I survey, but were not recognised for what they were. From this reassessment we can consider:

- We have learned to look at data differently. Basic assumptions of what features will look like in the geophysical anomalies are not enough. On many occasions interpretation of anomalies must go beyond normal data review processes. Only through the actual excavation for ground truthing and after an intensive period of data processing and interpretation have some of the archaeological features from the Phase II of survey come to light in the data.
- GPR anomalies were identified which lay beneath the broad plough furrows crossing Area A2. Some of these anomalies appeared to correspond to features on the excavation plan and may be post-pits. In this particular application, GPR may be put forward as an effective survey tool to 'see' beneath other 'masking' features.
- The data from the topsoil survey and subsoil survey, each taken at comparable depths, should provide us with even more information on the influence of the topsoil, surrounding geology and archaeological features on final geophysical survey maps.

6.2.2 GIS and ArcIms

The WRM project is managed in a GIS. All additional Phase II project data and results should be input to the GIS for further analysis and interpretation. Because of the complex nature of the project, a comprehensive presentation of data and results is challenging. This report presents the results of the geophysical survey and an assessment of the data. The detail and nuances of the data are difficult to express in

textual format. It is suggested that a more efficient and flexible way to present the true 3D nature of the data and results would be through ArcIMS.

All data from the project GIS can be uploaded directly to an ArcIMS mapserver. ArcIMS enables global access to project data immediately after its integration into the GIS. Viewed through an internet browser, project information can be password protected for research collaborators while public access can be made available for selected project results. This format for data presentation is a powerful tool which can be used in future investigations enabling fast access to and dissemination of data with the ability to connect to mobile devices in the field. ArcIMS provides a basic GIS format for data display, queries and assessment.

6.2.3 Data Fusion, Modelling and Visualisation

One of the main conflicts encountered when using a GIS for data interpretation and display is the lack of the expression of 3D space. Though ArcGIS has 3D Analyst, this is geared toward planimetric 3D mapping and does not take into account the nature of the closed 3D surfaces investigated in geophysical data. The definitive third dimension of GPR survey enabled an informed analysis of the effects of modern and past land-use in the Focus Area and also provides insight to the structure of archaeological features, such as the shape, volume and deposits in pits in Area A1. Resistivity data collected in vertical profiles across each survey area presents a rich 3D environment for data assessment and interpretation, which is not possible through conventional 2D display methods.

The 3D nature of data sampling across the six areas and in the 2m x 5m sub-areas demanded a more innovative platform for integrated data investigation and interpretation. Visualisation software Amira is able to work with various data types and provides a true 3D environment which can be viewed either through 3D projection methods or with more virtual techniques using head-tracking capabilities. Different data types can be loaded into a single grid with accurate geospatial information enabling comparison of the form and strength of archaeological features as they are mapped through varying geophysical methods.

The visualisation environment enables solid modelling through feature surfaces of geophysical anomalies and archaeological features for data investigation and interpretations. Taken as an example, the GPR and resistivity data from pits in Area A1 illustrate the rich potential of 3D geophysical data. As can be seen in the images below, the traditional display of GPR and resistivity data revealed pits along the pit-alignment.

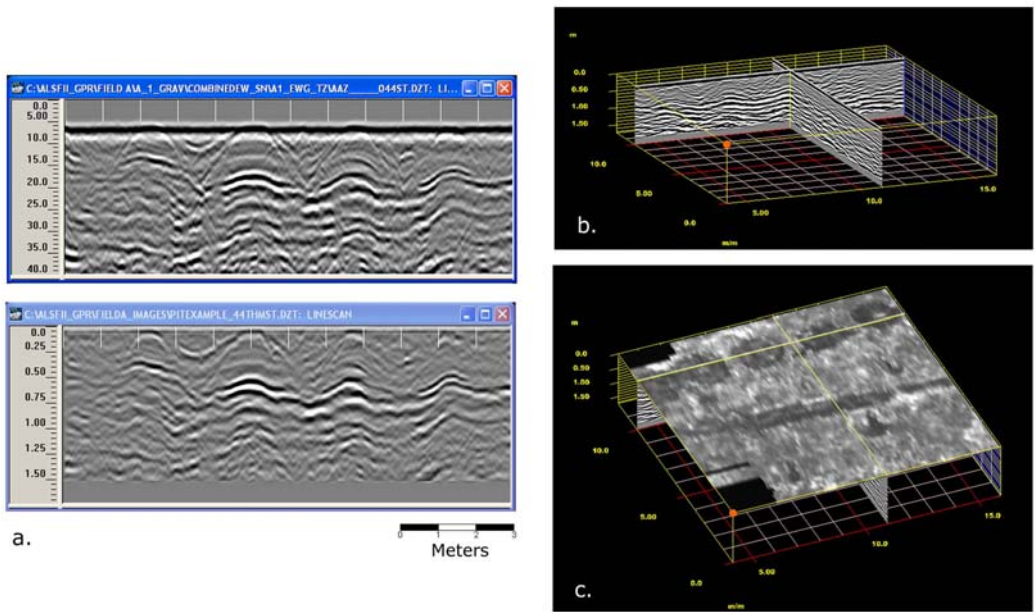


Figure 111. Traditional GPR profiles (a.), fence diagram (b.) and 3D cube with time slices (c.)

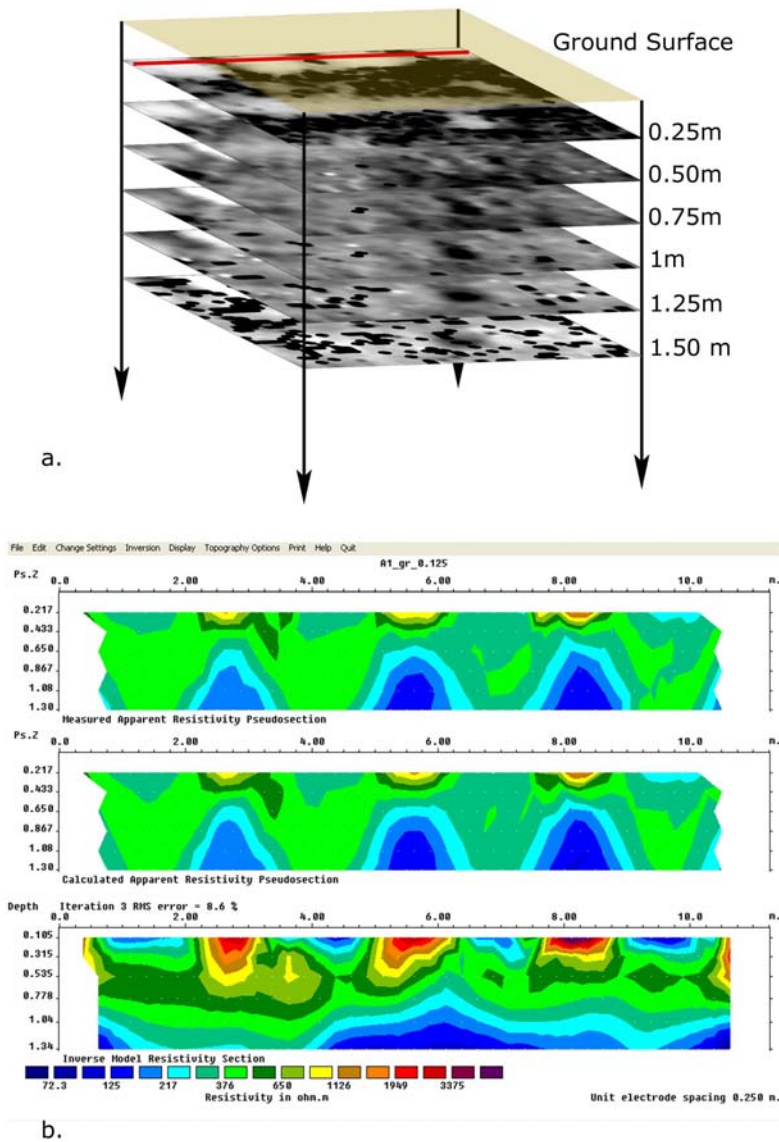


Figure 112. Resistivity plan maps (a.) and inverted pseudosections (b.)

GPR and resistivity data are imaged above as vertical profiles and plan views. Both formats present good information regarding the position, structure and geophysical properties of the archaeological feature but they fall short of presenting the true nature of the features. Only through 3D assessment can this goal be achieved.

In order to investigate innovative methods for data analysis, both GPR and resistivity data were read into the same environment in Amira and registered geospatially. The creation of label fields enables the user to select voxels of interest that cross different values to define archaeological features visible in the data. The label fields are interpolated to create surfaces that define the 3D shape of the feature selected. At this stage, Amira tools enable various types of visual and quantitative analyses between all data in the environment. Functions such as volume and shape comparison of each data type begin to reveal information on how different geophysical methods visualise the earth and how they are influenced not only by the archaeological features they are targeting but also by the subsurface geology and the environment. Further comparison of the shape and character of rendered geophysical features to models created from excavated archaeological information and additional soil analysis,

provided a 3D environment in which we were able to consider data in an entirely new perspective.

The example below presents preliminary images rendering the pit-alignment and associated features from Area A1 in GPR data (a.), resistivity data (b.) and of both data sets overlain for comparison (c.). The GPR and resistivity rendered pit-alignment features differ significantly in shape, presumably as a result of the nature of equipment arrays and data collection methods, the physical properties of the pit fills and the materials from which they were excavated. Continuing research and data assessment will investigate further the nature of these data visualisation methods.

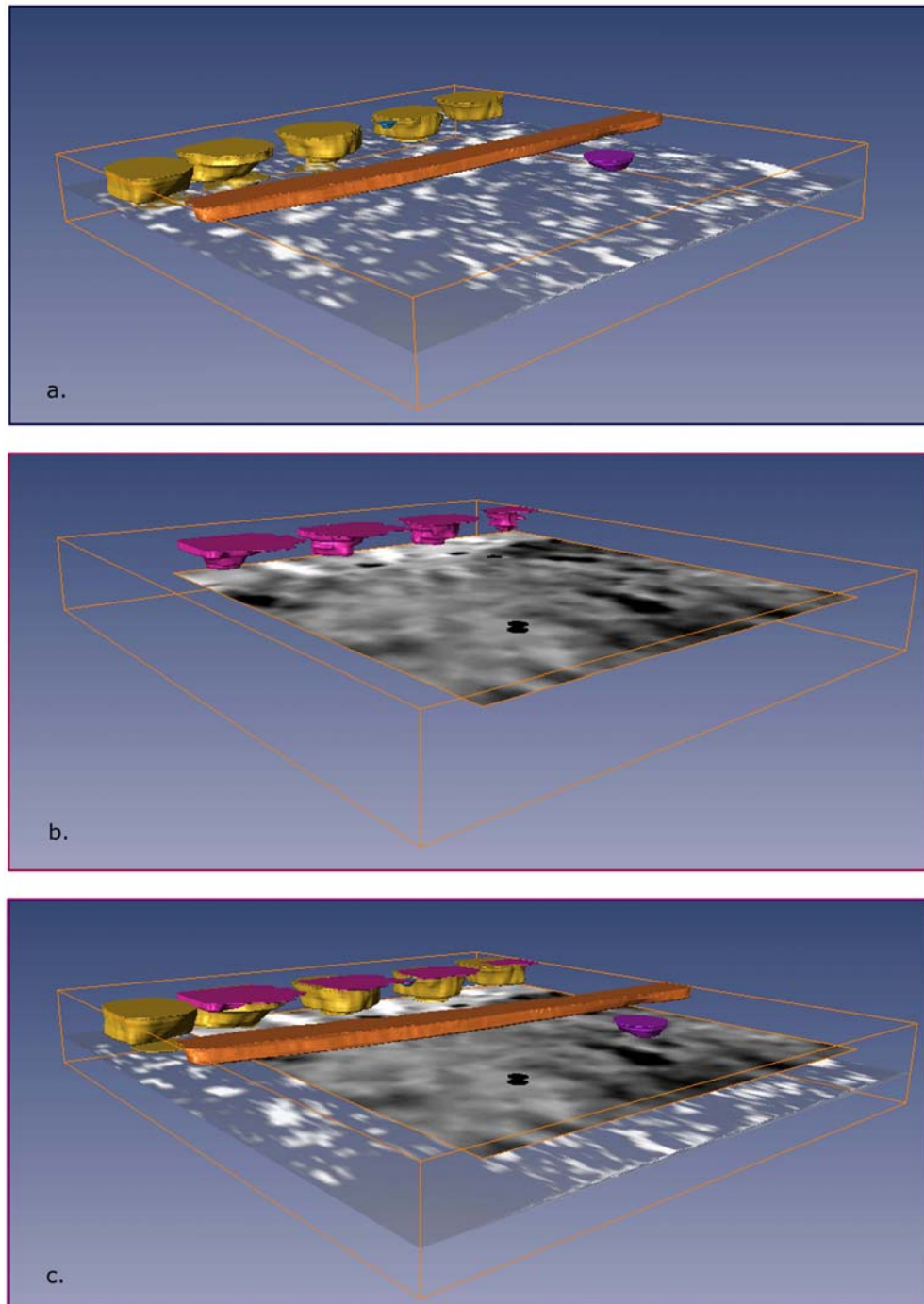


Figure 113. 3D visualised GPR and resistivity data from Area A1.

Visualisation analyses can readily be output to a variety of data formats in order to allow integration back into a project GIS or other management software. Combined processing and analysis of geophysical data through specialised geophysical programs, GIS and visualisation applications have the capability to present the full spectrum of geophysical data in a descriptive, visual and comprehensive format.

7.0 Bibliography

Breiner, S. 1973. *Applications Manual for Portable Magnetometers, Rev. A.* Geometrics, San Jose, California.

Buteux, S. 2002. Where Rivers Meet: Landscape, Ritual, Settlement and the Archaeology of River Gravels, Project design submitted to English Heritage.

Buteux S. Forthcoming. *Archaeological Synthesis.* Aggregates Levy Sustainability Fund (ALSF) Where Rivers Meet Phase I Report, London: English Heritage: Vol 1.

Chanzy A., Tarussov A., Judge A. and Bonn. F., 1996, Soil Water Content Determination Using a Digital GPR. *Soil Science Society of America Journal*, vol.60, no.5., pp.1318-26.

Clark, A. J., 1996. *Seeing Beneath the Soil: Prospecting Methods in Archaeology* (New Edition). Revised Edition. B. T. Batsford Ltd., London.

Conyers, L.B. and D. Goodman. (1997). *Ground-Penetrating Radar: An introduction for Archaeologists.* Altamira Press, Walnut Creek, California.

Daniels, D. J. (1996). *Surface-Penetrating Radar.* Institution of Electrical Engineers Radar Series no. 6.

Gaffney, Chris and J. Gater. (2003). *Revealing the Buried Past Geophysics for Archaeologists.* Tempus Publishing, Ltd.

GSSI, 2002. RADAN User's Manual, Geophysical Survey Systems, Inc.

Scollar, I., A. Tabbagh, A. Hesse, and I. Herzog. (1990). *Archaeological Prospecting and Remote Sensing.* Cambridge University Press, Cambridge.

Watters, M. and J. Hunter, 2003. *Geophysics and Burials: Field Experience and Software Development*, in Pye, K. and Croft, D. (eds.) *Forensic Geosciences*, Geological Society of London.

Watters M. Forthcoming. *Aggregates Levy Sustainability Fund: Where Rivers Meet Geophysical Survey At Catholme.* Aggregates Levy Sustainability Fund (ALSF) Where Rivers Meet Phase I Report, London: English Heritage: Vol 3.

Grey Literature for ALSF Study Area Geophysical Survey

Bartlett A. 2001. Barton Business Park Staffordshire. Report on Archaeogeophysical Survey 2001. Bartlett-Clark Consultancy, for Phoenix Consulting Archaeology, Ltd.

Bartlett, A. 1998. Whitemoor Haye, Alrewas, Staffordshire. Report on Archaeogeophysical Survey, 1998. Bartlett-Clark Consultancy, for Phoenix Consulting Archaeology, Ltd.

Bartlett, A. 1995. Whitemoor Haye, Alrewas, Staffordshire. Report on Archaeogeophysical Survey, 1995. Bartlett-Clark Consultancy, for Tempus Reparatum Archaeological and Historical Associates, Ltd.

BUFAU, 1992. An Archaeological Evaluation at Whitemoor Haye, Alrewas, Staffordshire 1992. Report No. 231, Birmingham University Field Archaeology Unit.

Coates, G. and G. Hughes, 1999. The excavation of a prehistoric pit-alignment and enclosure at Fatholm Farm, Barton-Under-Needwood, Staffordshire: an interim report. Project No. 630, Birmingham University Field Archaeology Unit.

Hughes, G. and Coates, G., 1999. An archaeological Evaluation at Catholme, Barton-Under-Needwood, Staffordshire: Trial Trenching Phase, BUFAU Report 620.2.

Hughes, G. 1993. Barton Turn Marina, Staffordshire, 1993: An Archaeological Evaluation. Report No. 268, Birmingham University Field Archaeology Unit.

Losco-Bradley, S. and Kinsley, G., 2002. Catholme: An Anglo-Saxon settlement on the Trent gravels in Staffordshire, Nottinghamshire Studies in Archaeology Vol. 3, Nottingham University Press.

Richmond, A. 2001. Specification for Archaeological Evaluation, Barton Business Park Barton-Under-Needwood, Staffordshire. P138G, Phoenix Consulting.

Rose, S. 2000, Archaeological Evaluation of Land at Barton Quarry, Barton-Under-Needwood, Staffordshire. Northamptonshire County Council Northamptonshire Archaeology, for Hanson Aggregates.